

**Induced pluripotent stem cells from patients with  
hypoplastic left heart syndrome (HLHS)  
as a model to study functional contribution of  
endothelial-mesenchymal transition (EndMT) in HLHS**

**Doctoral Thesis**

*(Cumulative Doctoral Thesis)*

*In partial fulfillment of the requirements for the degree*

*“Doctor rerum naturalium (Dr. rer. nat.)”*

*in the Molecular Medicine Study Program*

*at the Georg-August University Göttingen*



*submitted by*

**Xiaopeng Liu**

*born in Inner Mongolia, China*

*Göttingen 2016*

## **Members of the thesis committee:**

*Supervisor:*

**Prof. Dr. med. Elisabeth Zeisberg**

*Department of Cardiology and Pneumology*

*University Medical Center, Georg-August University of Göttingen*

*Second member of the thesis committee:*

**Prof. Dr. rer. nat. Kaomei Guan**

*Department of Cardiology and Pneumology*

*University Medical Center, Georg-August University of Göttingen*

*Third member of the thesis committee:*

**Prof. Dr. med. Frauke Alves**

*Molecular Imaging in Oncology*

*Max Planck Institute of Experimental Medicine, Göttingen*

*Date of Disputation:*

## **AFFIDAVIT**

*Here I declare that my doctoral thesis entitled:*

**“Induced pluripotent stem cells from patients with  
hypoplastic left heart syndrome (HLHS)  
as a model to study functional contribution of  
endothelial-mesenchymal transition (EndMT) in HLHS”**

*has been written independently with no other sources and aids than  
quoted.*

*Xiaopeng Liu*

*Göttingen, November 2016*

## List of publications and posters:

### Publications:

1. **Liu X**, Qi J, Xu X, Zeisberg M, Guan K, Zeisberg EM. Differentiation of functional endothelial cells from human induced pluripotent stem cells: a novel, highly efficient and cost effective method.

“Differentiation” 2016. DOI: 10.1016/j.diff.2016.05.004

2. Xu X, Tan X, Tampe B, Nyamsuren G, **Liu X**, Maier LS, Sossalla S, Kalluri R, Zeisberg M, Hasenfuss G, Zeisberg EM. Epigenetic balance of aberrant Rasaf1 promoter methylation and hydroxymethylation regulates cardiac fibrosis.

“Cardiovasc Res” 2015. DOI: 10.1093/cvr/cvv015

3. Charytan DM, Padera R, Helfand AM, Zeisberg M, Xu X, **Liu X**, Himmelfarb J, Cinelli A, Kalluri R, Zeisberg EM. Increased concentration of circulating angiogenesis and nitric oxide inhibitors induces endothelial to mesenchymal transition and myocardial fibrosis in patients with chronic kidney disease.

“Int J Cardiol” 2014. DOI: 10.1016/j.ijcard.2014.06.062

### Posters:

1. Title: Induced pluripotent stem cells from patients with hypoplastic left heart syndrome (HLHS) as a model to study functional contribution of EndMT in HLHS

Authors: Xiaopeng Liu, Kaomei Guan and Elisabeth Zeisberg

Occasion: 2014 Molecular Medicine PhD program Annual Retreat

Location: Braunlage

2. Title: iPS cell-derived endothelial cells: a new tool to study mechanisms of endocardial fibroelastosis in congenital heart diseases

Authors: Xiaopeng Liu, Kaomei Guan and Elisabeth Zeisberg

Occasion: 2015 ISSCR Annual Meeting

Location: Stockholm



**Table of contents**

<i>Abbreviations</i> .....	1
<i>Summary</i> .....	4
<b>1. Introduction</b> .....	<b>5</b>
1.1 <i>Hypoplastic left heart syndrome</i> .....	5
1.1.1 <i>General overview</i> .....	5
1.1.2 <i>Genetic backgrounds of HLHS</i> .....	7
1.1.3 <i>Endocardial fibroelastosis in HLHS</i> .....	10
1.2 <i>EndMT</i> .....	10
1.2.1 <i>EndMT in heart development</i> .....	10
1.2.2 <i>EndMT in pathological process</i> .....	11
1.2.3 <i>Molecular mechanisms of EndMT</i> .....	13
1.3 <i>Disease-specific hiPSCs and endothelial cell generation</i> .....	15
1.3.1 <i>Disease-specific human iPSCs</i> .....	15
1.3.2 <i>Endothelial cell generation from hiPSCs</i> .....	16
1.4 <i>Aims and objectives</i> .....	17
<b>2. Original Publications</b> .....	<b>18</b>
2.1 <i>Differentiation of functional endothelial cells from human induced pluripotent stem cells: a novel, highly efficient and cost effective method</i> .	19
2.1.1 <i>Declaration of my contribution</i> .....	19
2.2 <i>Increased concentration of circulating angiogenesis and nitric oxide inhibitors induces endothelial to mesenchymal transition and myocardial fibrosis in patients with chronic kidney disease</i> .....	39
2.2.1 <i>Declaration of my contribution</i> .....	39
<b>3. Unpublished data</b> .....	<b>54</b>
3.1 <i>Patient-specific iPSC models for HLHS</i> .....	54
3.1.1 <i>Abstract</i> .....	54
3.1.2 <i>Introduction</i> .....	55
3.1.3 <i>Materials and Methods</i> .....	55
3.1.3.1 <i>HLHS-hiPSC generation</i> .....	55
3.1.3.2 <i>Alkaline phosphatase (ALP) staining</i> .....	56
3.1.3.3 <i>In vitro ECs differentiation</i> .....	56
3.1.3.4 <i>Flow cytometry and fluorescence-activated cell sorting</i> .....	56

## Table of Contents

---

3.1.3.5 Immunofluorescence staining .....	57
3.1.3.6 RNA isolation and real-time PCR.....	57
3.1.3.7 Reverse transcription PCR (RT-PCR).....	58
3.1.3.8 Statistical Analysis .....	58
3.1.4 Results .....	59
3.1.4.1 Generation of HLHS-hiPSCs .....	59
3.1.4.2 Generation and characterization of HLHS-hiPSC-ECs and WT-hiPSC-ECs .....	61
3.1.4.3 Susceptibility of hiPSC-ECs to EndMT .....	62
3.1.5 Discussion .....	65
4. Discussion .....	67
4.1 Establishment of a novel endothelial cell differentiation method.....	67
4.2 Modeling of HLHS by hiPSCs .....	69
5. Conclusion and future perspectives .....	72
6 Reference.....	73
7 Acknowledgement .....	89
Curriculum Vitae .....	90

**List of figures:**

*Figure 1. The scheme of heart structure in HLHS patient. .... 7*

*Figure 2. Origins of cardiac fibrosis. .... 13*

*Figure 3. Pluripotency characterization of HLHS-hiPSCs..... 60*

*Figure 4. Characterization of HLHS-hiPSC-ECs. .... 62*

*Figure 5. Susceptibility of HLHS-hiPSC-ECs to TGF $\beta$ 1 treatment and hypoxia  
condition..... 64*

**List of tables:**

*Table 1. HLHS related gene mutations .....9*

*Table 2. PCR primers list: .....58*

**Abbreviations**

<b>AFP</b>	<i>Alpha-1-fetoprotein</i>
<b>ALP</b>	<i>Alkaline phosphatase</i>
<b>ANG</b>	<i>Angiopoietin</i>
<b>AVS</b>	<i>Aortic valve stenosis</i>
<b>bFGF</b>	<i>Basic fibroblast growth factor</i>
<b>BMP</b>	<i>Bone morphogenetic proteins</i>
<b>BSA</b>	<i>Bovine serum albumin</i>
<b>CD31</b>	<i>PECAM-1</i>
<b>CHD</b>	<i>Congenital heart disease</i>
<b>CHIR</b>	<i>CHIR99021</i>
<b>CKD</b>	<i>Chronic kidney disease</i>
<b>CNVs</b>	<i>Copy number variances</i>
<b>CoA</b>	<i>Coarctation of the aorta</i>
<b>DNA</b>	<i>Deoxyribonucleic acid</i>
<b>DMEM</b>	<i>Dulbecco's Modified Eagle Medium</i>
<b>EB</b>	<i>Embryoid bodies</i>
<b>EC</b>	<i>Endothelial cell</i>
<b>ECM</b>	<i>Extracellular matrix</i>
<b>EFE</b>	<i>Endocardial fibroelastosis</i>
<b>EMT</b>	<i>Epithelial-mesenchymal transition</i>
<b>END</b>	<i>Endostatin</i>
<b>EndMT</b>	<i>Endothelial-mesenchymal transition</i>
<b>GATA 4</b>	<i>GATA binding protein 4</i>
<b>GJA1</b>	<i>Gap junction protein alpha 1</i>
<b>GSK3</b>	<i>Glycogen synthase kinase 3</i>
<b>HAND 1</b>	<i>Heart and neural crest derivatives expressed 1</i>
<b>HCAEC</b>	<i>Human coronary artery endothelial cells</i>
<b>hESC</b>	<i>Human embryonic stem cell</i>
<b>HIF-1</b>	<i>Hypoxia inducible factor-1</i>

## Abbreviations

---

<b>hiPSC</b>	<i>Human induced pluripotent stem cell</i>
<b>hiPSC-EC</b>	<i>Endothelial cell derived from hiPSC</i>
<b>HLHS</b>	<i>Hypoplastic left heart syndrome</i>
<b>HREs</b>	<i>HIF-responsive elements</i>
<b>iPSC</b>	<i>Induced pluripotent stem cell</i>
<b>JAM3</b>	<i>Junctional adhesion molecule 3</i>
<b>LDL</b>	<i>Low density lipoprotein</i>
<b>LVNC</b>	<i>Left ventricular noncompaction</i>
<b>LVOT</b>	<i>Left ventricular outflow obstruction</i>
<b>NANOG</b>	<i>Nanog homeobox</i>
<b>NKX2-5</b>	<i>NK2 homeobox 5</i>
<b>NR2F2</b>	<i>Nuclear receptor subfamily 2 group F member 2</i>
<b>NO</b>	<i>Nitric oxide</i>
<b>OCT4</b>	<i>Octamer binding transcription factor 4</i>
<b>OMIM</b>	<i>Online mendelian inheritance in man</i>
<b>PBS</b>	<i>Phosphate-buffered saline</i>
<b>PCR</b>	<i>Polymerase chain reaction</i>
<b>PFA</b>	<i>Paraformaldehyde</i>
<b>RASAL1</b>	<i>RAS protein activator like 1</i>
<b>RNA</b>	<i>Ribonucleic acid</i>
<b>ROCK</b>	<i>Rho-associated protein kinase</i>
<b>S100B</b>	<i>S100 calcium binding protein B</i>
<b>SMA</b>	<i>Smooth muscle actin</i>
<b>SNP</b>	<i>Single nucleotide polymorphism</i>
<b>SOX2</b>	<i>SRY (Sex determining region Y)-box 2</i>
<b>SSEA4</b>	<i>Stage-specific embryonic antigen-4</i>
<b>TBX5</b>	<i>T-box 5</i>
<b>TGF<math>\beta</math></b>	<i>Transforming growth factor beta</i>
<b>TIMP</b>	<i>Tissue inhibitor of metalloproteinases</i>
<b>TNF-<math>\alpha</math></b>	<i>Tumor necrosis factor-<math>\alpha</math></i>
<b>TSP</b>	<i>Thrombospondin</i>

## Abbreviations

---

<b>VEGF</b>	<i>Vascular endothelial growth factor</i>
<b>VE-Cad</b>	<i>VE-cadherin/ CDH5</i>
<b>VWF</b>	<i>Von Willebrand factor</i>
<b>WT</b>	<i>Wild-type control/ Healthy control</i>
<b>ZEB1</b>	<i>Zinc finger E-Box binding homeobox 1</i>
<b>ml</b>	<i>Milliliter</i>
<b>µg</b>	<i>Microgram</i>
<b>µM</b>	<i>Micromolar</i>

## Summary

*Hypoplastic left heart syndrome (HLHS) is one of the most lethal congenital heart diseases (CHD) and its pathological mechanism remains unclear. Endocardial fibroelastosis (EFE) is a hallmark of HLHS which impairs myocardial growth. EFE tissue originates from aberrant EndMT. Thus, we hypothesized that potential disorders in endothelial cells of HLHS could facilitate the EndMT, which eventually lead to the EFE formation. Human induced pluripotent stem cells (hiPSCs) provide a new access for modeling HLHS because of their ability of differentiation into desired cell types. We developed a simple endothelial cells (ECs) differentiation protocol from hiPSCs by monolayer differentiation approach. Three different combinations of cytokines were confirmed to contribute towards endothelial cell generation in this protocol. Furthermore, stage-specific medium was optimized and simplified to increase the efficiency of endothelial cells differentiation. We also demonstrated that the endothelial cell growth medium was supportive for maintaining and expanding hiPSCs derived ECs (hiPSC-ECs). To explore the underlying molecular mechanisms of HLHS, patient-specific hiPSCs (HLHS-hiPSCs) were generated and characterized to be pluripotent. All the endothelial cells derived from the HLHS-hiPSC lines were generated based on this endothelial cell differentiation protocol. Endothelial cells derived from HLHS-hiPSCs (HLHS-hiPSC-ECs) showed similar morphological and genetic properties as the wild type control (WT-hiPSC-ECs). Thereafter, we investigated whether the HLHS-hiPSC-ECs were more susceptible to EndMT, induced by TGF $\beta$ 1 treatment or hypoxia condition than WT-hiPSC-ECs. The expression of SNAIL (SNAIL1), and SLUG (SNAIL2), as key indicators of EndMT, implied no significant phenotypic and expression differences between HLHS-hiPSC-ECs and WT-hiPSC-ECs. In sum, it needs further optimization to study EndMT by using hiPSC-ECs, such as enrichment of specific subtype of endothelial cells.*

## 1. Introduction

*Congenital heart disease, also known as congenital heart defect (CHD), is the most common birth defect. HLHS is one of the life-threatening CHD characterized by an undeveloped left heart. Despite the cause of HLHS remains elusive, former studies point out that it is most likely to be a genetic disease (Benson et al., 2016; Grossfeld et al., 2009; Grossfeld, 2007b; Hinton et al., 2007). Numerous gene mutations and genomic disorders have been identified, although investigators are prone to believe that HLHS is multifactorial in etiology. EFE is considered as a hallmark of HLHS, which has been implied to result from pathological EndMT (Xu et al., 2015a). EndMT is a biological process, which plays an important role in both normal heart development and pathological aspects of heart disease. It seems that endocardial endothelial cells contribute to the EFE tissue formation by aberrant EndMT, which might be caused by disrupted transforming growth factor  $\beta$  (TGF $\beta$ ), hypoxia and other factors (Xu et al., 2015c; Yu et al., 2014; Zeisberg et al., 2007b).*

### 1.1 Hypoplastic left heart syndrome

#### 1.1.1 General overview

*HLHS is a rare, fatal and complex CHD, which is characterized by abnormally underdeveloped left ventricle and hypoplastic ascending aorta. HLHS accounts for 2% to 9% of all CHD patients (Fruitman, 2000). Furthermore, among all the infants who are born with CHD, approximately 20% to 25% of neonatal mortality are caused by HLHS (Fruitman, 2000; Grossfeld, 2007a). HLHS is a heterogeneous disease with different phenotypes of severe congenital left heart malformations (Tchervenkov et al., 2006). The common complex phenotypes of HLHS also include a smaller left atrium, and stenotic aortic and mitral valve. Interestingly, the left heart hypoplasia is correlated with hypertrophy of the heart in some reported cases (Andersen et al., 2015; Grant and Robertson, 1972; Rychik et al., 1999). For the HLHS fetus, a thick-walled cavity and EFE are usually*



*regarded as a clinical manifestation of the disease, yet the pathological mechanism between these correlated phenotypes is not fully proven (Figure 1).*

*In HLHS infants, the oxygen-rich blood is mixed with oxygen-low blood. Besides, the hypoplasia of left heart cannot properly pump the oxygen-rich blood because of the influence of the defective left ventricle. Consequently, the rest of the body is starved of the oxygen-rich blood. Therefore, the infant would require surgical procedure or cardiac transplantation after birth to rectify these defects (Figure 1) (Bertram et al., 2008). There are different treatments of HLHS available now, including the Norwood operation, the Sano modification and the hybrid procedure (Brescia et al., 2014). Although the diagnosis and treatment of HLHS have been improved in the past few decades, mortality is still high and the cause of HLHS is still largely unknown. Recently, accumulated evidences support the contribution of genetic etiology to the HLHS pathological process (Glidewell et al., 2015; Grossfeld et al., 2009; Grossfeld, 2007b).*

*HLHS is believed to share similar genetic disorders or genotypic milieus with two other types of cardiac diseases, aortic valve stenosis (AVS) and coarctation of the aorta (CoA) due to their feature of left ventricular outflow tract obstruction (LVOT) (Chu et al., 2016; McBride et al., 2009). Chromosomal abnormalities seem to be associated with these cardiac malformations (AVS, CoA, HLHS), such as monosomy X in Turner's syndrome and 11q terminal deletion in Jacobsen's syndrome (Gotzsche et al., 1994; Grossfeld et al., 2004b). Besides, genetic disorders, such as NOTCH1 and NKX2-5 mutations, have been reported in LVOT malformations including HLHS (McBride et al., 2009; McElhinney et al., 2003b; Mohamed et al., 2006).*

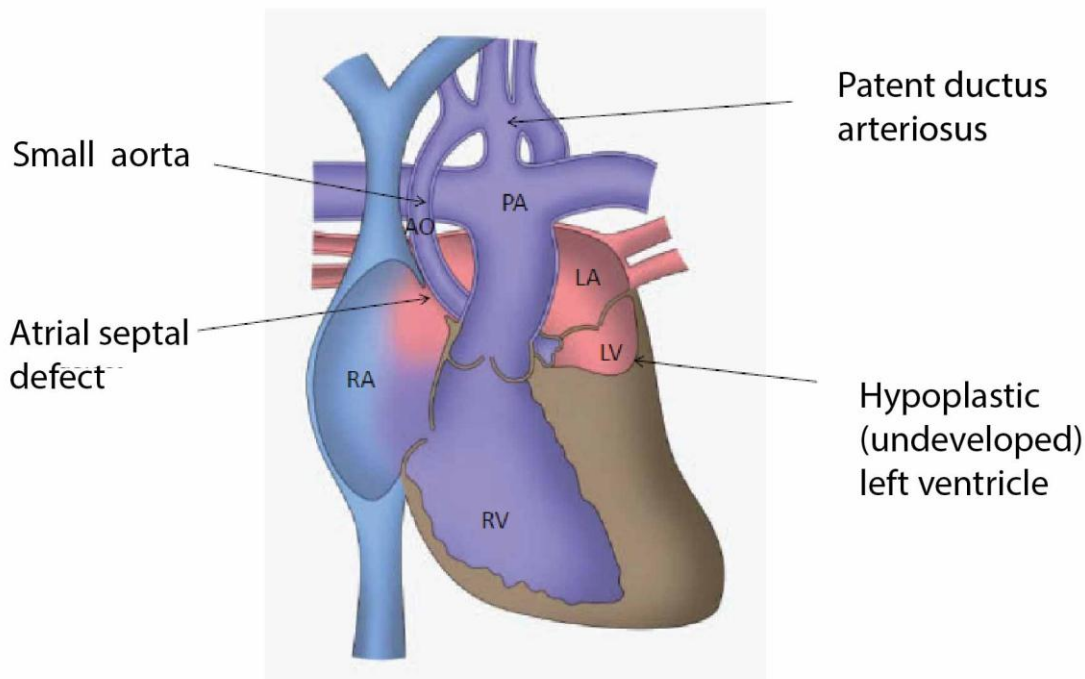


**Figure 1. The scheme of heart structure in HLHS patient.**

The heart structure of HLHS patient is severely affected. The typical structure-abnormality is a hypoplastic left ventricle. Besides, the narrow aorta, atrial septal defects and patent ductus arteriosus are also found in a large numbers of HLHS patients. AO=Aorta, PA=Pulmonary Artery, LA= Left Atrium, RA= Right Atrium, LV= Left Ventricle, RV= Right Ventricle. The picture of heart shape is adapted from: (Kobayashi et al., 2014).

### 1.1.2 Genetic backgrounds of HLHS

It has been shown that HLHS is associated with several gene mutations or gene copy number variances (CNVs) (Grossfeld, 2007b; Sifrim et al., 2016). Mutations in the genes that play important roles during the embryonic heart formation seem to be related with the heart malformation during development of HLHS, such as *GJA1* (6q22), *NKX2-5* (5q35), *NOTCH1* (9q34), and *HAND1* (5q33) (Dasgupta et al., 2001; Elliott et al., 2003; Garg et al., 2005; Iacone et al., 2012; Kanady et al., 2011; McElhinney et al., 2003a; Reamon-Buettner et al., 2008; Shay et al., 2011). Additionally, mutations of genes related to cardiac and endothelial development are

*reported to be involved in HLHS (Table 1).*

*Genomic imbalance refers to the abnormal copy number of genes due to chromosomal rearrangements or aneuploidy, which alters the gene dosage, thus affecting gene expression levels. This accounts for 12.7% of infants with HLHS and about 2% of healthy infants (Glessner et al., 2014). Recent reports have shown that CNVs are associated with HLHS pathogenesis (Glidewell et al., 2015; lascone et al., 2012). CNVs encompassing NKX2-5 were previously demonstrated to contribute to the genetic etiology of HLHS (Baekvad-Hansen et al., 2006; Glessner et al., 2014). Besides, CNVs may potentially influence expression level of neighboring genes by alterations of the chromosomal structure (Breckpot et al., 2011; Glidewell et al., 2015). Furthermore, other associated genomic imbalances, like trisomy 13, trisomy 18 and chromosome X monosomy are also found in HLHS patients (Grossfeld et al., 2009; Grossfeld et al., 2004a; McBride et al., 2009).*

*Identified susceptibility loci or other genetic disorder at these reported cases in HLHS patients can however only account for a minority of HLHS patients. Therefore, it needs more efforts to solve the puzzle of the underlying molecular mechanism of HLHS (Lahm et al., 2015).*

**Table 1. HLHS-related gene mutations**

Gene name Gene ID	Gene location	Mutation	Role in HLHS	Documented Involvement in EndMT or EMT	Vascular development	cardiac development
GJA1 OMIM: 121014	6q22	Yes	Yes (Dasgupta et al., 2001)	Yes (Nakano et al., 2008)	Yes (Kanady et al., 2011)	Yes
NKX2-5 OMIM: 600584	5q35	Yes	Yes (Elliott et al., 2003)		Yes	Yes
HAND1 OMIM:602 406	5q33	Yes	Yes (Reamon-Buettner et al., 2008)	Yes (Asuthkar et al., 2016)	Yes	Yes
GATA4 OMIM: 600576	8p23	Yes	Yes (Reamon-Buettner et al., 2008)	Yes (Kondratyeva et al., 2016)	Yes	Yes (Moskowitz et al., 2011)
FOXC2 OMIM:602 402	16q24	Yes	Yes (Iascone et al., 2012)	Yes (Kume, 2012)	Yes	
S100B OMIM:176 990	21q22	Yes	Yes (Bokesch et al., 2002)	Yes (Xu et al., 2014)	Yes (Bokesch et al., 2002)	
JAM3 OMIM: 606871	11q25	Yes	Yes (Phillips et al., 2002)		Yes (Ebnet et al., 2003)	
NOTCH 1 OMIM:190 198	9q34.3	Yes	Yes (Garg et al., 2005)	Yes (Li et al., 2013)	Yes (Gridley, 2007; Wu et al., 2014)	
NR2F2 OMIM:107 773	15q26	Yes	Yes (Al Turki et al., 2014)	Yes (Zhang et al., 2014)		Yes (Lin et al., 2012b)
TBX5 OMIM:601 620	12q24.1	Yes	Yes (Shay et al., 2011)	Yes (Gros and Tabin, 2014)		Yes

**Table 1.** Summary of HLHS-related gene mutations in published case reports of HLHS. OMIM: Online mendelian inheritance in man.

### **1.1.3 Endocardial fibroelastosis in HLHS**

*Fetal EFE is one of the hallmarks of HLHS, which is characterized by a thick layer of fibro-elastic tissue in the left ventricular endocardium. EFE appears to play an important role in the HLHS pathological process (Friehs et al., 2012; Shimada et al., 2015). Generally, in the left ventricle of HLHS patients, a thick layer of EFE tissue is frequently observed to restrict the growth of myocardium. Abundant elastin and collagen fibers are also found in the thickened endocardium. Surgical removal of EFE tissue in HLHS patients will allow the myocardium to grow and a biventricular repair can be achieved in a subset of patients (Emani et al., 2012; McElhinney et al., 2010). EFE is also found in other left ventricular noncompaction (LVNC) related diseases (Ezon et al., 2012; Ozgur et al., 2011; Seki et al., 2013; Sjoberg et al., 2007) as well as in neonatal lupus, aortic stenosis or atresia and Barth Syndrome (Brito-Zeron et al., 2015; Capone et al., 2012).*

*Cardiac valves and septum are derived from the mesenchymal layer (called endocardial cushion) which is generated by the process of EndMT from endocardial cells in the atrioventricular canal. Hypoplastic (or stenotic) valves may suggest the developmental defect of endocardial cushion during embryonic heart formation (Hickey et al., 2012; Tripathi et al., 2012). In this process, abnormal EndMT of the endocardium contributes to the EFE occurrence in the endocardial layer of HLHS patient (Xu et al., 2015a; Zeisberg et al., 2009). Among all the reported HLHS mutated genes, many of them have been shown to play a role in endothelial cell biology in general or even EndMT/EMT (epithelial-mesenchymal transition) specifically (Xu et al., 2015a).*

## **1.2 EndMT**

### **1.2.1 EndMT in heart development**

*EndMT is a complex process, which is characterized by the acquisition of mesenchymal characteristics and loss of the endothelial properties. EndMT is*

*considered as a form of EMT. EMT is an evolutionary conserved process, during which epithelial cells gradually develop mesenchymal-like cell features (Kalluri and Weinberg, 2009). During EMT or EndMT, original cells gradually acquire the properties of migratory, invasiveness, and resistance to apoptosis. Both EMT and EndMT are vital mechanisms for embryonic development (Kovacic et al., 2012).*

*Fetal heart as a life indicator is the first functional organ of human life during pregnancy (Bruneau, 2013). EndMT is known to play an important role in embryonic heart formation (Eisenberg and Markwald, 1995; Guan and Couldwell, 2013; Lin et al., 2012a), for instance, heart valves formation. Heart valves originate from the endocardial cushion of heart (Xiong et al., 2012). During early heart development, endocardium and myocardium are separated by cardiac jelly (Kovacic et al., 2012). Endothelial cells undergo EndMT process and transform into mesenchymal cells. The mesenchymal cells generated from EndMT invade the cardiac jelly to form endocardial cushion tissue in atrioventricular canal and out flow tract (Markwald et al., 1977). Semi-lunar valves are developed from endocardial cushion in outflow tract, while mitral and tricuspid valves are generated from endocardial cushion tissue in atrioventricular canal (Kisanuki et al., 2001; Kovacic et al., 2012; Thiery et al., 2009).*

### **1.2.2 EndMT in pathological process**

*All chronic heart diseases are associated with cardiac fibrosis. In the experimental cardiac fibrosis model of ascending aortic constriction, approximately 30% of pathologic cardiac fibroblasts have been shown to be generated by EndMT (Zeisberg et al., 2007b). EndMT contributes to fibrosis generation in two ways: fibroblast proliferation and microvascular rarefaction (Krenning et al., 2010; Zeisberg et al., 2008; Zeisberg et al., 2007b). Cardiac fibrosis causes increased stiffness of the heart and is a hallmark of diastolic dysfunction (Beggah et al., 2002; Burlew and Weber, 2002). Fibrosis found in other organs such as the kidney, lung or gut suggests that the etiological mechanisms of fibrosis formation are similar,*

*which is generated by abnormal EndMT, EMT or activation of fibroblast progenitors (Figure 2) (Hashimoto et al., 2010; Krenning et al., 2010; Rieder et al., 2011; Zeisberg et al., 2008; Zeisberg et al., 2007b). EndMT also contributes to the pathological process of cancer-associated myofibroblast generation (Zeisberg et al., 2007a; Zeisberg et al., 2007b).*

*Cardiac fibrosis is further commonly observed in patients with chronic kidney disease (CKD) (Lopez et al., 2008). CKD patients have high risks of developing cardiovascular disease, and therefore high mortality (Charytan et al., 2014). A series of mechanical and circulating factors that deteriorate kidney functions of CKD patients may also be responsible for the development of cardiovascular disorders. According to existing studies, serological factors, e.g. the circulating angiogenesis and nitric oxide (NO) inhibitors are potential triggers for the linkage between CKD and heart disease (Bhandari et al., 2012; Chen et al., 2012; Fleck et al., 2001; Reinecke et al., 2013; Wang et al., 2015). The causative effects between aforementioned risk factors and CKD have been demonstrated in animal models (Amann et al., 1997; Jacobi et al., 2006). The pathogenic concentrations of these serological factors in CKD could induce the susceptibility of EndMT that trigger several downstream effects such as microvascular rarefaction and fibroblast accumulation. Abnormal concentration of circulating factors in CKD patient's blood could induce not only the pathological change of human myocardial but also fibrosis generation (Charytan et al., 2014). Although evidence has been accumulated from decades of studies, the connection between chronic kidney disease and cardiovascular disease has still not been fully elucidated.*

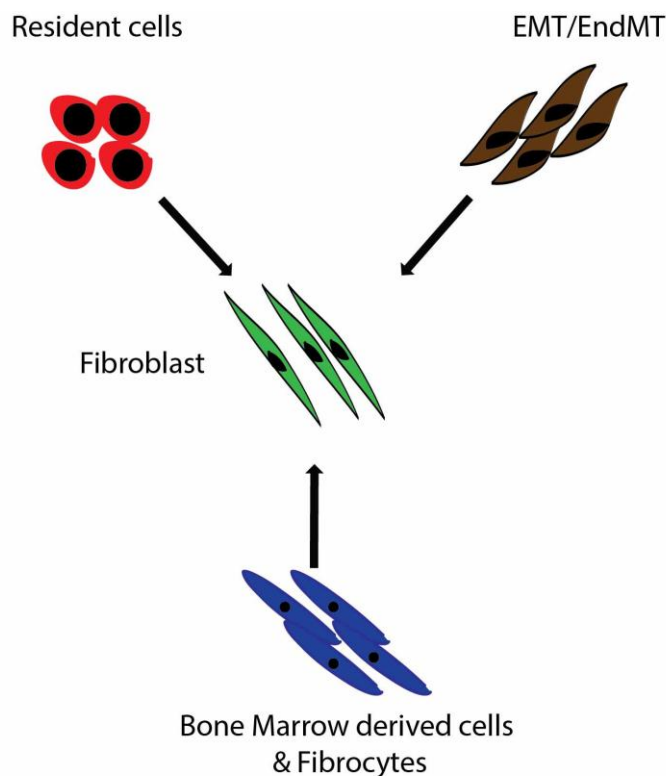


### Figure 2. Origins of cardiac fibrosis.

During the formation of cardiac fibrosis, the outside stimulus could trigger the resident or quiescent fibroblast to proliferate. EMT or EndMT could also react to the heart injuries and contribute to the cardiac fibrosis. Bone marrow derived cells are recruited to the injury site and differentiate into fibroblast.

### 1.2.3 Molecular mechanisms of EndMT

Plasticity of endothelial cells plays an important role in both heart development and pathological conditions like cardiac fibrosis. A large number of stimuli are proved to induce EndMT including  $TGF\beta$  proteins, inflammatory factors, hypoxia, and even microRNAs. These stimuli can trigger the EndMT process by different signaling pathways, which are not mutually exclusive. In particular,  $TGF\beta 1$  and  $TGF\beta 2$  are the most commonly known cytokines associated with both Smad-dependent and Smad-independent pathways (Medici et al., 2011; Piera-Velazquez et al., 2011; van Meeteren and ten Dijke, 2012). In addition, interferon- $\gamma$  could induce EndMT by increasing the  $TGF\beta 2$  level that could lead to fibrogenesis. Also, ischemia and injury associated hypoxia can activate the  $TGF\beta$  proteins by hypoxia inducible factor-1 $\alpha$  (HIF-1 $\alpha$ ) (Choi et al., 2015a; Xu et al., 2015c). Several specific



*microRNAs are reported to be involved in EndMT. MiR-9, miR-21 and miR-31 regulate the endothelial cell transition by controlling the secretion of different cytokines, e.g. tumor necrosis factor- $\alpha$  (TNF- $\alpha$ ) and TGF $\beta$ s (Chakraborty et al., 2015; Katsura et al., 2016; Kumarswamy et al., 2012).*

*In particular, studies of cardiac pressure overload-induced mouse models have demonstrated that TGF $\beta$  pathways play crucial roles in cardiac fibrosis generation and pathological EndMT (Kovacic et al., 2012; Xu et al., 2015b; Zeisberg et al., 2007b). TGF $\beta$ 1 and TGF $\beta$ 2 are the most powerful known pro-fibrotic inducers of EndMT. Furthermore, inhibition of the TGF $\beta$ s has been shown to promote endothelial cell proliferation during endothelial cell differentiation in vitro (Atkins et al., 2011b; James et al., 2010). Upon TGF $\beta$ 1 or TGF $\beta$ 2 stimulation, several transcriptional factors (SNAIL, SLUG, ZEB1, and TWIST1) have been implicated as the downstream targets (Peinado et al., 2007; Peinado et al., 2004; Saito, 2013). Among these transcriptional factors, SNAIL and SLUG have been demonstrated to be the key regulators during the EndMT or EMT, which are up-regulated during TGF $\beta$ 1 or TGF $\beta$ 2 stimulation (Cooley et al., 2014; Lin et al., 2012a).*

*Recently, several reports show that hypoxia is another inducer of EndMT (Choi et al., 2015b; Higgins et al., 2008; Xu et al., 2015c). Hypoxia is a condition where cells and tissues have insufficient oxygen supply and undergo a series of changes of their morphology and function. HIF-1 is a highly-conserved heterodimeric complex, composed by an alpha and a beta subunit. Once heart injury occurs, the environment becomes hypoxic, and oxygen shortage activates HIF-1 $\alpha$ , a transcription factor responsible for stimulating expression of endothelial growth factors to induce EndMT (Medici and Kalluri, 2012; Xu et al., 2015c). HIF-1 $\alpha$  binding to HIF-responsive elements (HREs) causes the stimulation of cascade response mediators of hypoxia. SNAIL has been shown as the direct mediator of hypoxia to induce EndMT (Xu et al., 2015c).*

### **1.3 Disease-specific hiPSCs and endothelial cell generation**

#### **1.3.1 Disease-specific human iPSCs**

*hiPSC disease models hold great potential for advancing our understanding of the pathogenic mechanisms in various diseases. iPSCs are firstly generated by introducing four ectopic expression transcription factors, Oct3/4, Sox2, Klf4 and c-Myc (these four transcription factors are also commonly known as Yamanaka factors) to mouse or human fibroblasts (Takahashi et al., 2007; Takahashi and Yamanaka, 2006; Yu et al., 2007). Like all other pluripotent stem cells, iPSCs have the abilities of long term self-renewal and differentiation into all derivatives of three germ layers (ectoderm, mesoderm, and endoderm) (Drawnel et al., 2014; Ebert et al., 2012).*

*Various methods have been established to generate iPSCs including integration-free DNA virus, RNA virus, synthetic mRNA, recombinant protein and even small molecules compounds (Fusaki et al., 2009; Hou et al., 2013; Kim et al., 2009; Liu et al., 2016; Liu et al., 2013; Warren et al., 2010; Zhou et al., 2009). Different sources of somatic cells have also been used to generate hiPSCs, for example, dermal fibroblast, hair follicle cells, blood peripheral mononuclear cells and even epithelial cells excreted within the urine (Streckfuss-Bomeke et al., 2013; Zhou et al., 2012).*

*hiPSCs can potentially provide an unlimited supply of cell source to avoid the ethical dilemmas involving the use of human embryonic stem cells (hESCs), thus it is a suitable approach for modeling diseases and drug screening. However, one of the limitations for hiPSCs application is the lack of stable differentiation protocol of endothelial cells. In vitro remodeling the dysfunctional ECs are promising for unmasking the underlying pathogenic mechanism of human vascular diseases and disease associated with EFE such as HLHS (Adams et al., 2013).*

### 1.3.2 Endothelial cell generation from hiPSCs

*In the process of in vivo vasculogenesis, endothelial cells are believed to be generated from angioblasts which are derived from mesodermal layer origin (Belaousoff et al., 1998; Marcelo et al., 2013; Vokes and Krieg, 2002). Several reports show that short-term treatment with CHIR in a high concentration or long term treatment in a low-concentration can both generate the mesodermal cell from hiPSCs (Borchin et al., 2013; Lian et al., 2012; Lian et al., 2013). CHIR mediated  $\beta$ -catenin phosphorylation is an important step of Wnt/ $\beta$ -catenin signaling activation, which stimulates mesoderm differentiation (Denham et al., 2012; Lian et al., 2013; Wu et al., 2013). In the first stage of EC differentiation, some pan-mesodermal markers are significantly upregulated after the treatment with CHIR, for instance, BRACHYURY (T) and ACTA2 (Tan et al., 2013; Yang et al., 2008).*

*From previous studies, cytokines are observed to play an important role in differentiation of different progenitor lineages (Yang et al., 2008). Fibroblast growth factor 2 (FGF2 or bFGF) has been shown to induce mesodermal cell differentiation by targeting FGF receptor (Marom et al., 2005; Saxton and Pawson, 1999). BMP4 initiates the EC differentiation and interacts with a FGF2-dependent progress to regulate the specification of angioblasts (Hirashima, 2009; Marcelo et al., 2013; Pearson et al., 2008; Yamaguchi et al., 1994). Vascular endothelial growth factor (VEGF) signaling regulates numerous endothelial transcription factors both in vitro and in vivo. VEGF exerts its angiogenic function in the generation of endothelial cells and endothelial precursors usually through attributing to VEGFR1 and VEGFR2 activation (Yan et al., 2008). ACTIVIN A is believed to be involved in the process of cardiac vasculogenesis, which is reported in several protocols of endothelial cell differentiation (Chiang and Wong, 2011; McLean et al., 2007; Wu et al., 2015). Proper combinations of chemicals and cytokines could enable the specification of endothelial cells (Atkins et al., 2011a; Cao et al., 2013; Kume, 2010; Li et al., 2011b; Li et al., 2009).*

*For functional characterization of hiPSC-ECs, one of the most widely accepted methods is in vitro endothelial tube formation assay (Li et al., 2011a; Li et al., 2009). In this assay, capillary-like structures generates a hollow network of connecting tubes, representing the in vivo angiogenesis capability of endothelial cells. Another EC functional assessment is the low-density lipoprotein (LDL) uptake assay. LDL receptors mediated LDL uptake plays a key role in the cellular cholesterol level (Voyta et al., 1984). By the spheroid sprouting assay, the ability of self-aggregation of endothelial cells could be evaluated in in vitro three-dimension way (Glaser et al., 2011; Li et al., 2011a).*

#### **1.4 Aims and objectives**

*The overall aim of this thesis was to test if endothelial cells generated from HLHS-hiPSCs (HLHS-hiPSC-ECs) have a higher susceptibility to undergo EndMT as compared to endothelial cells generated from hiPSCs from healthy individuals (WT-hiPSC-ECs). For this purpose the individual objectives were:*

- 1. To establish a highly efficient, easy and cost effective endothelial cell differentiation method.*
- 2. Generation of hiPSCs from patients with HLHS.*
- 3. To test different stimuli of EndMT, such as TGF $\beta$  and hypoxia, in HLHS-hiPSC-ECs versus WT-hiPSC-ECs in EndMT assays in vitro.*

## 2. Original Publications

*The following manuscripts have been published before the submission date of this thesis.*

### **1. Differentiation of functional endothelial cells from human induced pluripotent stem cells: a novel, highly efficient and cost effective method.**

**Liu X**, Qi J, Xu X, Zeisberg M, Guan K, Zeisberg EM.

*First author*

*Differentiation. 2016. DOI: 10.1016/j.diff.2016.05.004*

### **2. Epigenetic balance of aberrant Rasal1 promoter methylation and hydroxymethylation regulates cardiac fibrosis.**

Xu X, Tan X, Tampe B, Nyamsuren G, **Liu X**, Maier LS, Sossalla S, Kalluri R, Zeisberg M, Hasenfuss G, Zeisberg EM.

*Coauthor*

*Cardiovasc Res. 2015. DOI: 10.1093/cvr/cvv015*

### **3. Increased concentration of circulating angiogenesis and nitric oxide inhibitors induces endothelial to mesenchymal transition and myocardial fibrosis in patients with chronic kidney disease.**

Charytan DM, Padera R, Helfand AM, Zeisberg M, Xu X, **Liu X**, Himmelfarb J, Cinelli A, Kalluri R, Zeisberg EM.

*Coauthor*

*Int J Cardiol. 2014. DOI: 10.1016/j.ijcard.2014.06.062*

## **2.1 Differentiation of functional endothelial cells from human induced pluripotent stem cells: a novel, highly efficient and cost effective method**

*hiPSCs generated from patients carry identical genetic information as in the patients, which may re-implement the disease phenotype in vitro. Functional endothelial cells derived from patient-specific hiPSCs are a promising model to study the cardiac vascular disease. In this part, a highly efficient differentiation method of functional endothelial cells was established. At first, hiPSCs were treated with CHIR for 2 days to generate the mesoderm cells. Following, different combinations of cytokines were used to differentiate mesoderm cells into endothelial cells. At last, the derived CD31 and VE-cadherin double-positive endothelial cells were enriched and cultivated for further analysis. hiPSC-ECs showed similar properties with human coronary artery endothelial cells (HCAEC), including uptake of low-density, formation of capillary-like tubes and angiogenic sprouting from spheroids. Here, the differentiation efficiency of endothelial cells is as high as 80% within 12 days by the indication of double staining of CD31 and VE-cadherin. Comparing with former reported protocols, this protocol is superior in generating endothelial cells with respect to both cost and time.*

### **2.1.1 Declaration of my contribution**

*Xiaopeng Liu: conceived and designed this study, performed experiments, data analysis, data interpretation, and help of drafting the manuscript.*

*Prof. Dr. Elisabeth Zeisberg: conceived and designed this study, data interpretation, drafted the manuscript.*

*Prof. Dr. Kaomei Guan: conceived and designed this study, data interpretation.*

*Prof. Dr. Michael Zeisberg: drafted the manuscript.*

*Jing Qi: conceived and designed this study, performed experiments, data analysis, and data interpretation.*

*Xingbo Xu: data analysis, data interpretation.*



Contents lists available at ScienceDirect

Differentiation

journal homepage: [www.elsevier.com/locate/diff](http://www.elsevier.com/locate/diff)

## Differentiation of functional endothelial cells from human induced pluripotent stem cells: A novel, highly efficient and cost effective method

Xiaopeng Liu<sup>a</sup>, Jing Qi<sup>a</sup>, Xingbo Xu<sup>a,c</sup>, Michael Zeisberg<sup>b,c</sup>, Kaomei Guan<sup>a,d,1</sup>, Elisabeth M. Zeisberg<sup>a,c,\*</sup>

<sup>a</sup> Department of Cardiology and Pneumology, University Medical Center of Göttingen, Georg August University, 37075 Göttingen, Germany

<sup>b</sup> Department of Nephrology and Rheumatology, University Medical Center of Göttingen, Georg August University, 37075 Göttingen, Germany

<sup>c</sup> DZHK (German Centre for Cardiovascular Research) Partner Site Göttingen, 37075 Göttingen, Germany

<sup>d</sup> Department of Pharmacology and Toxicology, TU Dresden, 01307 Dresden, Germany

### ARTICLE INFO

#### Article history:

Received 13 November 2015

Received in revised form

26 April 2016

Accepted 13 May 2016

#### Keywords:

hiPSC

EC

Highly efficient differentiation method

### ABSTRACT

Endothelial cells derived from human induced pluripotent stem cells (hiPSC-EC) are of significant value for research on human vascular development, *in vitro* disease models and drug screening. Here we report an alternative, highly efficient and cost-effective simple three step method (mesoderm induction, endothelial cell differentiation and endothelial cell expansion) to differentiate hiPSC directly into endothelial cells. We demonstrate that efficiency of described method to derive CD31<sup>+</sup> and VE-Cadherin<sup>+</sup> double positive cells is higher than 80% in 12 days. Most notably we established that hiPSC-EC differentiation efficacy depends on optimization of both mesoderm differentiation and endothelial cell differentiation steps.

© 2016 International Society of Differentiation. Published by Elsevier B.V. All rights reserved.

### 1. Introduction

Endothelial cells line the entire circulatory system, from the heart to capillaries and lymphatics. Due to their widespread distribution and their vast array of biological functions, endothelial cells are indispensable for development and growth and they play central roles in numerous diseases, ranging from congenital heart disease, to cancer and diabetes mellitus (Hink et al., 2001; Moretti et al., 2013). Despite such prominent interest in endothelial cell biology, studies involving cultured endothelial cells are still challenging, because it is difficult to generate primary endothelial cells from adult organs in substantial quantities, because endothelial cell lines de-differentiate and do not lend themselves for representative cell assays and because the derived endothelial cells often do not represent the intricate organ- and vessel type-specific phenotype encountered *in vivo*. Such limitations are even more concerning when studying genetic diseases, where derivation of

isogenic endothelial cells is essential for meaningful experiments.

In this regard differentiating induced pluripotent stem (iPS) cells *in vitro* holds promise to solve these limitations, because iPS cells could be amplified unlimitedly *in vitro* in a chemically defined system (Chen et al., 2011; Orlova et al., 2014). As for endothelial cell generation from human pluripotent stem cells, currently two different principles are commonly used: embryoid body (EB) formation and monolayer differentiation (Table 1) (Lian et al., 2014; Orlova et al., 2014; Patsch et al., 2015; Sahara et al., 2014; Tatsumi et al., 2011; Yang et al., 2008). All fore-mentioned groups developed their unique protocols to successfully generate endothelial cells, although with various time and cost efficiency.

Here, we report a highly efficient, consistent, and cost effective protocol for generation of cells with phenotypic and functional properties of endothelial cells from hiPSCs. We achieved this through optimization of cell density and colony size for mesodermal differentiation, and optimization of growth factors for mesodermal to endothelial differentiation.

### 2. Material and methods

#### 2.1. Cell culture

Human induced pluripotent stem cells (hiPSCs) used here were previously established and characterized (Dudek et al., 2013;

**Abbreviations:** iPSC, induced pluripotent stem cell; hiPSC, human induced pluripotent stem cell; iPSC-EC, induced pluripotent stem cell-derived endothelial cell; EC, endothelial cell; HCAEC, human coronary artery endothelial cells; vWF, von Willebrand factor; Ac-LDL, acetylated-low density lipoprotein

\* Corresponding author at: Department of Cardiology and Pneumology, University Medical Center of Göttingen, Georg August University, 37075 Göttingen, Germany.

E-mail address: [elisabeth.zeisberg@med.uni-goettingen.de](mailto:elisabeth.zeisberg@med.uni-goettingen.de) (E.M. Zeisberg).

<sup>1</sup> Equal contribution as last authors.

<http://dx.doi.org/10.1016/j.diff.2016.05.004>

Join the International Society for Differentiation ([www.isdifferentiation.org](http://www.isdifferentiation.org))

0301-4681/© 2016 International Society of Differentiation. Published by Elsevier B.V. All rights reserved.

Please cite this article as: Liu, X., et al., Differentiation of functional endothelial cells from human induced pluripotent stem cells: A novel, highly efficient and cost effective method. *Differentiation* (2016), <http://dx.doi.org/10.1016/j.diff.2016.05.004>



**Table 1.** Comparison of different EC differentiation protocols.

Publications	Highest Efficiency	Enrichment needed	Duration	Reagents	Estimated cost <sup>a</sup>
Yang et al. (2008)	30% CD31+ Endothelial Progenitors	Indirect Differentiation; Enrichment needed	14 days	BMP4, F12 bFGF, Activin A, StemPro34, VEGFA	~40 Euros
Tatsumi et al. (2011)	20% CD144+ VEGFR2+ Endothelial Progenitors	Indirect Differentiation; Enrichment Needed	5 days	ES medium, DMEM/F12, N2/B27, BIO Stem pro34, VEGFA	~32 Euros
Orlova et al. (2014)	19.9% CD31+ CD144+ Endothelial cell	Direct Differentiation; No enrichment	10 days	BPEL/APEL, Activin A, BMP4, VEGF, SB431542	~120 Euros
Sahara et al. (2014)	64.3% CD31+ CD144+ Endothelial cell	Direct Differentiation; No enrichment	7 days	ROCK inhibitor N2/B27, DMEM/F12, StemPro-34, BMP4, VEGFA	~44 Euros
Lian et al. (2014)	Protocol 1: 20.55% CD31+ CD34+ Endothelial Progenitors	Direct Differentiation; No enrichment	5 days	Advanced DMEM/F12, Ascorbic acid, GlutaMAX, CHIR99021, StemPro-34, VEGFA	Protocol1 ~42 Euros, Protocol2 ~12 Euros
Patsch et al. (2015)	69.2% CD144+ Endothelial Progenitors	Direct Differentiation; No enrichment	6 days	StemPro-34, 200 ng ml <sup>-1</sup> VEGF-A, 2 μM forskolin, N2/B27, 8 μM CHIR, 1 μM CP21, 25 ng/ml BMP4	~100 Euros
Our protocol	81% CD31+ CD144+ Endothelial cell	Direct Differentiation; No enrichment	10 days	DMEM/F12, CHIR, EBM, VEGFA, bFGF, EMV2	28 Euros

<sup>a</sup> Listed reagents and cost from different protocols compared to ours. The estimated cost is calculated from induction of one complete 6-well plate (2 ml medium per well) hiPSCs into desired cell types (endothelial progenitors or endothelial cells). Detailed information on the companies from which prices for reagents were used is provided in the supplementary information.

Streckfuss-Bomeke et al., 2013) (Table S6). hiPSC were maintained in Essential 8 basal medium (Gibco Life Technologies) supplemented with Essential 8 Supplement (Gibco Life Technologies), and Penicillin-Streptomycin (Sigma-Aldrich). hiPSCs were cultured on Geltrex Reduced Growth Factors (Millipore) coated tissue culture dishes, and treated with Versene solution (Life technology) for passaging. Human Coronary Artery Endothelial Cells (HCAEC) were cultured in HCAEC growth medium (GENLANTIS) on the attachment factor coated (GENLANTIS) flasks. All cultured cells were kept in standard physical growth conditions (37 °C, 5% CO<sub>2</sub>).

## 2.2. In vitro ECs differentiation methods

hiPSCs were seeded onto Geltrex coated dishes and cultured with Essential 8 Medium supplemented with pro survival factor (Millipore), which is cell-permeable pyrrolidine, a small molecule which promotes single human iPSC cell or stem cell survival. To determine the size of the hiPSC colonies, fully confluent hiPSC layers were examined under the microscope at day 0 and colony sized was measured by using the AxioVision microscope software (Carl Zeiss). The colonies were gently scraped off from the dish and seeded onto Matrigel coated dishes. When cells had attached after 24 h, medium was changed to DMEM/F12 supplemented with 4 μM Chir99021 (Millipore). After 2 further days, medium was replaced with Endothelial cell basal medium (Promocell) supplemented with growth factors bFGF (Peprotech) and VEGFA (R&D) or Activin A (Peprotech) and BMP4 (Peprotech). After four further days, medium was replaced with EMV2 (Promo cell) medium supplemented with VEGFA, and medium was changed every other day until cell analysis. Experimental set-up is summarized in Fig. 1(A).

## 2.3. Flow cytometry and Fluorescence-activated cell sorting (FACS)

hiPSC derived endothelial cell progenitors were harvested after trypsin-EDTA digestion and washed in cold PBS. Pellets were resuspended in 2% v/v bovine serum albumin (BSA), cell suspensions were standardized to a concentration of  $1 \times 10^6$  cells/ml. After cells were incubated at 37 °C incubator for 30 min to allow for recovery from trypsinization, directly-labeled antibodies were added to cell suspensions (PE conjugated CD 31 antibody (BD Pharmingen) and Alexa Fluor 647 conjugated VE-cadherin antibody (BD Pharmingen)). After 1 h incubation, samples were centrifuged and supernatants decanted. Cells were then resuspended in ice-cold FACS buffer to final concentrations of  $1 \times 10^6$  cells/ml. Cells were then filtered through 100 μm cell strainers and fixed in 4% PFA for 5 min at room temperature for FACS analysis. For cell sorting experiments, all samples were blocked in blocking buffer with 5% BSA for 1 h before antibody was added, and incubated at 37 °C for 2 h (for living cell sorting) or 4 °C overnight (only for fixed cells). After PBS washing for three times, cell concentration was adjusted to  $1 \times 10^6$  cells/ml for FACS sorting.

## 2.4. Culture of FACS-isolated cell populations

FACS-sorted CD31+ and VE-cadherin+ double positive cells were plated onto tissue culture plates coated with attachment factor (GENLANTIS) in Endothelial Cell growth medium (EMV2) supplemented with 15 ng/ml VEGFA. Once settled, sorted cells were cultured in EMV2 growth medium until passage 3 for functional analysis.

## 2.5. Immunofluorescence labeling of adherent cells

Cells growing in chamber slides were fixed by 4% paraformaldehyde, permeabilized in 0.1% TritonX-100 for 10 min and blocked in 5% BSA for 30 min before antibodies were added.



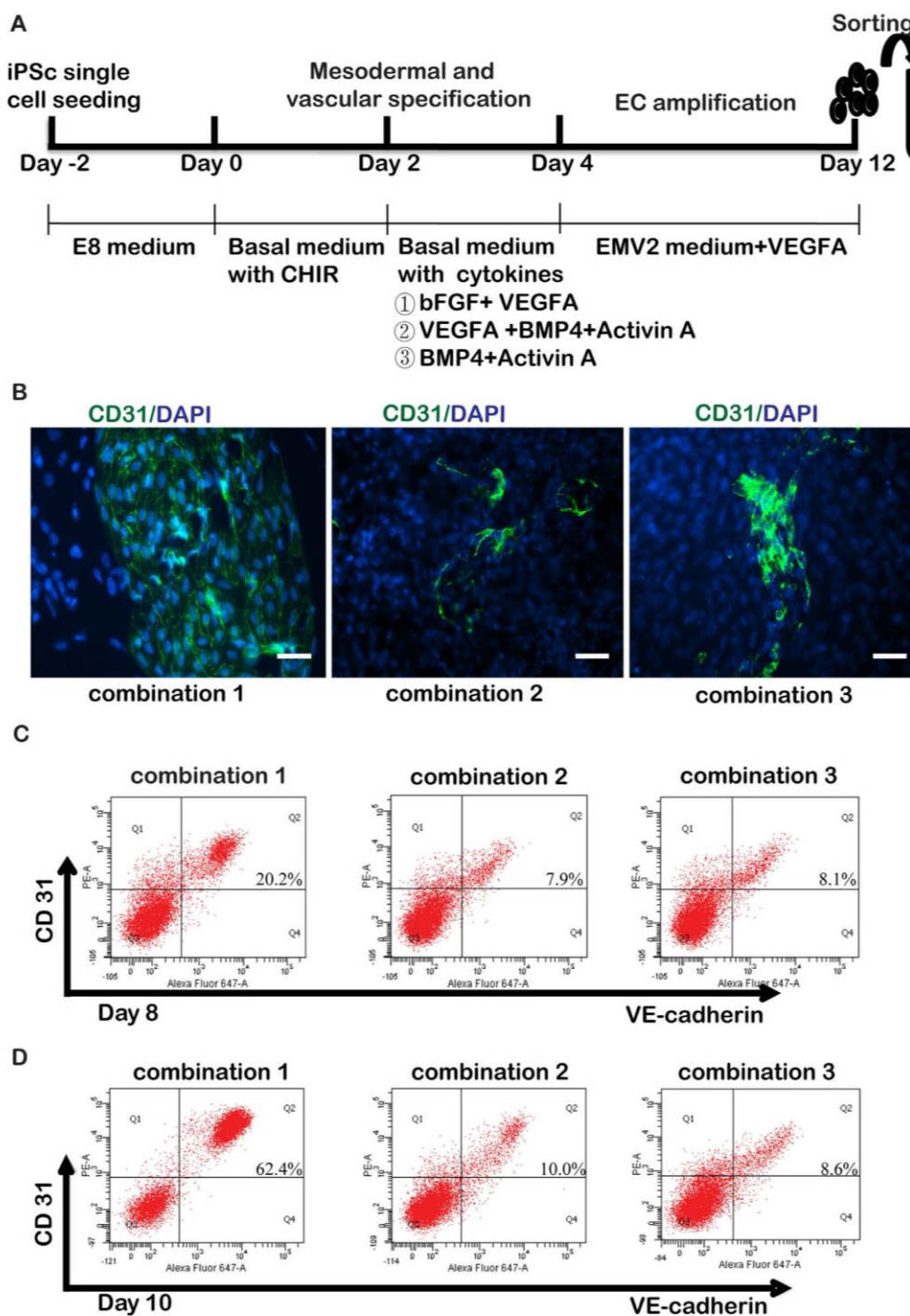


**Fig. 1. Endothelial cells derived from human induced pluripotent stem cells.** A. Schematic illustration of experimental design. hiPSCs were seeded at low density and maintained in E8 medium until single colonies had established (day -2 to day 0). For mesodermal specification, hiPSCs were exposed for two days to basal medium supplemented with CHIR (day 0 to day 2). For endothelial specification hiPSCs were then exposed for two days to basal medium supplemented with different combinations of cytokines as indicated (day 2 to day 4). Upon endothelial specification, cells were maintained for eight days in EMV2 medium supplemented with VEGFA (day 4 to day 12) and subsequently analyzed. B. CD31 immunolabeling. Upon completion of endothelial cell differentiation protocols, cells were immunolabeled with antibodies to CD31 (green). The pictures display representative immunofluorescence micrographs of each group. Scale bar: 50  $\mu$ m. C. FACS analysis after 8 days of differentiation protocol, hiPSC-ECs were labeled with antibodies to endothelial markers CD31 (PECAM1) and VE-cadherin (CDH5) at day 8. The graphs display representative scatter plots of each group. D. FACS analysis after 10 days of differentiation protocol. Endothelial markers CD31 (PECAM1) and VE-cadherin (CDH5) were analyzed by FACS at day 10. Differentiation was performed at an initial cell density of  $2.5 \times 10^4$  per well without control of colony size (which ranged from  $< 60 \mu$ m to  $> 200 \mu$ m). The data were generated from two independent hiPSCs cell lines (WTBLD and WTD2) and showed consistency between the different cell lines.

Primary antibodies used were specific for CD31 (Dako), VE-cadherin (Cell Signal Tech), von Willebrand factor (vWF, Abcam). Secondary antibodies used were goat anti-Rabbit Alexa Fluor 546 (Life Technologies), goat anti-mouse Alexa Fluor 546 (Life Technologies), goat anti-mouse Alexa Fluor 488 (Life Technologies), goat anti-rabbit Alexa Fluor 488 (Life Technologies). Staining was analyzed by fluorescence microscopy (Carl Zeiss) with 20x magnification.

#### 2.6. RNA isolation and quantitative real-time PCR

RNA was extracted from hiPSC-ECs and HCAEC using the Trizol (Invitrogen) and reverse transcribed using SuperScript reverse transcriptase (RT) kit (Invitrogen) according to manufacturers' recommendations. Real-time polymerase chain reaction (qPCR) was carried out using SYBR Master Mix kit (Applied Biosystems) on an ABI StepOne PCR instrument (Applied Biosystems). Analysis was conducted using the CT method (according to the Applied Biosystems protocol Performing Relative Quantitation of Gene Expression Using Real-Time Quantitative PCR). The list of primers used in this study is available in Supplementary Table S1.

#### 2.7. Acetylated-low density lipoprotein (Ac-LDL) uptake assay

Sorted hiPSC-ECs or HCAEC were seeded in 24-well cell culture plates at densities of  $10 \times 10^4$  per well in endothelial cell growth medium. After removing the culture medium and washing for three times with PBS, 2.5  $\mu\text{g}/\text{ml}$  DiI-labelled Ac-LDL was added and incubated at 37 °C for 1 h. Cells were then washed with PBS, fixed with 4% PFA and analyzed using a fluorescence microscope.

#### 2.8. Vascular tube formation assay

Growth factor-reduced Matrigel (Millipore) was added into a 48-well plate and kept in 37 °C incubator to solidify the Matrigel for 1 h. Sorted hiPSC-ECs or HCAEC were seeded onto solidified Matrigel ( $3 \times 10^4$  cells per well in endothelial cell growth medium) and incubated at 37 °C for 12 h to allow for tube formation.

#### 2.9. Spheroid angiogenesis assay

To generate spheroids, a total of  $4 \times 10^4$  sorted hiPSC-ECs or HCAEC were suspended in cell type-dependent growth medium containing 20% methyl cellulose (Sigma-Aldrich) solution supplemented with Penicillin/Streptomycin (P/S) and incubated in round-bottom 96-well plates at 37 °C for 24 h. Type I rat-tail collagen (BD Biosciences) was mixed with 0.1% acetic acid in a 1:1 dilution (v/v), mixed with 10 x M199 medium (in a ratio of 9: 1 v/v), and neutralized with 0.2 N NaOH. Spheroids were harvested in methylcellulose solution and suspended in 24-well plates (containing about 40 spheroids per well) and incubated at 37 °C for 30 min. After incubation, 100  $\mu\text{l}$  of endothelial cell growth medium were added and cell samples were incubated in a 37 °C incubator for 24 h. Sprouting measurement results are available in supplementary data Table S5.

#### 2.10. Statistical analysis

Student's *t* test was used to compare the statistical differences between different samples, *p* values  $<=0.05$  were considered significant.

### 3. Results

#### 3.1. Co-stimulation with vascular endothelial growth factor-A and basic fibroblast growth factor is an optimal stimulus to differentiate

#### hiPSC mesodermal cell to endothelial cell progenitors

Based on defined factors which have been shown to promote embryoid body endothelial differentiation, we hypothesized that these factors could also enhance endothelial monolayer differentiation (Yang et al., 2008). Besides, it has been found that *in vitro* endothelial cell differentiation starts from mesodermal cells induced by activation of WNT/ $\beta$ -catenin (by addition of CHIR). Sequentially other factors have been demonstrated to promote mesoderm to endothelial cell transition. We therefore tested if different combinations in embryoid body endothelial differentiation might enable optimization of the monolayer direct endothelial cell differentiation (Lian et al., 2014; Yang et al., 2008). We first established a three-step protocol, consisting of a mesodermal differentiation step, a mesodermal cell to endothelial progenitor differentiation to endothelial cell differentiation step and finally an endothelial cell expansion step (Fig. 1(A)). For maintenance, hiPSCs were cultured on Matrigel-coated plates with ES cell culture Essential 8 medium (the commonly used xeno-free and feeder-free medium specially formulated for the growth and expansion of human pluripotent stem cells) until cells were fully confluent. To prepare hiPSCs for differentiation, cells were passaged at low density to obtain "super small colonies" (diameter from 30  $\mu\text{m}$  to 280  $\mu\text{m}$ ) and maintained in E8 medium supplemented with Pro Survival Factor (PSF) for 48 h (Bauwens et al., 2008; Rosowski et al., 2015).

During the process of vasculogenesis, preliminary vascular endothelial progenitor cells are believed to originate from angioblasts generated from mesoderm (Belousoff et al., 1998; Marcelo et al., 2013; Vokes and Krieg, 2002; Yang et al., 2008). Thus, generation of pure mesoderm cells is essential for derivation of endothelial progenitor cells to be differentiated into all types of endothelial lineages. Generation of pure mesoderm cells was initiated by switching the E8 medium to serum-free Endothelial Basal Medium (EBM) supplemented with GSK-3 $\beta$  inhibitor CHIR 99021 (CHIR) (Lian et al., 2014). Thereby, the morphology of hiPSCs gradually changed into mesodermal progenitor cell shape through activating the WNT/  $\beta$ -Catenin signaling pathway, as previously described (Supplementary Fig. 1) (Davidson et al., 2012; Lian et al., 2012).

We next aimed to establish a protocol to effectively differentiate mesodermal cells to endothelial progenitor cells. Based on existing literature, we decided to follow a two-step strategy in which induction of endothelial cell differentiation (for 48 h) was followed by an expansion step of endothelial progenitor cells by cultivation within endothelial cell growth medium MV2 (EMV2 medium) supplemented with VEGFA (vascular endothelial growth factor-A) for six to eight days (Lian et al., 2014; Lian et al., 2012; Marcelo et al., 2013; Sahara et al., 2014; Yang et al., 2008) (Fig. 1(A)).

For differentiation of mesodermal cells into endothelial cells via endothelial cell progenitors, we aimed to compare different combinations of growth factors which had been implied in this process either in embryonic vasculogenesis (where angioblasts derive from mesoderm and then give rise to vascular progenitor cells) or in previously established differentiation protocols (Bao et al., 2015; Orlova et al., 2014; Rufaihah et al., 2013). In this regard, basic fibroblast growth factor (FGF2 or bFGF) and bone morphogenetic protein 4 (BMP4) are known to promote specification of mesoderm (Marom et al., 2005; Saxton and Pawson, 1999) and endothelial cell progenitor *in vitro* (Hirashima, 2009; Marcelo et al., 2013; Yamaguchi et al., 1994). Vascular endothelial growth factor (VEGF) exerts its angiogenic function in endothelial cells and endothelial precursors by attributing to VEGFR1 (vascular endothelial growth factor receptor 1) and VEGFR2 activation (Yan et al., 2008). As a member of the TGF  $\beta$  superfamily, Activin A was reported to induce cardiomyogenesis together with BMP4 (Kim et al., 2015;



Teo et al., 2012). bFGF and VEGFA, which stimulate different vascular downstream genes expression profiles (Jih et al., 2001), were previously demonstrated to induce endothelial cell differentiation (Li et al., 2011; Li et al., 2009).

Based on these studies, we compared three different media for endothelial progenitor cell differentiation: Endothelial Basal Medium (EBM) supplemented with 5 ng/ml bFGF and 10 ng/ml VEGFA ("combination 1"), EBM supplemented with 10 ng/ml VEGFA, 4 ng/ml BMP4 and 15 ng/ml Activin A ("combination 2") and EBM supplemented with 4 ng/ml BMP4 and 15 ng/ml Activin A ("combination 3"). Upon exposure for 48 h to different "combinations", we expanded cells in EMV2 medium supplemented with VEGFA before comparing efficacies to induce endothelial cell differentiation among different protocols.

Explorative analysis of cultured cells by immunofluorescence-labeling with antibodies to the endothelial cell marker CD31 revealed robust CD31 immunolabeling in cells which had been exposed to "combination 1" (bFGF and VEGF-A) and only modest staining in cells which had been exposed to "combination 2" (VEGF, BMP4 and Activin A) or "combination 3" (BMP4 and Activin A, Fig. 1(B)). This observation was corroborated by FACS analysis using antibodies to CD31 and VE-cadherin, which revealed that upon exposure to "combination 1" 60.14% of all cells were CD31<sup>+</sup>VE-cad<sup>+</sup> (identifying them as cells of endothelial lineage), whereas only 10.0% (or 8.6% respectively) of all cells had acquired an endothelial phenotype when "combination 2" (or "combination 3") was used (Fig. 1(C) and Supplementary Fig. 1).

### 3.2. Further characterization of hiPSC-derived endothelial cell progenitors confirms bFGF and VEGF-A as most efficient cytokine combination for endothelial differentiation

We next analyzed expression of genes which are typically linked to specific endothelial cell populations, including common endothelial cell markers PECAM1 (CD31), CDH5 (VE-cadherin) and vWF (Von Willebrand factor) by quantitative real-time PCR after treatment with the three different cytokine combinations (Fig. 2(A)). All three markers showed highest expression after exposure to "combination 1" (bFGF and VEGFA).

For further validation of an endothelial phenotype of differentiated hiPSC we next characterized cells which had been isolated through FACS sorting, utilizing antibodies to CD31 and VE-cadherin. We plated CD31<sup>+</sup>VE-cadherin<sup>+</sup> double-positive cells onto tissue culture plates coated with attachment factor in Endothelial Cell growth medium supplemented with 15 ng/ml VEGFA, and once settled, cells were cultured in EMV2 growth medium until analysis. Almost all sorted cells stained positive for endothelial cell markers CD31, VE-cadherin and vWF, irrespective of the "differentiation combination" which had been used (Fig. 2(B)). These observations suggested that hiPSCs could be differentiated into hiPSCs with endothelial cell phenotype (hiPSC-EC) and that different growth factor combinations tested differed substantially in the quantitative effectiveness to generate hiPSC-EC, but that cells did not appear to differ significantly once they had been differentiated, regardless of growth factor combination that had been used. However, cells generated from combination 2 and 3 were not suitable for prolonged culture as cell morphology suggested a higher rate of apoptotic cells (Fig. 2(B)).

### 3.3. Optimization of mesodermal cell differentiating further improves endothelial cell differentiation efficiency

In our differentiation experiments, we noticed that initial cell density and colony size of hiPSC play another key role in differentiation, which is in line with previous reports (Bauwens et al., 2008; Tan et al., 2013). Thus, once among the 3 combinations

tested, combination 1 has been established as the most effective cytokine combination to differentiate endothelial cells, we aimed to further enhance efficiency of hiPSC-ECs by further optimizing the protocol with respect to cell density and colony size (this modified experiment set-up is summarized in Fig. 3(A)). In these experiments, we first established that initial cell density of hiPSCs played a key role in efficacy of hiPSC differentiation, and that a cell density of  $2.5 \times 10^4$  cells per 6-well plate was most efficient (Supplementary Table S2). However, while a higher cell density was associated with a tendency to larger colony sizes, even optimal cell density still produced colonies ranging from <60 to >200  $\mu\text{m}$  in size. We further established that the size of hiPSC colony is a critical factor for the initiation of the ECs differentiation. Colony sizes from <60 to >200  $\mu\text{m}$  were tested in our differentiation protocol and a colony diameter of around 60  $\mu\text{m}$  of hiPSCs was shown optimal for further improving the efficiency in this modified protocol (Supplementary Table S3). These efforts resulted in further increased EC-differentiating efficiency of >80% by day12, as shown by FACS analysis for CD31 and VE-cadherin (Fig. 3 B). We next explored necessity of the two-step approach, omitting either the GSK-3beta inhibitor CHIR 99021 (CHIR) step (Fig. 3(C), left panels) or the addition of growth factors (Fig. 3(C), right panels). Omission of either step prevented differentiation to CD31<sup>+</sup>/VE-cadherin<sup>+</sup> cells (Fig. 3(C)). However, we established that the DMEM/F12 could sufficiently substitute endothelial cell basal medium during the first 2 days, further reducing cost of differentiation (Fig. 3(B)).

### 3.4. Phenotypic characterization of hiPSC-EC upon protocol optimization

In order to further characterize the hiPSC-EC differentiated upon the optimized protocol, we first compared expression of additional endothelial cell markers CD31, VE-cadherin, Tie1 and vWF among iPS cells, fully differentiated iPSC-ECs (after 12 days of differentiation protocol) and native human coronary artery endothelial cells (HCAEC). Expression of all selected endothelial specific markers were significantly induced in iPSC-ECs and comparable to (or higher than) expression levels in HCAEC (Fig. 4 A). Robust upregulation of endothelial markers in iPSC-EC was additionally confirmed by immunofluorescence-labeling experiments (Fig. 4(B)). In order to test if cell sorting and consecutive culturing of cells alters purity of endothelial markers, cells were maintained in normal endothelial cell growth medium for additional two weeks after primary endothelial cell sorting, and re-analyzed by FACS analysis for the endothelial markers CD31 and VE-cadherin. CD31<sup>+</sup>VE-cadherin<sup>+</sup> double-positive cells comprised up to 96.63% of all cells, further illustrating the high homogeneity as well as proliferation capability of the hiPSC-derived EC (Fig. 4(C)). Observation of cell population proliferation showed that after cultivation of cells for 2 weeks, cell population had increased to 6-fold of initial cell number (data not shown).

### 3.5. Development of endothelial versus mesodermal phenotype over time of differentiation

In order to document the differentiation steps from undifferentiated iPSCs to mesodermal to endothelial differentiation, we performed time-course analysis of KDR (vascular endothelial growth factor receptor 2), Brachyury and CD34 (all indicating endothelial progenitor cells) as well as CD31, Tie1 and vWF (indicating endothelial differentiation) by quantitative real-time PCR. Analysis revealed that after 12 days of previously established differentiation protocol expression of CD31, Tie1 and vWF were robustly increased, phenocopying expression levels of HCAEC and thereby suggesting that after 12 days optimal endothelial

Please cite this article as: Liu, X., et al., Differentiation of functional endothelial cells from human induced pluripotent stem cells: A novel, highly efficient and cost effective method. *Differentiation* (2016), <http://dx.doi.org/10.1016/j.diff.2016.05.004>

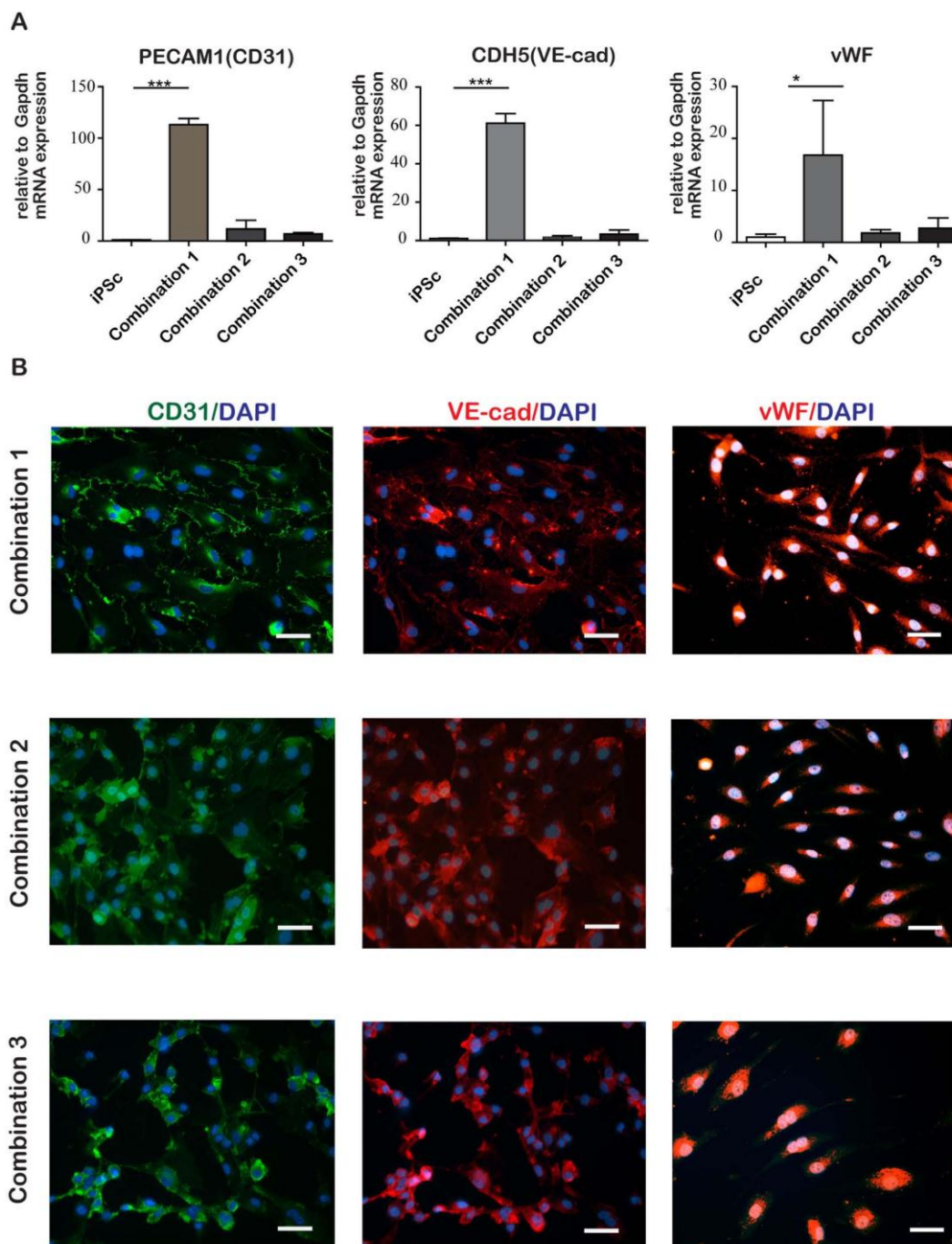


**Fig. 2. Further Characterization of EC derived from hiPSC.** A. Expression of endothelial cells markers in response to different differentiation protocols. Before sorting, hiPSCs were subjected to 10-day differentiation protocols including different combinations of cytokine supplements of either Endothelial Basal Medium (EBM) supplemented with 5 ng/ml bFGF and 10 ng/ml VEGFA ("combination 1"), EBM supplemented with 10 ng/ml VEGFA, 4 ng/ml BMP4 and 15 ng/ml Activin A ("combination 2") and EBM supplemented with 4 ng/ml BMP4 and 15 ng/ml Activin A ("combination 3"). The bar graphs summarize results of quantitative real-time PCR analysis of CD31 (PECAM1), VE-cadherin (CDH5) and vWF (Von Willebrand factor) expression before sorting in relation to un-induced hiPSC (mean  $\pm$  SD, \*\* $p \leq 0.01 < 0.005$ ; \*\*\* $p \leq 0.005$ ). The values represent the average level of triplicates. B. CD31/VE-cadherin and vWF immunolabeling. Sorted cells were immunolabeled with antibodies to CD31 (green), VE-cadherin (red), and vWF (red). DAPI was used to visualize nuclei. The pictures display merged representative immunofluorescence-micrographs upon exposure to cytokine combinations 1, 2, or 3. Scale bar: 50  $\mu$ m. Differentiation was performed at an initial cell density of  $2.5 \times 10^4$  per well without control of colony size (which ranged from  $< 60 \mu$ m to  $> 200 \mu$ m). The data were generated from two independent hiPSCs cell lines (WTBLD and WTD2) and showed consistency between the two different cell lines.



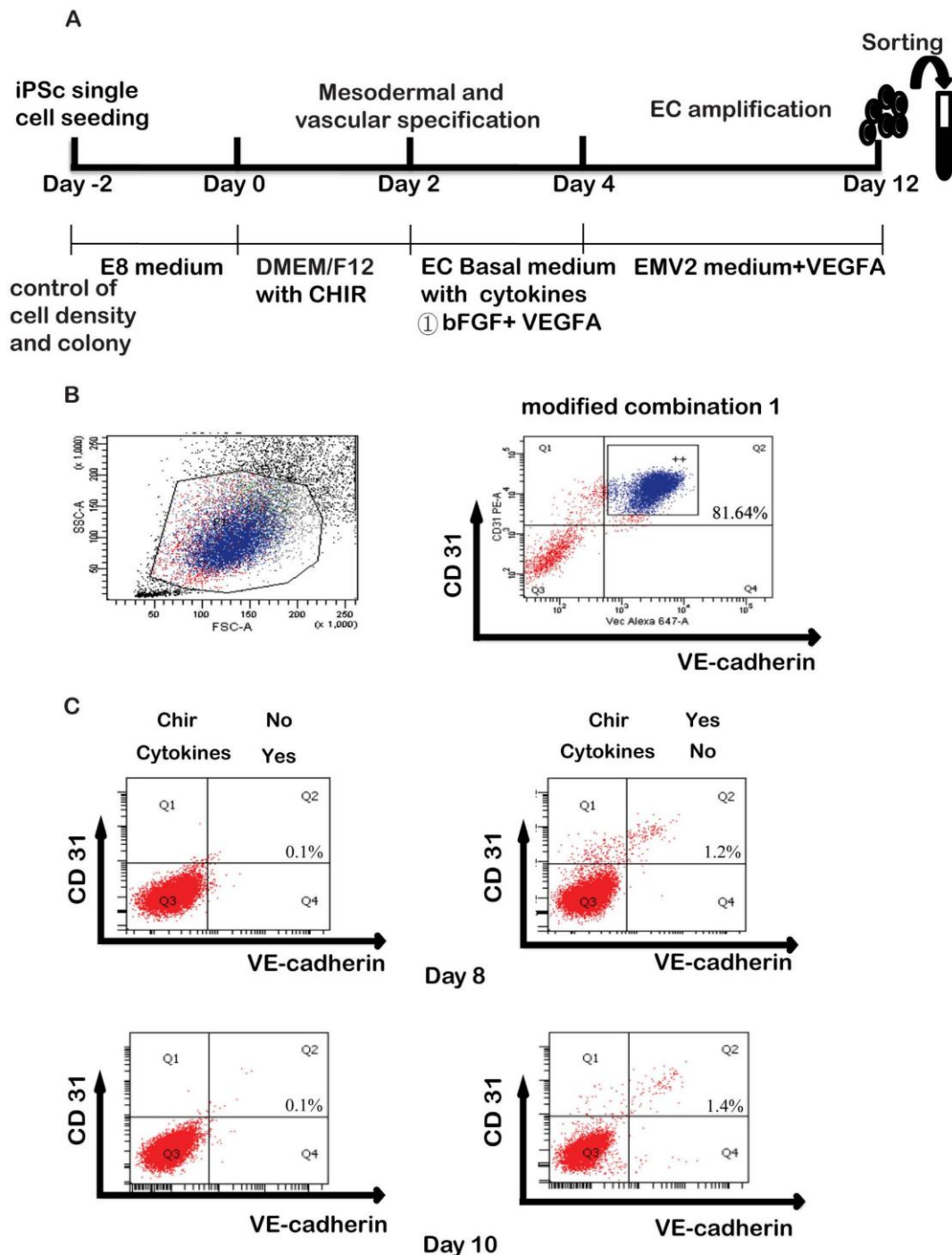


**Fig. 3. Control of cell density and colony size improves ECs generation efficiency.** A. Schematic illustration of experimental design. hiPSCs were seeded at low density and maintained in E8 medium until single colonies had established (day -2 to day 0). For mesodermal specification, hiPSCs were exposed to DMEM/F12 medium supplemented with CHIR for two days (day 1 to day 2). For endothelial specification, hiPSCs were then exposed for two days to basal medium supplemented with different combinations of cytokines as indicated (day 2 to day 4). Upon endothelial specification, cells were maintained in EMV2 medium supplemented with VEGFA for amplification for eight days (day 4 to day 12) and subsequently analyzed. B. FACS analysis showing the CD31/VE-cadherin double positive cells population upon modified protocol. FACS sorting by the endothelial markers CD31 and VE-cadherin at day 10. Efficiency to generate CD31+/VE-cadherin+ double-positive cells was 81.64%. C. Effect of CHIR or growth factor-omission on endothelial cell differentiation efficacy. We either omitted addition of CHIR (left panels) or growth factors (right panels) and analyzed CD31 and VE-cadherin expression by FACS after 8 days (top row) and 10 days (bottom row). Representative scatter plots are displayed. Differentiation was performed at an initial cell density of  $2.5 \times 10^4$  per well and at an optimized colony size of  $60 \mu\text{m}$ . Data were generated from three independent hiPSCs cell lines (WTBLD, WTD2 and IC113) and showed consistency between all three different cell lines.

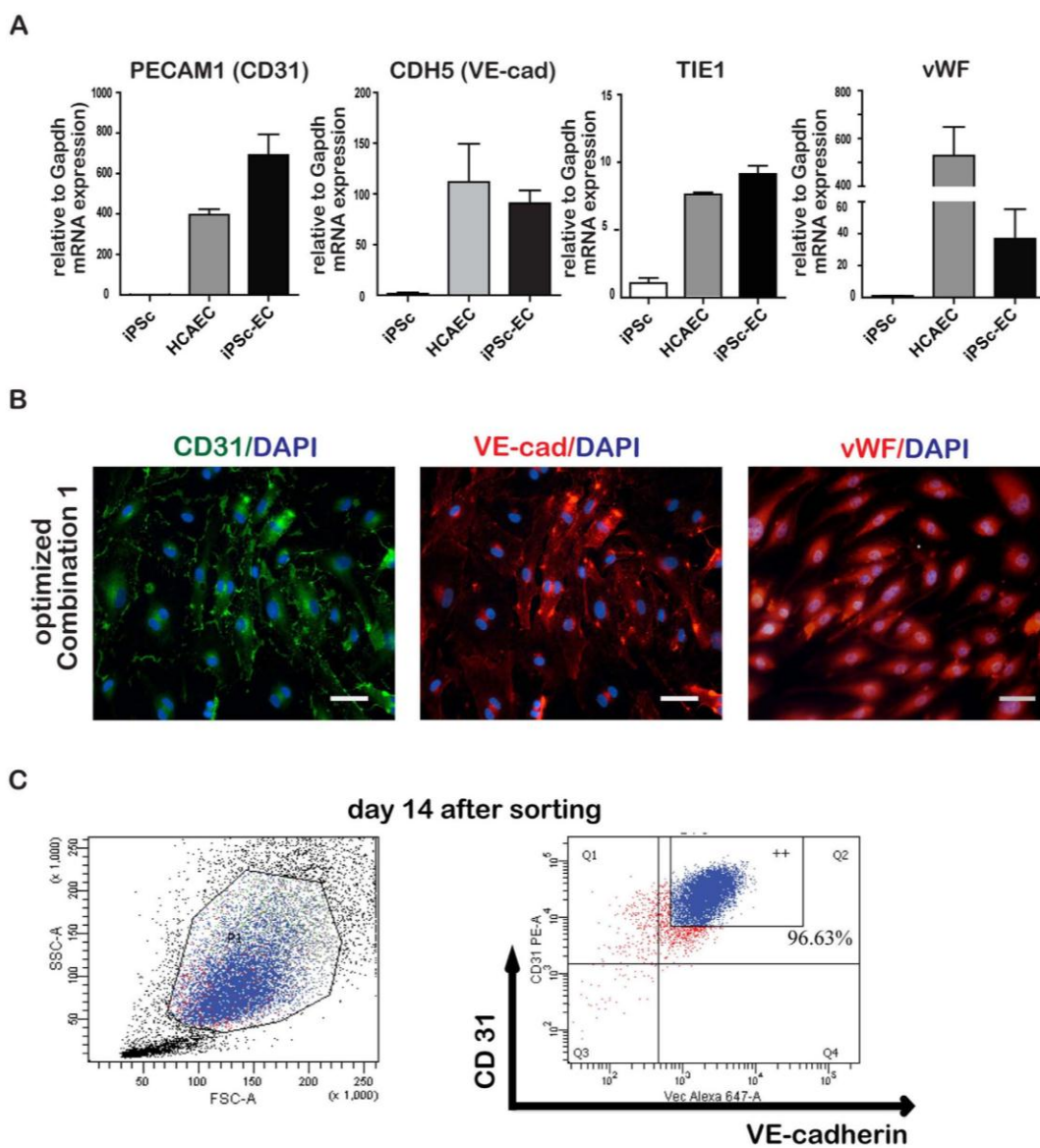


**Fig. 4. Expression of common endothelial markers upon optimized differentiation protocol.** A. CD31 (PECAM1), VE-cadherin (CDH5), TIE1 and vWF (Von Willebrand factor) mRNA expression. Upon completion of optimized differentiation protocol we compared expression of indicated genes in un-induced hiPSC to HCAEC and differentiated hiPSC-EC 4 days after sorting. The bar graphs summarize relative expression of indicated genes. The values represent the average level of triplicates. B. Immunofluorescence labeling. After completion of optimized differentiation protocol we labeled cells (4 days after sorting) with antibodies specific to CD31 (left picture, green) and VE-cadherin (middle picture, red) and vWF (right picture, red) and DAPI (blue) was used to visualize nuclei. Representative photomicrographs obtained on a fluorescence microscope are displayed. Scale bar: 50  $\mu\text{m}$ . C. CD31/VE-cadherin FACS analysis upon 2 weeks culture of the hiPSC induced ECs. FACS sorting by the endothelial markers CD31 and VE-cadherin after 2 weeks cultured in normal endothelial cell growth medium. Differentiation was performed at an initial cell density of  $2.5 \times 10^4$  per well and at a colony size of  $\sim 60 \mu\text{m}$ . Data were generated from two independent hiPSC cell lines (WTBLD and WTD2) and showed consistency between the different cell lines.

differentiation was achieved (Fig. 5(A)). Brachyury and CD34 showed highest expression on days 4 and 7, which is when mesodermal differentiation is assumed (Fig. 5(B)) (Era et al., 2008; Kane et al., 2010). KDR on the other hand also showed an increase of expression on day 7 as compared to previous time points (indicative of mesodermal differentiation), but had highest expression level on day 12, when endothelial differentiation has already

occurred (Fig. 5(B)). This likely reflects the fact that KDR is also abundantly expressed on vascular endothelial cells (Koch and Claesson-Welsh, 2012; Neufeld et al., 1999; Olsson et al., 2006). KDR also plays a specific role in arteriogenesis and studies comparing arterial and venous umbilical endothelial cells furthermore showed a two-fold higher KDR expression in arterial as compared to venous cells (Aranguren et al., 2013; Babiak et al., 2004).

Please cite this article as: Liu, X., et al., Differentiation of functional endothelial cells from human induced pluripotent stem cells: A novel, highly efficient and cost effective method. Differentiation (2016), <http://dx.doi.org/10.1016/j.diff.2016.05.004>

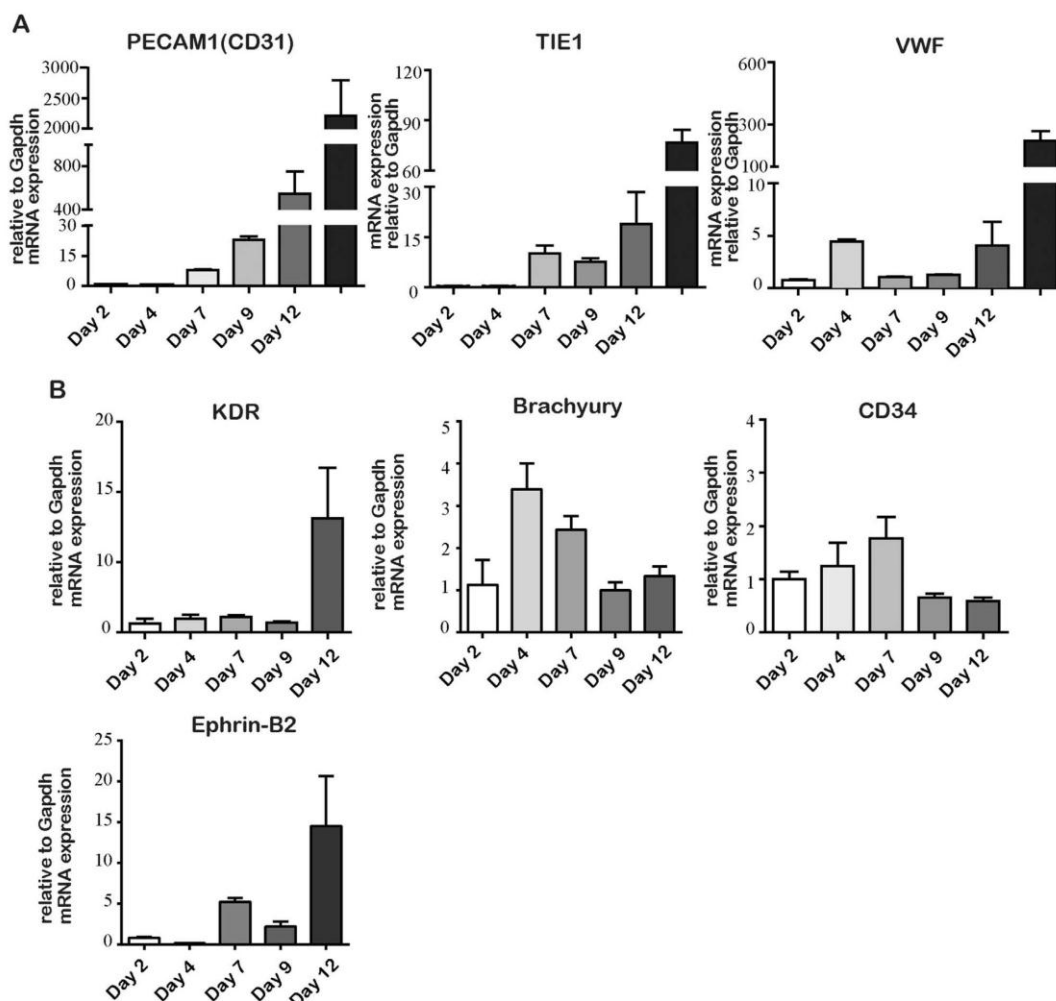


**Fig. 5. Time course analysis of expression of genes associated with endothelial cell differentiation.** A. Expression of endothelial markers during the course of hiPSC differentiation. Three endothelial cell markers CD31, Tie1 and vWF were analyzed by quantitative real time PCR over the time course of endothelial cell differentiation. B. Expression of mesodermal markers during the course of hiPSC differentiation. KDR, Brachyury, CD34 and Ephrin-B2 were analyzed by quantitative real time PCR over the time course of endothelial cell differentiation. The graphs summarize relative gene expression at indicated time points. Data were generated from two independent hiPSC cell lines (WTBLD and WTD2) and showed consistency between the different cell lines.

Therefore, we also tested Ephrin-B2 (a purely arterial marker) at different time points, and similarly found highest expression at day 12, further suggesting a more arterial endothelial phenotype of our iPSC-derived endothelial cells. (Fig. 5(B))(Swift and Weinstein, 2009).

### 3.6. Functional characterization of hiPSC-EC upon protocol optimization

To gain insights into utility of hiPSC-derived endothelial cells to serve as representative model for endothelial cells, we next compared their phenotype and functional properties to that of human coronary endothelial cells (HCAEC). We compared iPSC-ECs to HCAEC in functional LDL-uptake and tube formation assays. Sorted iPSC-ECs were as efficient as HCAEC to take up ac-Dil-LDL (Fig. 6 (A)-(B)). Furthermore, we performed tube formation assays on

matrigel-coated plates and observed that iPSC-ECs mirrored capacity of HCAEC to form tube like structures (Fig. 6(C)). We finally compared capacity of iPSC-ECs and HCAEC to form 3-dimensional angiogenic spheroids within type I collagen gels. After 48 h in mix with collagen type I, both cell types had formed angiogenic spheres to an indistinguishable degree (Fig. 6(D)).

## 4. Discussion

While it was previously established that endothelial cells could be derived through differentiation of hiPSC, differentiation efficiency and cost or the combination of both are still not at the optimal level (Bao et al., 2015; Lian et al., 2014; Orlova et al., 2014; Patsch et al., 2015; Sahara et al., 2014; Tatsumi et al., 2011; Yang et al., 2008). Here, we report an alternative highly efficient, simple



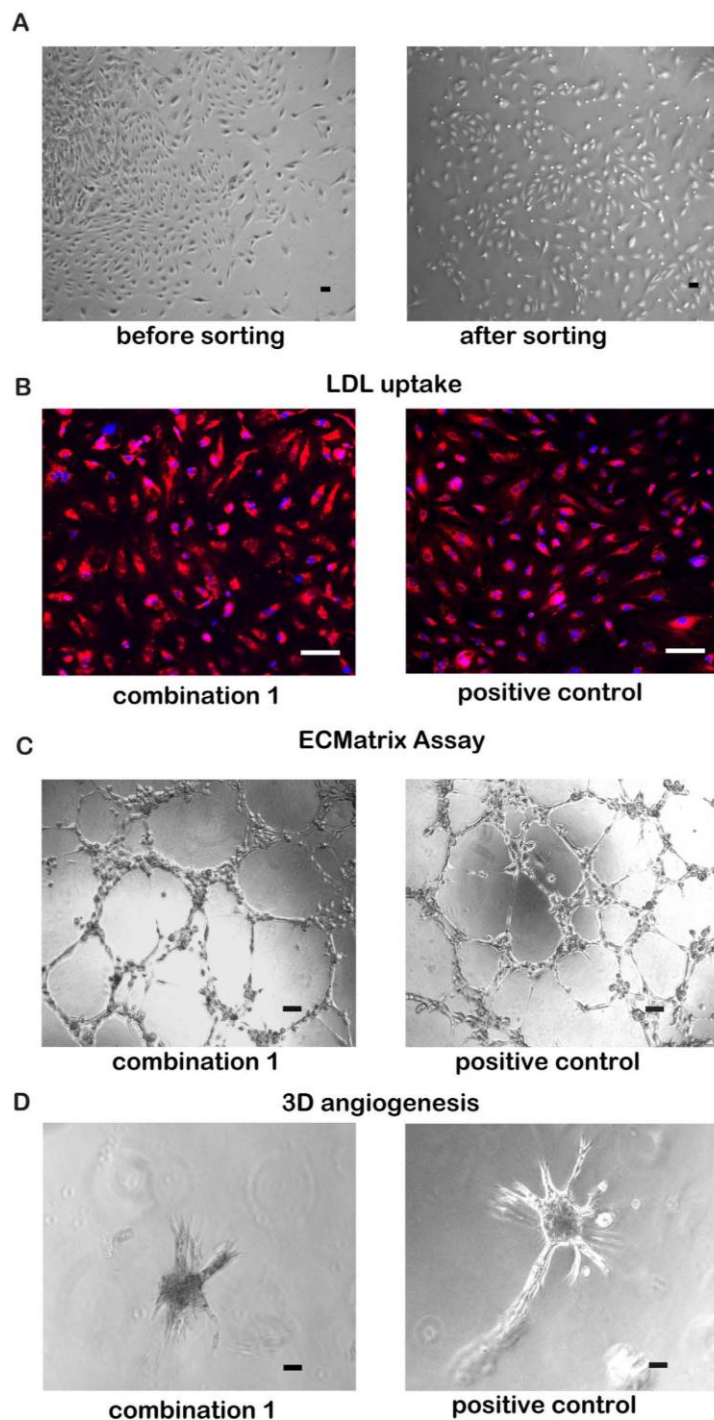


**Fig. 6. Functional characterization of iPSC derived ECs.** A. Phase-contrast microscopy. We compared cell morphology of hiPSC-EC before (left picture) and after FACS sorting (right picture). Cells displayed a similar morphology before and after undergoing the cell sorting procedure. B. LDL-uptake. Ac-Dil-LDL was added to culture media of sorted iPSC-EC (left) and of HCAEC (right). LDL-uptake was visualized using a fluorescence microscope (red). The pictures display representative photomicrographs of each cell type. C. Tube formation assay. hiPSC-EC (left) and HCAEC were seeded onto matrigel-coated plates. Formation of tube-like structures was documented by light-microscopy, representative pictures are displayed. D. 3D angiogenesis assay. Cells were allowed to form angiogenic spheres within type I collagen. The pictures display representative photomicrographs of hiPSC (left) and HCAEC (right). Scale bars: 50  $\mu$ m. Data were generated from two (Figure 6 D) or three (Figure 6 A, B, C) independent hiPSCs cell lines (WTBLD, WTD2 and IC113) and showed consistency between the different cell lines.



three step method (mesoderm induction, endothelial cell differentiation and endothelial cell expansion) to differentiate hiPSC into endothelial cells. We report that efficiency of described method to derive CD31<sup>+</sup> VE-Cadherin<sup>+</sup> double-positive cells is higher than 80% in 12 days. Most notably we established that hiPSC-EC differentiation efficacy depends on optimization of both mesoderm differentiation and endothelial cell differentiation steps. With regard to mesoderm differentiation, seeding cell density (hiPSC colony diameter around 60 μm) and addition of 4 μM Chir99021 are critical, whereas expensive endothelial basal medium could be replaced with DMEM/F12 without impacting differentiation efficiency (Supplementary data Table S3). For endothelial cell differentiation, combination of Endothelial Basal Medium (EBM) supplemented with 5 ng/ml bFGF and 10 ng/ml VEGFA was optimal and a 12-day differentiation protocol yielded best results. In this study, three different hiPSCs lines were used and no bias on a particular hiPSCs cell line could be observed.

Endothelial cells obtained here were defined through their expression of endothelial cell markers CD31, vWF and VE-cadherin and their capacity for LDL-uptake, endothelial tube formation and formation of angiogenic spheres in 3D-culture. In this regard, hiPSC-ECs did not differ from HCAEC, demonstrating their utility for future studies.

#### Author disclosure statement

The authors declare that no competing financial interests exist in this study.

#### Acknowledgements

This work was supported by the German Heart Research Foundation DSHF F/55/13 (to E.Z.). It was further supported by the University Medical Center of Göttingen and Deutsche Forschungsgemeinschaft (DFG) Grant SFB1002/C01 (to E.Z.) and SFB1002/A04 (to K.G.), IRTG1816 (International Research Training Group 1816, to J.Q. and X.L.), DFG Grants ZE523/2-1 and ZE523/3-1 and Else Kröner Memorial Stipend 2005/59 (to M.Z.).

#### Appendix A. Supplementary material

Supplementary data associated with this article can be found in the online version at <http://dx.doi.org/10.1016/j.diff.2016.05.004>.

#### References

- Aranguren, X.L., Agirre, X., Beerens, M., Coppiello, G., Ufrix, M., Vandersmissen, I., Benkhell, M., Panadero, J., Aguado, N., Pascual-Montano, A., et al., 2013. Unraveling a novel transcription factor code determining the human arterial-specific endothelial cell signature. *Blood* 122, 3982–3992.
- Babiak, A., Schumm, A.M., Wangler, C., Loukas, M., Wu, J.B., Dombrowski, S., Matuschek, C., Kotzerke, J., Dehio, C., Waltenberger, J., 2004. Coordinated activation of VEGFR-1 and VEGFR-2 is a potent arteriogenic stimulus leading to enhancement of regional perfusion. *Cardiovasc Res* 61, 789–795.
- Bao, X., Lian, X., Dunn, K.K., Shi, M., Han, T., Qian, T., Bhute, V.J., Canfield, S.G., Palecek, S.P., 2015. Chemically-defined albumin-free differentiation of human pluripotent stem cells to endothelial progenitor cells. *Stem Cell Res* 15, 122–129.
- Bauwens, C.L., Peerani, R., Niebruegge, S., Woodhouse, K.A., Kumacheva, E., Husain, M., Zandstra, P.W., 2008. Control of human embryonic stem cell colony and aggregate size heterogeneity influences differentiation trajectories. *Stem Cells* 26, 2300–2310.
- Belousoff, M., Farrington, S.M., Baron, M.H., 1998. Hematopoietic induction and respecification of A-P identity by visceral endoderm signaling in the mouse embryo. *Development* 125, 5009–5018.
- Chen, G., Gulbranson, D.R., Hou, Z., Bolin, J.M., Ruotti, V., Probasco, M.D., Smuga-

- Otto, K., Howden, S.E., Diol, N.R., Propson, N.E., et al., 2011. Chemically defined conditions for human iPSC derivation and culture. *Nat. Methods* 8, 424–429.
- Davidson, K.C., Adams, A.M., Goodson, J.M., McDonald, C.E., Potter, J.C., Berndt, J.D., Biechele, T.L., Taylor, R.J., Moon, R.T., 2012. Wnt/beta-catenin signaling promotes differentiation, not self-renewal, of human embryonic stem cells and is repressed by Oct4. *Proc. Natl. Acad. Sci. USA* 109, 4485–4490.
- Dudek, J., Cheng, I.F., Balleininger, M., Vaz, F.M., Streckfuss-Bomeke, K., Hubscher, D., Vukotic, M., Wanders, R.J.A., Rehling, P., Guan, K.M., 2013. Cardiolipin deficiency affects respiratory chain function and organization in an induced pluripotent stem cell model of Barth syndrome. *Stem Cell Res* 11, 806–819.
- Era, T., Izumi, N., Hayashi, M., Tada, S., Nishikawa, S., Nishikawa, S.L., 2008. Multiple mesoderm subsets give rise to endothelial cells, whereas hematopoietic cells are differentiated only from a restricted subset in embryonic stem cell differentiation culture. *Stem Cells* 26, 401–411.
- Hink, U., Li, H., Mollnau, H., Oelze, M., Matheis, E., Hartmann, M., Skatchkov, M., Thais, F., Stahl, R.A., Warnholtz, A., et al., 2001. Mechanisms underlying endothelial dysfunction in diabetes mellitus. *Circ. Res* 88, E14–E22.
- Hirashima, M., 2009. Regulation of endothelial cell differentiation and arterial specification by VEGF and Notch signaling. *Anat. Sci. Int.* 84, 95–101.
- Jih, Y.J., Lien, W.H., Tsai, W.C., Yang, G.W., Li, C., Wu, L.W., 2001. Distinct regulation of genes by bFGF and VEGF-A in endothelial cells. *Angiogenesis* 4, 313–321.
- Kane, N.M., Meloni, M., Spencer, H.L., Craig, M.A., Strehl, R., Milligan, G., Houstlay, M. D., Mountford, J.C., Emanuelli, C., Baker, A.H., 2010. Derivation of endothelial cells from human embryonic stem cells by directed differentiation analysis of MicroRNA and angiogenesis *in vitro* and *in vivo*. *Arterioscl. Throm. Vas.* 30 1389–1319.
- Kim, M.S., Horst, A., Blinks, S., Stamm, K., Mahne, D., Schuman, J., Gundry, R., Tomita-Mitchell, A., Lough, J., 2015. Activin-A and Bmp4 levels modulate cell type specification during CHIR-induced cardiomyogenesis. *PLoS One* 10, e0118670.
- Koch, S., Claesson-Welsh, L., 2012. Signal transduction by vascular endothelial growth factor receptors. *Cold Spring Harb. Perspect. Med.* 2.
- Li, Z.J., Hu, S.J., Ghosh, Z., Han, Z.C., Wu, J.C., 2011. Functional characterization and expression profiling of human induced pluripotent stem cell- and embryonic stem cell-derived endothelial cells. *Stem Cells Dev.* 20, 1701–1710.
- Li, Z.J., Wilson, K.D., Smith, B., Kraft, D.L., Jia, F.J., Huang, M., Xie, X.Y., Robbins, R.C., Gambhir, S.S., Weissman, I.L., Wu, J.C., 2009. Functional and transcriptional characterization of human embryonic stem cell-derived endothelial cells for treatment of myocardial infarction. *PLoS One*, 4.
- Lian, X., Bao, X., Al-Ahmad, A., Liu, J., Wu, Y., Dong, W., Dunn, K.K., Shusta, E.V., Palecek, S.P., 2014. Efficient differentiation of human pluripotent stem cells to endothelial progenitors via small-molecule activation of WNT signaling. *Stem Cell Rep.* 3, 804–816.
- Lian, X.J., Hsiao, C., Wilson, G., Zhu, K.X., Hazeltine, L.B., Azarin, S.M., Raval, K.K., Zhang, J.H., Kamp, T.J., Palecek, S.P., 2012. Robust cardiomyocyte differentiation from human pluripotent stem cells via temporal modulation of canonical Wnt signaling. *Proc. Natl. Acad. Sci. USA* 109, E1848–E1857.
- Marcelo, K.L., Goldie, L.C., Hirschi, K.K., 2013. Regulation of endothelial cell differentiation and specification. *Circ. Res* 112, 1272–1287.
- Marom, K., Levy, V., Pillemer, G., Fainsod, A., 2005. Temporal analysis of the early BMP functions identifies distinct anti-organizer and mesoderm patterning phases. *Dev. Biol.* 282, 442–454.
- Moretti, A., Laugwitz, K.L., Dorn, T., Sinnecker, D., Mummery, C., 2013. Pluripotent stem cell models of human heart disease. *Cold Spring Harb. Perspect. Med.* 3.
- Neufeld, G., Cohen, T., Gengrinovitch, S., Poltorak, Z., 1999. Vascular endothelial growth factor (VEGF) and its receptors. *FASEB J.* 13, 9–22.
- Olsson, A.K., Dimberg, A., Kreuger, J., Claesson-Welsh, L., 2006. VEGF receptor signaling – in control of vascular function. *Nat. Rev. Mol. Cell Biol.* 7, 359–371.
- Orlova, V.V., van den Hil, E.E., Petrus-Reurer, S., Drabsch, Y., ten Dijke, P., Mummery, C.L., 2014. Generation, expansion and functional analysis of endothelial cells and pericytes derived from human pluripotent stem cells. *Nat. Protoc.* 9, 1514–1531.
- Patsch, C., Challet-Meylan, L., Thoma, E.C., Ulrich, E., Heckel, T., O'Sullivan, J.F., Grainger, S.J., Kapp, F.G., Sun, L., Christensen, K., et al., 2015. Generation of vascular endothelial and smooth muscle cells from human pluripotent stem cells. *Nat. Cell Biol.*
- Rosowski, K.A., Mertz, A.F., Norcross, S., Dufresne, E.R., Horsley, V., 2015. Edges of human embryonic stem cell colonies display distinct mechanical properties and differentiation potential. *Sci. Rep.* 5.
- Rufaihah, A.J., Huang, N.F., Kim, J., Herold, J., Volz, K.S., Park, T.S., Lee, J.C., Zambidis, E.T., Reijo-Pera, R., Cooke, J.P., 2013. Human induced pluripotent stem cell-derived endothelial cells exhibit functional heterogeneity. *Am. J. Transl. Res.* 5, 21–U122.
- Sahara, M., Hansson, E.M., Wernet, O., Lui, K.O., Spater, D., Chien, K.R., 2014. Manipulation of a VEGF-Notch signaling circuit drives formation of functional vascular endothelial progenitors from human pluripotent stem cells. *Cell Res* 24, 820–841.
- Saxton, T.M., Pawson, T., 1999. Morphogenetic movements at gastrulation require the SH2 tyrosine phosphatase Shp2. *Proc. Natl. Acad. Sci. USA* 96, 3790–3795.
- Streckfuss-Bomeke, K., Wolf, F., Azizian, A., Stauske, M., Tiburcy, M., Wagner, S., Hubscher, D., Dressel, R., Chen, S., Jenke, J., et al., 2013. Comparative study of human-induced pluripotent stem cells derived from bone marrow cells, hair keratinocytes, and skin fibroblasts. *Eur. Heart J.* 34, 2618–2629.
- Swift, M.R., Weinstein, B.M., 2009. Arterial-venous specification during development. *Circ. Res.* 104, 576–588.
- Tan, J.Y., Sriram, G., Rufaihah, A.J., Neoh, K.G., Cao, T., 2013. Efficient derivation of

Please cite this article as: Liu, X., et al., Differentiation of functional endothelial cells from human induced pluripotent stem cells: A novel, highly efficient and cost effective method. *Differentiation* (2016), <http://dx.doi.org/10.1016/j.diff.2016.05.004>

## ARTICLE IN PRESS

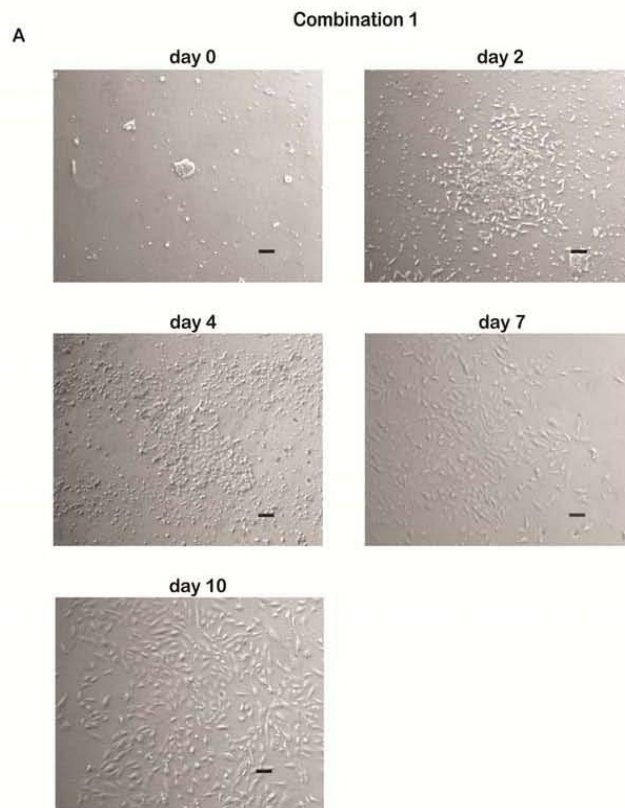
12

X. Liu et al. / *Differentiation* ■ (■■■■) ■■■-■■■

- lateral plate and paraxial mesoderm subtypes from human embryonic stem cells through GSKi-mediated differentiation. *Stem Cells Dev.* 22, 1893–1906.
- Tatsumi, R., Suzuki, Y., Sumi, T., Sone, M., Suemori, H., Nakatsuji, N., 2011. Simple and highly efficient method for production of endothelial cells from human embryonic stem cells. *Cell Transplant.* 20, 1423–1430.
- Teo, A.K., Ali, Y., Wong, K.Y., Chipperfield, H., Sadasivam, A., Poobalan, Y., Tan, E.K., Wang, S.T., Abraham, S., Tsuneyoshi, N., et al., 2012. Activin and BMP4 synergistically promote formation of definitive endoderm in human embryonic stem cells. *Stem Cells* 30, 631–642.
- Vokes, S.A., Krieg, P.A., 2002. Endoderm is required for vascular endothelial tube formation, but not for angioblast specification. *Development* 129, 775–785.
- Yamaguchi, T.P., Harpal, K., Henkemeyer, M., Rossant, J., 1994. Fgfr-1 is required for embryonic growth and mesodermal patterning during mouse gastrulation. *Gene Dev.* 8, 3032–3044.
- Yan, W., Bentley, B., Shao, R., 2008. Distinct angiogenic mediators are required for basic fibroblast growth factor- and vascular endothelial growth factor-induced angiogenesis: the role of cytoplasmic tyrosine kinase c-Abl in tumor angiogenesis. *Mol. Biol. Cell* 19, 2278–2288.
- Yang, L., Soonpaa, M.H., Adler, E.D., Roepke, T.K., Kattman, S.J., Kennedy, M., Henckaerts, E., Bonham, K., Abbott, G.W., Linden, R.M., et al., 2008. Human cardiovascular progenitor cells develop from a KDR+ embryonic-stem-cell-derived population. *Nature* 453, 524–528.

Please cite this article as: Liu, X., et al., Differentiation of functional endothelial cells from human induced pluripotent stem cells: A novel, highly efficient and cost effective method. *Differentiation* (2016), <http://dx.doi.org/10.1016/j.diff.2016.05.004>

Supplementary Figure 1 Phase-contrast images of EC differentiation



Supplementary Figure 1. Phase contrast images during the hiPSCs differentiated into ECs.

A. Representative pictures to show the cell morphology change at different time points during different treatment. Single cell seeding method was performed at Day -1. Cell morphology changed into mesodermal cell like cells at Day 2 after CHIR treatment. After the different cytokines combination treatments, colony of cobblestone morphology like endothelial cell cluster was expanded. Scale bars: 100  $\mu$ m. Data were generated from two independent hiPSCs cell lines (WTBLD and WTD2) and showed consistency between the different cell lines.



**Table S1. Semi-Quantitative Polymerase Chain Reaction Primers**

Gene name	F/R	sequence	Reference
CD31(PECAM1)	Forward	5'-ATT GCA GTG GTT ATC ATC GGA GTG-3'	Self-designed
	Reverse	5'-CTC GTT GTT GGA GTTCAG AAG TGG-3'	Self-designed
VE-cadherin(CDH5)	Forward	5'- AGA CAC CCC CAA CAT GCT AC -3'	Self-designed
	Reverse	5'- GCA AAC TCT CCT TGG AGC AC-3	Self-designed
Ephrin-B2(EFNB2)	Forward	5'-TGA TAA AAG ACC AAG CAG ACA GAT -3'	primerdesign
	Reverse	5'-TCT TGA AAC TTG ATG GTG AAT TGA -3'	primerdesign
TIE1	Forward	5'-CTG TGC TCC TGT CCA CCA A-3'	primerdesign
	Reverse	5'-CAC TCC CAG AAC CCA CTG TC-3'	primerdesign
vWF	Forward	5'-GGG GTC ATC TCT GGA TTC AAG -3'	primerdesign
	Reverse	5'-TCT GTC CTC CTC TTA GCT GAA-3'	primerdesign
Brachyury	Forward	5'-TAAGGTGGATCTTCAGGTAGC-3'	(Inoue et al., 2010)
	Reverse	5'-CATCTCATTGGTGGAGCTCCCT-3'	
CD34	Forward	5'-TTGACAACAACGGTACTGCTAC-3'	(Dome et al., 2009)
	Reverse	5'-TGGTGAACACTGTGCTGATTAC-3'	

NOTE: Primerdesign is the supplier who supply all these primers marked as 'primerdesign'.

**Table S2. Influence of cell density on hiPSC- EC differentiation efficiency**

<i>cell density (6-well plate)</i>	<i>Efficiency at day 10(%)</i>
$1 \times 10^4$	0.00
$2 \times 10^4$	16.62
$2.5 \times 10^4$	>20%
$4 \times 10^4$	18.71
$12 \times 10^4$	0.80
$20 \times 10^4$	0.10

*Table S2: hiPSCs were cultured according to the combination 1 protocol (4 $\mu$ M CHIR treatment for 2 days, followed by another 2 days in EBM medium supplemented with bFGF and VEGFA, then changed into EMV2 medium with VEGFA). The percentage of endothelial cell efficiency was determined by flow cytometry analysis of CD31+ VE-cadherin+ double positive cells at day 10 of the endothelial differentiation protocol. Differentiation was performed without colony size control, and colony sizes ranged from <60  $\mu$ m to >200 $\mu$ m. The data were generated from two independent hiPSCs cell lines (WTBLD and WTD2) and showed consistency between the different cell lines. Two or more independent replicates were performed for each line.*

**Table S3. Influence of colony size on hiPSC-EC differentiation efficiency**

<i>colony size</i>	<i>Efficiency at day 10 (%)</i>
<i>&gt;200 <math>\mu\text{m}</math></i>	<i>~6.14</i>
<i>150- 200 <math>\mu\text{m}</math></i>	<i>~33.95</i>
<i>90<math>\mu\text{m}</math>-150 <math>\mu\text{m}</math></i>	<i>~39.00</i>
<i>60<math>\mu\text{m}</math></i>	<i>~80.00</i>
<i>&lt; 60<math>\mu\text{m}</math></i>	<i>Not applicable</i>

*Table S3: hiPSCs were cultured according to the combination 1 protocol at an initial cell density of  $2.5 \times 10^4$  per well in a 6-well plate. At day 0 colonies of different sizes were selected and further differentiated. Percentage of endothelial cell efficiency was determined by flow cytometry analysis of CD31+ VE-cadherin+ double positive cells at day 10. The data were generated from two independent hiPSCs cell lines (WTBLD and WTD2) and showed consistency between the different cell lines. Two or more independent replicates were performed for each line.*

**Table S4. Influence of CHIR concentration on hiPSC- EC differentiation efficiency**

<i>CHIR concentration (6well plate)</i>	<i>Efficiency at day 10 (%)</i>
<i>2 <math>\mu</math>M</i>	<i>74.9</i>
<i>4 <math>\mu</math>M</i>	<i>77.5</i>
<i>6 <math>\mu</math>M</i>	<i>64.6</i>
<i>8 <math>\mu</math>M</i>	<i>50.5</i>
<i>10 <math>\mu</math>M</i>	<i>39.9</i>
<i>12 <math>\mu</math>M</i>	<i>51</i>
<i>18 <math>\mu</math>M</i>	<i>Cell death</i>

*Table S4: hiPSCs were cultured at an initial cell density of  $2.5 \times 10^4$  per well in a 6-well plate according to the combination 1, and different CHIR concentrations were tested for 2 days, followed by another 2 days in EBM medium supplemented with bFGF and VEGFA, then changed into EMV2 medium with VEGFA. Colony size ranged between  $>60 \mu\text{m}$  to  $>200 \mu\text{m}$  and was not controlled. The percentage of endothelial cell efficiency was determined by flow cytometry analysis of CD31+ VE-cadherin+ double positive cells. The data were generated from two independent hiPSCs cell lines (WTBLD and WTD2), and showed consistency between the different cell lines. Two or more independent replicates were performed for each line.*

**Table S5. Measurement of 3D Angiogenesis sprouting**

HCAEC1	HCAEC2	HCAEC3	HCAEC4	hiPSC-EC1	hiPSC-EC 2	hiPSC-EC 3	hiPSC-EC 4
68.75	88.57	35.06	48.08	81.02	40.99	165.87	94.36
52.70	31.47	33.69	37.78	68.51	92.98	67.93	92.18
54.03	43.62	37.37	92.32	48.39	62.14	53.47	79.50
48.51	62.69	62.53	94.86	65.62	55.43	52.55	112.85
36.75	46.80	65.80	43.75	62.91	78.46	72.87	
25.42		19.86	34.86	63.69			
56.61			42.00				
60.88							

Table S5: Endothelial cell spheroids assay was performed as a model of the *in vivo* basement membrane environment to induce vessel sprouts... Each column represents one endothelial cell spheroid, consisting either of HCAECs (columns 1-4) or of hiPSC-derived endothelial cells (columns 5-8). Sprout outgrowth was quantified by measuring the length of the sprouts. The data were generated from two independent hiPSCs cell lines (WTBLD and WTD2) and showed consistency between the different cell lines. There were no statistically significant differences between group means as determined by one-way ANOVA ( $F = 1.9037$ ,  $p = 0.09$ ).



Table S6. hiPSC cell lines which were used in this study.

iPSc name	Origin	Characterization	Publication	FACS <sup>1</sup>	Immunostaining <sup>2</sup>	qPCR	ECmatrix <sup>3</sup>	3D Angiogenesis <sup>4</sup>
WTD2	Healthy skin fibroblasts	yes	(Streckfuss-Bomeke et al., 2013)	yes	yes	yes	yes	yes
IC113	Healthy skin fibroblasts	yes	(Dudek et al., 2013)	yes	no	yes	yes	no
IsWTbid	Healthy peripheral blood mononuclear cells	yes	manuscript in preparation	yes	yes	yes	yes	yes

Note:

1. The samples were analyzed by FACS with the endothelial cell markers CD31 and VE-Cadherin.
2. The samples were analyzed by immunofluorescence staining with the endothelial cell markers CD31 and VE-Cadherin and vWF.
3. The samples were analyzed by real time PCR with endothelial cell markers CD31 and VE-Cadherin and vWF.
4. The samples were analyzed by tube formation assay (ECmatrix).
5. The samples were analyzed by 3D angiogenesis sprouting.

#### Detailed information for Table 1:

All the mentioned reagents in Table 1 are calculated according to the price of 2015: ES primate medium without bFGF (Stem Cell tech); N-2 Supplement (Life Tech); B27 (Life Tech); DMEMF12 (Life Tech); BIO (Sigma-Aldrich); StemPro-34 SFM (Life Tech); VEGF (R&D); CHIR99021 (Sigma-Aldrich); endothelial cell basal medium (Promo cell); bFGF (R&D); advanced DMEMF12 (Life Tech); L-Ascorbic acid (Sigma-Aldrich); mTeSR medium (Stem Cell tech); Rock inhibitor (R&D); BMP4 (R&D); Activin A (R&D); SB431542 (Tocris Bioscience); IMDM (Life Tech); PFHMI (Life Tech); Lipids (Life Tech); ITS (Life Tech); aMTG (Sigma-Aldrich); AA2P (Sigma-Aldrich).

## **2.2 Increased concentration of circulating angiogenesis and nitric oxide inhibitors induces endothelial to mesenchymal transition and myocardial fibrosis in patients with chronic kidney disease**

*Chronic kidney disease (CKD) patients have a high risk of suffering from cardiovascular disease. According to previous studies, circulating angiogenesis and NO (nitrogen oxide) inhibitors were proposed to play a role in the development of cardiovascular disease within CKD patients. In this study, our aim was to verify if these factors are elevated in a cohort of patients with CKD and what the effect of these factors is on coronary endothelial cells, in order to unravel the association between CKD and cardiac fibrosis. Therefore, the circulating angiogenesis and NO inhibitors including asymmetric ADMA (asymmetric dimethyl arginine), END (endostatin), ANG (angiopoietin) and TSP (thrombospondin) were measured in CKD patients' blood serum, and cardiac fibrosis and capillary density were analyzed in heart tissue of CKD patients. The data implied that the severity of CKD correlates with increasing concentrations of circulating angiogenesis and NO inhibitors. Furthermore, HCAEC were used for testing if these inhibitors could induce EndMT, which might contribute to the generation of myocardial fibrosis in patients with CKD. The results concluded that increased concentration of circulating angiogenesis and NO inhibitors could promote EndMT and cardiac fibrosis in CKD patients.*

### **2.2.1 Declaration of my contribution**

*Xiaoepng Liu: data analysis and interpretation, performed experiments of serum treatments of HCAEC and gene expression analysis.*



Contents lists available at ScienceDirect

International Journal of Cardiology

journal homepage: [www.elsevier.com/locate/ijcard](http://www.elsevier.com/locate/ijcard)

## Increased concentration of circulating angiogenesis and nitric oxide inhibitors induces endothelial to mesenchymal transition and myocardial fibrosis in patients with chronic kidney disease



David M. Charytan<sup>a,\*</sup>, Robert Padera<sup>b</sup>, Alexander M. Helfand<sup>a</sup>, Michael Zeisberg<sup>c</sup>, Xingbo Xu<sup>d</sup>, Xiaopeng Liu<sup>d</sup>, Jonathan Himmelfarb<sup>e</sup>, Angeles Cinelli<sup>a</sup>, Raghu Kalluri<sup>f</sup>, Elisabeth M. Zeisberg<sup>d,g</sup>

<sup>a</sup> Renal Division, Department of Medicine, Brigham & Women's Hospital, Boston, MA, United States

<sup>b</sup> Department of Pathology, Brigham & Women's Hospital, Boston, MA, United States

<sup>c</sup> Department of Nephrology and Rheumatology, Georg-August University, Göttingen, Germany

<sup>d</sup> Department of Cardiology and Pneumology, University Medical Center, Georg-August University, Göttingen, Germany

<sup>e</sup> Department of Medicine, University of Washington School of Medicine, MD Anderson Cancer Center, Houston, TX, United States

<sup>f</sup> Department of Cancer Biology, MD Anderson Cancer Center, Houston, TX, United States

<sup>g</sup> DZHK (German Centre for Cardiovascular Research), partner site Göttingen, Germany

### ARTICLE INFO

#### Article history:

Received 9 April 2014

Received in revised form 19 May 2014

Accepted 28 June 2014

Available online 6 July 2014

#### Keywords:

CKD

ESRD

Fibrosis

Endothelial to mesenchymal transition

Cardiovascular disease

Angiogenesis inhibitor

### ABSTRACT

**Background:** Sudden cardiovascular death is increased in chronic kidney disease (CKD). Experimental CKD models suggest that angiogenesis and nitric oxide (NO) inhibitors induce myocardial fibrosis and microvascular dropout thereby facilitating arrhythmogenesis. We undertook this study to characterize associations of CKD with human myocardial pathology, NO-related circulating angiogenesis inhibitors, and endothelial cell behavior.

**Methods:** We compared heart ( $n = 54$ ) and serum ( $n = 162$ ) samples from individuals with and without CKD, and assessed effects of serum on human coronary artery endothelial cells (HCAECs) in vitro. Left ventricular fibrosis and capillary density were quantified in post-mortem samples. Endothelial to mesenchymal transition (EndMT) was assessed by immunostaining of post-mortem samples and RNA expression in heart tissue obtained during cardiac surgery. Circulating asymmetric dimethylarginine (ADMA), endostatin (END), angiotensin-2 (ANG), and thrombospondin-2 (TSP) were measured, and the effect of these factors and of subject serum on proliferation, apoptosis, and EndMT of HCAEC was analyzed.

**Results:** Cardiac fibrosis increased 12% and 77% in stage 3–4 CKD and ESRD and microvascular density decreased 12% and 16% vs. preserved renal function. EndMT-derived fibroblast proportion was 17% higher in stage 3–4 CKD and ESRD ( $P_{\text{trend}} = 0.02$ ). ADMA, ANG, TSP, and END concentrations increased in CKD. Both individual factors and CKD serum increased HCAEC apoptosis ( $P = 0.02$ ), decreased proliferation ( $P = 0.03$ ), and induced EndMT. **Conclusions:** CKD is associated with an increase in circulating angiogenesis and NO inhibitors, which impact proliferation and apoptosis of cardiac endothelial cells and promote EndMT, leading to cardiac fibrosis and capillary rarefaction. These processes may play key roles in CKD-associated CV disease.

© 2014 Elsevier Ireland Ltd. All rights reserved.

### 1. Introduction

Individuals with chronic kidney disease (CKD) have high risks of developing and dying from cardiovascular (CV) disease and these risks are not fully explained by traditional risk factors [1]. Strong associations of

novel factors with CV events, a failure of standard therapies to substantially impact mortality in advanced CKD, and an outside risk of sudden death relative to myocardial infarction suggest that unique features underlie CVD in the setting of uremia [2].

Experimental models of uremia are characterized by myocardial fibrosis, loss of myocardial capillaries, and inhibition of ischemia driven neo-angiogenesis [3,4]. These changes increase capillary to myocyte distance, alter oxygen delivery, and disrupt myocardial conduction, thereby facilitating propagation of arrhythmias. Experimental studies also demonstrate altered nitric oxide (NO) bioavailability in uremia [5] which may induce secondary changes in the activity and concentration of additional angiogenesis inhibitors [6–8] thereby contributing to the observed myocardial fibrosis and capillary rarefaction. However, similar

**Abbreviations:** ADMA, asymmetric dimethyl arginine; ANG, angiotensin-2; CKD, chronic kidney disease; END, endostatin; EndMT, endothelial to mesenchymal transformation; ESRD, end stage renal disease; HCAECs, human coronary artery endothelial cells; NO, nitric oxide; TSP, thrombospondin-2.

\* Corresponding author at: Renal Division, Brigham & Women's Hospital, 1620 Tremont Street, 3rd Floor, Boston, MA 02120, United States. Tel: +1 617 525 7718; fax: +1 617 525 7752.

E-mail address: [dcharytan@partners.org](mailto:dcharytan@partners.org) (D.M. Charytan).

<http://dx.doi.org/10.1016/j.ijcard.2014.06.062>

0167-5273/© 2014 Elsevier Ireland Ltd. All rights reserved.

**Table 1**  
Baseline characteristics of the autopsy cohort.

Characteristic N (%)	Preserved function (N = 21)	Stage 3–4 CKD (N = 17)	Dialysis (N = 7)	P value*
<b>Demographics</b>				
Age (years), mean ± SD	58.0 ± 15.2	72.8 ± 10.5	66.6 ± 5.6	0.003
Male sex	12 (57.1)	9 (52.9)	5 (71.4)	0.70
<b>Race</b>				
White	16 (76.2)	13 (76.5)	3 (42.9)	0.33
Black	3 (14.3)	3 (17.7)	3 (42.9)	
<b>Labs (mean ± SD)</b>				
eGFR, mL/min/1.73 m <sup>2</sup>	101.7 ± 34.2	37.6 ± 16.2	2.0 ± 0.0	<0.001
Serum creatinine, mg/dL	70.7 ± 26.5	203.3 ± 159.1	707.2 ± 0.0	<0.001
<b>Medical history</b>				
Diabetes	2 (9.5)	10 (58.8)	6 (85.7)	<0.001
Hypertension	16 (76.2)	14 (82.4)	7 (100.0)	0.36
Coronary disease	6 (28.6)	7 (41.2)	5 (71.4)	0.13
Myocardial infarction	4 (19.1)	7 (41.2)	4 (57.1)	0.12
Atrial fibrillation	3 (15.0)	5 (29.4)	0 (0.0)	0.21
Congestive heart failure	2 (9.5)	5 (29.4)	3 (42.9)	0.12
Obesity	5 (23.8)	5 (29.4)	2 (28.6)	0.92
Hyperlipidemia	7 (33.3)	12 (75.0)	5 (71.4)	0.03
History of cancer	1 (4.8)	3 (17.7)	0 (0.0)	0.26
Anemia	3 (15.0)	8 (53.3)	4 (57.1)	0.03
Past or present smoking	11 (61.1)	8 (50.0)	2 (28.6)	0.34
Number of diseased coronary arteries (mean ± SD)*	1.4 ± 1.5	1.7 ± 1.2	1.9 ± 1.2	0.71
<b>Cause of death</b>				
Infection	5 (23.8)	5 (29.4)	3 (42.9)	0.51
Cardiovascular	6 (28.6)	8 (47.1)	2 (28.6)	
Other	10 (47.6)	4 (23.5)	2 (28.6)	
<b>Medications</b>				
Aspirin	5 (25.0)	10 (58.8)	6 (85.7)	0.01
ACE or ARB	6 (30.0)	9 (56.3)	3 (42.9)	0.28
Statin	7 (35.0)	9 (52.9)	5 (71.4)	0.22
Beta blocker	10 (50.0)	10 (58.8)	5 (83.3)	0.35

SD = standard deviation. eGFR—estimated GFR. \*ANOVA and non-parametric trend test for normally and non-normally distributed continuous variables, respectively. X<sup>2</sup> tests for count variables. \*Percent stenosis assessed pathologically was available for 17 patients with preserved function, 16 with Stage 3–4 CKD, and 7 on dialysis. Smoking status was missing in 4 individuals (preserved GFR-3, Stage 3–4 CKD-1). All dialysis patients were on hemodialysis.

data in human disease remains sparse. We undertook this study to characterize for the first time changes in human myocardial pathology across the spectrum of CKD and assess associations with NO-related circulating angiogenesis inhibitors and their effects on human coronary artery endothelial cells (HCAECs).

## 2. Materials and methods

### 2.1. Autopsy cohort

Autopsies performed at Brigham & Women's Hospital (BWH) between 2004 and 2006 (n = 45) were included. Cases without sufficient data to estimate kidney function, history of acute kidney injury lasting >1 week, cardiac transplant, active cancer, prior thoracic

irradiation, treatment with anthracyclines, congenital heart disease, idiopathic or viral cardiomyopathy, or insufficient tissue were excluded. Medical history and laboratory data were extracted from clinical records. Kidney function was estimated from outpatient serum creatinine or from the lowest stable value (replicated on ≥2 occasions) if outpatient values within 4 months were unavailable.

### 2.2. Serologic cohort

Individuals 18–80 years old were recruited from the coronary angiography and outpatient nephrology clinics at BWH (n = 162). Individuals with acute kidney injury, history of thoracic radiation, malignancy, receiving anti-angiogenic or immunosuppressive therapy, or requiring urgent angiography were excluded. Angiography subjects were excluded if they had a history of coronary bypass surgery. Serum and plasma were collected prior to angiography, centrifuged within 15 min at 1000 g, and stored at −80 °C. Clinical data

**Table 2**  
Histologic findings.

Characteristic mean ± SD	Preserved function-stage 1 CKD (N = 21)	Stage 3–4 CKD (N = 17)	Dialysis (N = 7)	P <sub>trend</sub>
<b>Histology</b>				
Fibrosis (%)	10.6 ± 4.8	11.9 ± 4.5	18.2 ± 6.6	0.003
Microvessels/field	459.1 ± 110.1	402.4 ± 69.7	386.9 ± 77.5	0.04
Cardiomyocytes/field	615.8 ± 214.3	573.2 ± 99.4	550.3 ± 121.9	0.31
Microvessel density (n/μM <sup>2</sup> )	612.2 ± 146.7	536.6 ± 92.9	515.8 ± 103.3	0.04
Myocyte size (μM <sup>2</sup> )	623.3 ± 222.8	645.4 ± 197.4	595.4 ± 222.6	0.90
Myocyte density (n/μM <sup>2</sup> )	821.0 ± 285.8	764.3 ± 132.5	733.8 ± 162.5	0.31
Vessels per myocyte	0.80 ± 0.19	0.73 ± 0.16	0.74 ± 0.18	0.24
<b>Immunofluorescence</b>				
FSP positive cells/field	(N = 11) 4.2 ± 1.4	(N = 8) 4.1 ± 2.0	(N = 4) 6.6 ± 0.7	0.04
Double FSP/CD-31 positive cells/field	0.9 ± 0.7	1.4 ± 0.7	2.3 ± 1.3	0.01
Ratio of double positive to all FSP-positive cells	0.19 ± 0.12	0.36 ± 0.11	0.36 ± 0.21	0.02

SD = standard deviation.

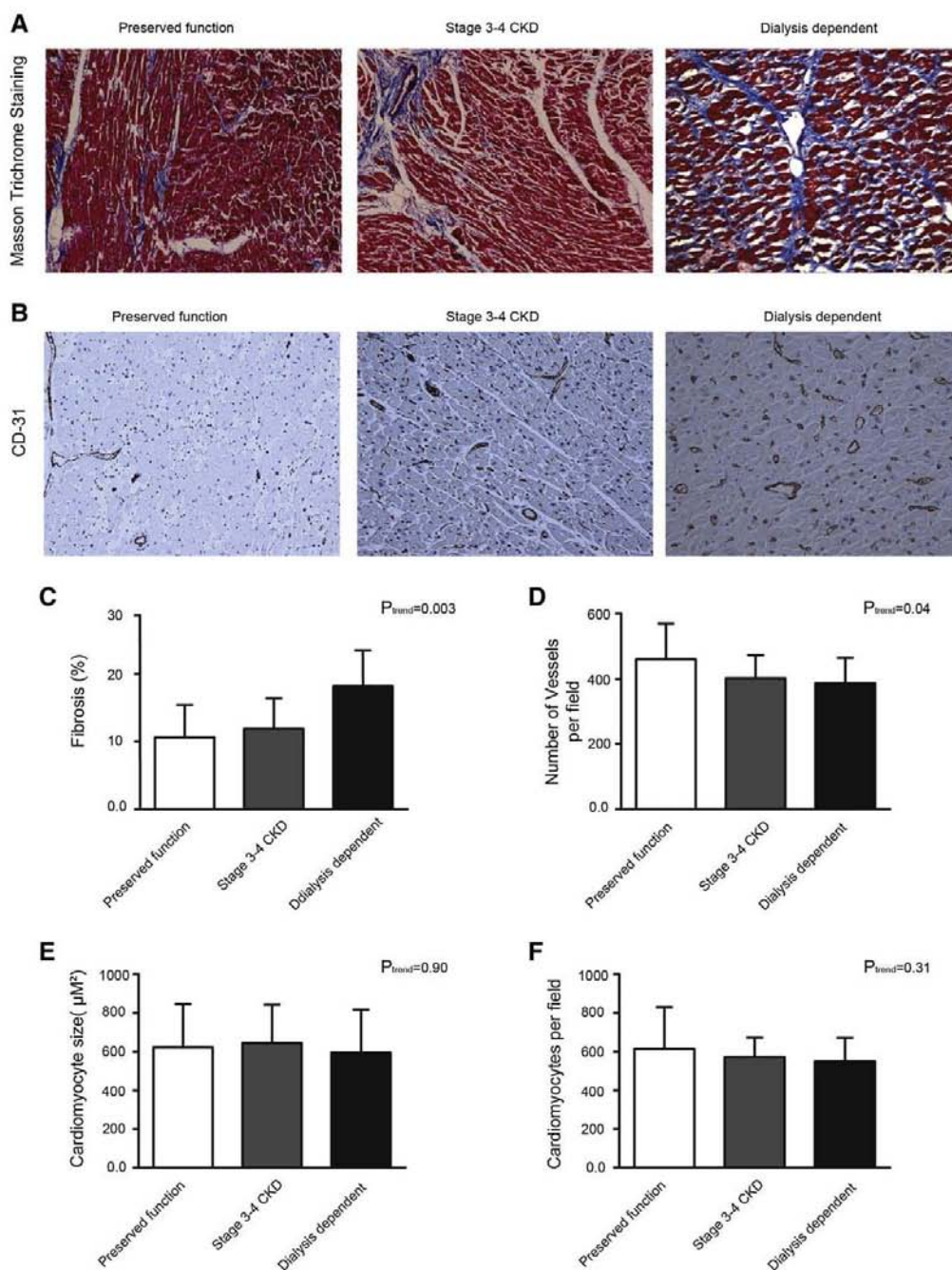


**Fig. 1.** Evaluation of fibrosis and microvessels in the LV. (A) Pictures show representative left ventricular sections stained with Masson-Trichrome to visualize fibrotic tissue (stained in blue). (B) Pictures show immunohistochemical anti-CD31 staining to label microvessels (stained in brown). (A, B) Left images show heart tissue from an individual with preserved GFR, middle images from a patient with stage 3–4 CKD, and right images from a dialysis patient. (C–F) Quantitative analysis of Masson-Trichrome and anti-CD31 stained sections from  $n = 21$  preserved GFR,  $n = 17$  stage 3–4 CKD, and  $n = 7$  dialysis patients for (C) fibrosis, (D) microvascular density, (E) myocyte size, and (F) myocyte density.



were obtained through interview and chart review. Serum creatinine, albumin, and hemoglobin were measured on the day of enrollment in the clinical laboratory. Cholesterol and urinary albumin and creatinine measurements within 6 months prior to enrollment were also recorded but urine was not collected.

In both cohorts, estimated glomerular filtration rate (eGFR) was calculated using the modified MDRD equation [9]. Given the sample size, individuals with preserved renal function and eGFR  $\geq 90$  (prospective cohort) or  $\geq 60$  mL/min/1.73 m<sup>2</sup> (autopsy) were considered jointly as preserved function/stage 1 or 1–2 CKD, according to standard definitions [10]. Stage 3–4 CKD was similarly combined. Patients with dialysis dependent ESRD were assigned a creatinine of 8.0 mg/dL (707.2  $\mu$ mol/L) and eGFR of 2 mL/min/1.73 m<sup>2</sup>.

### 2.3. Cardiac surgery cohort

Right atrial appendage was harvested as discarded tissue from 9 individuals undergoing non-emergent cardiac surgery. Appendages were snap frozen and stored at  $-80^{\circ}\text{C}$ . Renal function was estimated using pre-operative measurements of serum creatinine and clinical history was obtained via interview and chart review.

### 2.4. Circulating factors

Samples were batch analyzed in duplicate for serum endostatin (END) and angiotensin-2 (ANG) using Quantikine® ELISA (R&D Systems) with intra- and inter-assay coefficient of variations (CV)  $<7.0\%$  and  $10.5\%$ . Thrombospondin-2 (TSP) was measured using Luminex® assays (R&D Systems) with CVs  $<8.7\%$  and  $16.4\%$ , respectively. Plasma asymmetric dimethyl arginine (ADMA) was measured by HPLC as described by Teerlink [11] (intra and inter-assay CV  $<3.5\%$ ).

### 2.5. Microscopic analyses

Microscopic analyses were blinded. Five  $\mu\text{m}$  paraffin-embedded left ventricular (LV) sections were stained with hematoxylin or Masson's trichrome. After microscopic review to exclude infarcted myocardium, sections were incubated with phosphate buffered saline (negative control) or anti-CD31 antibodies (Pharmingen), followed by anti-rat or Envision™ anti-rabbit secondary antibodies (Dako), and developed with DAB (Dako).

An Olympus BX41 microscope and camera were used to capture digital images. Image Pro 6.2 (Media Cybernetics) was used to digitally label blue pixels and measure collagen deposition as the percentage of the total myocardium within  $\geq 10$  representative fields ( $100\times$  magnification). Microvascular density was measured at  $200\times$  ( $\geq 10$  fields/case). Myocytes and CD-31 positive, tubular structures of appropriate diameter were manually counted using digital calipers. Pixels enclosed within each cell were labeled, and the area occupied was measured.

Endothelial to mesenchymal transition (EndMT) was assessed in 5  $\mu\text{m}$  paraffin sections by double labeling with endothelial (CD31) and fibroblast (FSP1) markers. Following antigen retrieval in proteinase K (Dako) at  $37^{\circ}\text{C}$ , sections were incubated with anti-CD31 (Dako) and anti-FSP1 (Dako) and fluorescent-conjugated secondary antibodies (Invitrogen) and counterstained with DAPI (Invitrogen and/or Vector Labs). Sections were examined at  $630\times$  using confocal microscopy (Zeiss).

### 2.6. RNA extraction and quantitative PCR (qPCR) for EndMT

Total RNA was extracted using Trizol Reagent (Life technologies). RNA purification was performed using a PureLink RNA Mini Kit (Ambion) following the manufacturer's protocol. 250 ng of total RNA was digested with DNaseI (Sigma) and used for cDNA synthesis using Superscript II Reverse Transcriptase (Life Technologies) according to manufacturer's instructions. For qPCR analysis, diluted cDNA (1/10) was used as a template in a Fast SYBR Green Master Mix (Life Technologies) and run in StepOne Plus Instrument (Life Technologies). Primers were designed and purchased from PrimerDesign. TWIST, SLUG, and SNAIL RNA expression were measured as indices of EndMT [12]. All qPCR data for RNA expression analysis (two or more biological replicates with three technical replicates each) were calculated using the delta delta Ct method and standardized to the reference gene GAPDH expression.

### 2.7. Proliferation, apoptosis, and EndMT assays

HCAECs (Lonza), passage 5, were seeded at  $37^{\circ}\text{C}$  in  $5\%$  CO<sub>2</sub> on 96-well polystyrene plates (Becton Dickinson, Falcon) at  $8 \times 10^4$  cells/mL in EBM-2 medium (Lonza) supplemented with  $2\%$  fetal bovine serum (FBS, Sigma). After 24 h, medium was replaced and cells were cultured in duplicate for 24 h in  $2\%$  subject serum or in triplicate with  $2\%$  FBS spiked with physiologic concentrations of ADMA (Sigma), recombinant human END (Prospec Bio, Sigma), ANG, or TSP (both from R&D Systems). A proliferation detection

agent, WST-1 (Roche), was added after 20 h and cells were cultured an additional 4 h before measurement on a Versamax™ microplate reader (Molecular Devices) at 440 nm.

Apoptosis was measured in triplicate on HCAEC passage 5–7 on opaque polystyrene plates (Costar) using  $5\%$  FBS. Medium was replaced after 24 h with  $5\%$  subject serum or  $5\%$  FBS spiked with ADMA or recombinant factors. Human TNF- $\alpha$  (0.5–20 ng/mL, Promega) was used as a positive control. After 21 h, Caspase-Glo 3/7 Reagent (Promega) was added and plates were incubated at room temperature for 3 h. Luminescence was measured with a Spectramax-M5 microplate reader (Molecular Devices).

EndMT was measured in triplicate on HCAEC passage 5–7. As above, medium was replaced after 24 h and spiked with ADMA or recombinant factors. Cells were harvested after 48 h and total RNA was analyzed as above.

### 2.8. Statistical analysis

Data are presented as mean  $\pm$  standard deviation (SD), n (%) or median (inter-quartile range, IQR). Baseline differences were compared using ANOVA and non-parametric trend tests for continuous data and Chi-square tests for count data. Outcome variables including END, TSP, ANG and ADMA concentrations were logarithmically transformed to preserve normality. Differences across categories of CKD were assessed with ANOVA and the post-hoc Tukey–Kramer test to assess pairwise differences and non-parametric trend tests or orthogonal polynomial regression to assess trends. Continuous correlations were measured with the Pearson coefficient. Multivariable linear regression models were constructed to adjust for confounding factors. Model fit was tested graphically, by inspecting residuals, and by testing model specification. Analyses were performed in STATA 9.0 and 13.0 (STATA Corp.) with  $P < 0.05$  considered significant.

## 3. Results

### 3.1. Evaluation of cardiac fibrosis

The risk of sudden cardiac death increases dramatically as GFR declines [13]. Sudden cardiac death and overall mortality on the other hand are strongly associated with the presence of cardiac fibrosis [14]. We therefore aimed to systematically evaluate amount of cardiac fibrosis over various stages of CKD by analyzing heart tissue obtained from autopsy.

Among our autopsy cohort of 45 individuals, we identified 21 subjects with preserved kidney function, 17 with stage 3–4 CKD, and 7 with ESRD (Table 1). Mean eGFR was  $101.7 \pm 34.2$  in the group with preserved kidney function and  $37.6 \pm 16.2$  mL/min/1.73 m<sup>2</sup> in those with stage 3–4 CKD. Individuals with ESRD ( $66.6 \pm 5.6$  years) and stage 3–4 CKD ( $72.8 \pm 10.5$ ) were older than individuals with preserved function ( $58.0 \pm 15.2$ ,  $P = 0.003$ ). Diabetes ( $P < 0.001$ ) and hyperlipidemia ( $P = 0.03$ ) were more frequent, and there were non-significant trends towards a higher frequency of coronary disease ( $P = 0.13$ ) and prior MI ( $P = 0.12$ ) as CKD progressed.

The extent of interstitial fibrosis increased by 12% and 77% in individuals with stage 3–4 CKD and ESRD, respectively ( $P_{\text{trend}} = 0.003$ , Table 2 and Fig. 1A, C and G). Microvascular supply decreased by 12% and 16% in stage 3–4 CKD and ESRD, respectively ( $P_{\text{trend}} = 0.04$ , Fig. 1D–F, H). Associations between CKD group and percent fibrosis ( $P = 0.04$ ) or microvascular supply ( $P = 0.03$ ) remained significant in models adjusting for age, sex, diabetes, and hypertension, and in models adjusting for anemia or the use of either angiotensin converting enzyme inhibitors or angiotensin receptor blockers (Supplementary Tables A.2 and A.3). Numerical decreases in cardiomyocyte density were not significant (Fig. 1I, J). The number of fibroblasts (detected by FSP-1 positivity on confocal microscopy, Fig. 2) increased with CKD severity and was 57% higher with ESRD than with preserved renal function ( $P_{\text{trend}} = 0.04$ , Fig. 2A, B). Given the concurrent fibrosis and microvascular rarefaction, we analyzed the fibroblast-population derived from endothelial to mesenchymal

**Fig. 2** EndMT in the heart: Confocal microscopy and qPCR expression analysis. (A) Representative confocal images of left ventricular tissue after immunofluorescent staining with antibodies for the fibroblast marker FSP1 (green) and endothelial cell marker CD31 (red). Nuclei are stained with DAPI (blue). Top row shows tissue from an individual with preserved renal function, middle row from a patient with stage 3–4 CKD, and the bottom row from a dialysis patient. Dual FSP1/CD31 positive cells, indicative of EndMT (arrows), increase with decreasing renal function. Magnification  $\times 63$ . (B–D) Quantitative analysis of  $n = 11$  preserved GFR,  $n = 8$  stage 3–4 CKD, and  $n = 4$  dialysis patients for (B) FSP+ cells/visual field, (C) FSP1/CD-31 double positive cells/visual field, indicative of cells undergoing EndMT. (D) Ratio of FSP1/CD31 double positive cells to all FSP+ cells, indicative of the fraction of EndMT-derived FSP1-positive fibroblasts. (E, F, G) Bar graphs show quantitative real time PCR for EndMT marker genes SLUG (E), SNAIL (F), and TWIST (G) in right atrial appendage of individuals with preserved function ( $n = 3$ ), with CKD stage 3–4 ( $n = 3$ ), and dialysis patients ( $n = 3$ ).

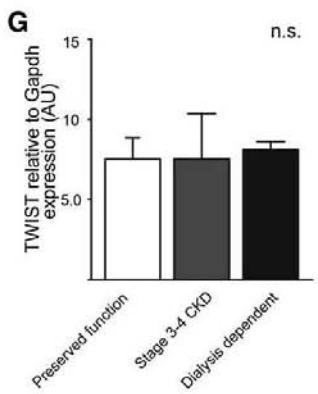
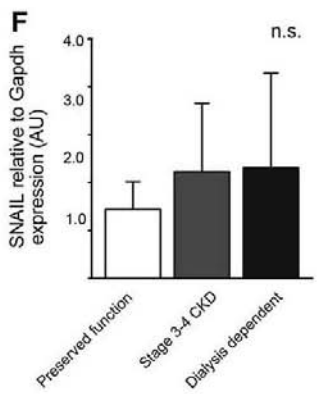
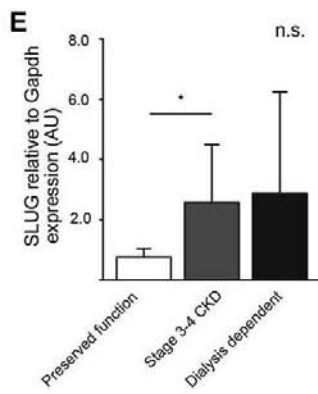
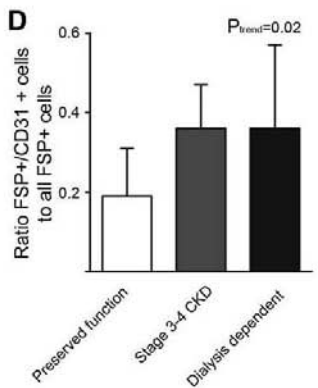
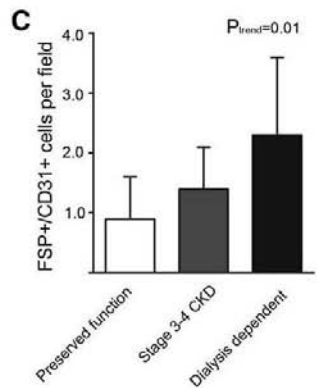
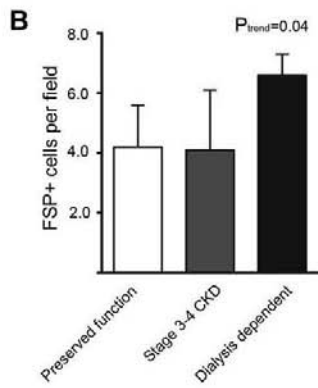
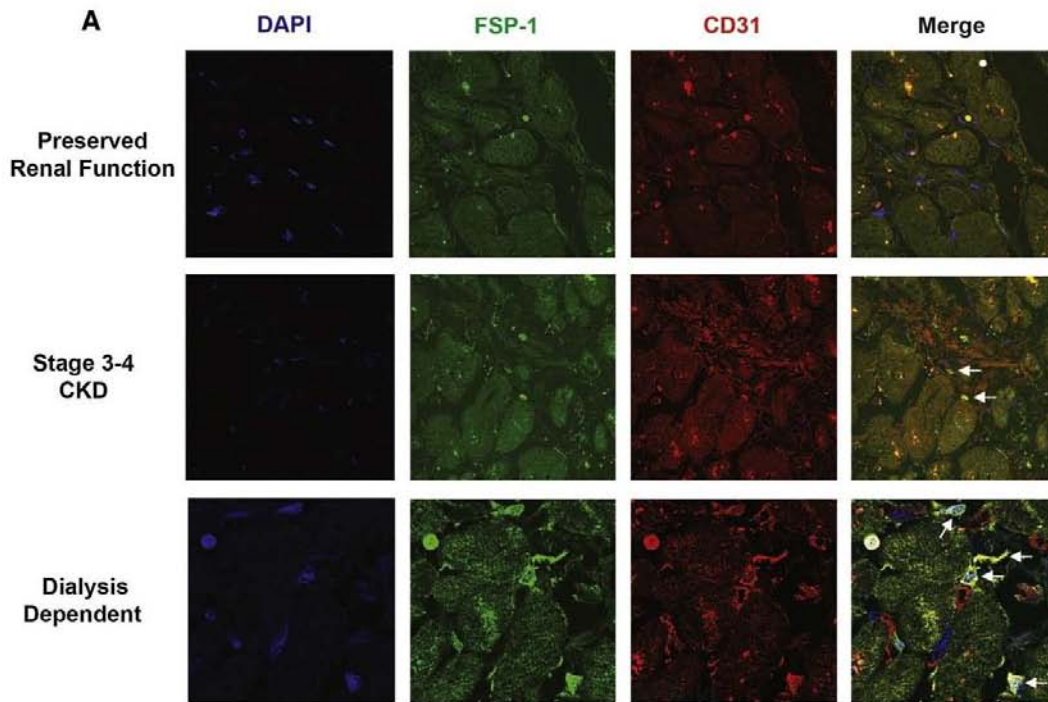




**Table 3**  
Baseline characteristics of the serologic cohort.

Characteristic N (%)	Preserved function (N = 30)	Stage 2 CKD (N = 58)	Stage 3–4 CKD (N = 60)	Stage 5 CKD (N = 14)	P value <sup>a</sup>
<b>Demographics</b>					
Age (years), mean ± SD	57.2 ± 8.3	61.1 ± 11.4	67.0 ± 11.8	48.9 ± 20.0	<0.001
Male sex	23 (76.7)	38 (65.5)	40 (66.7)	5 (35.7)	0.07
Race					0.01
White	26 (86.7)	45 (79.0)	46 (79.3)	5 (35.7)	
Black	3 (10.0)	7 (12.3)	5 (8.6)	6 (42.9)	
Other	1 (3.3)	5 (8.7)	7 (12.0)	3 (21.4)	
<b>Labs and physical exam</b>					
eGFR (mL/min/1.73 m <sup>2</sup> ), mean ± SD	105.4 (11.8)	74.3 ± 8.0	38.5 ± 13.4	4.3 ± 4.3	<0.001
Serum creatinine (mg/dL), median (IQR)	70.7 (62.2–79.5)	88.4 (79.6–106.1)	150.3 (123.8–221.0)	707.2 (707.2–707.2)	<0.001
Systolic pressure (mm Hg), mean ± SD	128.1 ± 24.2	123.3 ± 19.8	132.8 ± 21.5	138.3 ± 21.0	0.05
Diastolic pressure (mm Hg), mean ± SD	73.7 ± 13.2	69.9 ± 11.9	69.6 ± 16.0	77.4 ± 18.7	0.25
<b>Medical history</b>					
Dialysis-dependent	0 (0.0)	0 (0.0)	0 (0.0)	10 (71.4)	<0.001
Diabetes	9 (30.0)	18 (31.0)	37 (61.7)	6 (42.9)	0.003
Hypertension	21 (70.0)	42 (72.4)	50 (83.3)	14 (100.0)	0.07
Myocardial infarction	6 (20.0)	16 (27.6)	14 (23.3)	4 (33.3)	0.77
Congestive heart failure	4 (13.3)	14 (24.1)	17 (28.3)	5 (35.7)	0.33
Obstructive lung disease	0 (0.0)	2 (3.5)	6 (10.0)	1 (14.3)	0.12
Peripheral vascular disease	2 (6.7)	3 (5.2)	11 (18.3)	2 (14.3)	0.11
Hyperlipidemia	22 (73.3)	41 (70.7)	42 (70.0)	10 (71.4)	0.99
Current smoking	4 (14.8)	6 (10.9)	2 (3.5)	1 (8.3)	0.30
Anemia	3 (10.3)	12 (21.4)	29 (50.9)	9 (64.3)	<0.001
Cause of CKD					<0.001
Other/unknown	–	–	39 (65.0)	3 (21.4)	
Diabetes	–	–	12 (20.0)	4 (28.6)	
Hypertension	–	–	7 (11.7)	2 (14.3)	
Glomerulonephritis	–	–	1 (1.7)	5 (35.7)	
Renal artery stenosis	–	–	1 (1.7)	0 (0.0)	
<b>Medications</b>					
Aspirin	25 (83.3)	43 (74.1)	44 (73.3)	7 (50.0)	0.14
ACE or ARB	15 (50.0)	29 (50.0)	37 (61.7)	10 (71.4)	0.33
Statin	23 (76.7)	38 (65.5)	45 (75.0)	8 (57.1)	0.39
Beta blocker	18 (60.0)	38 (65.5)	45 (75.0)	8 (57.1)	0.38

SD = standard deviation, eGFR = estimated glomerular filtration rate, CKD = chronic kidney disease, IQR = interquartile range, ACE=angiotensin converting enzyme inhibitor, ARB=angiotensin receptor blocker. Race was missing in 1 participant. Smoking status was missing in 10%.

<sup>a</sup> ANOVA and non-parametric trend test for normally and non-normally distributed continuous variables, respectively.  $\chi^2$  tests for count variables.

transition (as evidenced by dual-positivity for FSP-1 and CD-31), as this mechanism potentially accounts for both findings. The proportion of CD31/FSP1 double positive fibroblasts likely derived from EndMT was 17% higher in stage 3–4 CKD and ESRD compared to preserved renal function ( $P_{\text{trend}} = 0.01$ ). Continuous measures of eGFR (mL/min/1.73 m<sup>2</sup>) were correlated with fibrosis, the number of microvessels/cross-sectional field, myocyte density, and the ratio of double-positive to all FSP-1<sup>+</sup> cells/field (Supplementary Table A.1).

In order to further investigate the confocal microscopy findings from the post-mortem samples suggesting an increase in myocardial EndMT with progressive renal impairment we performed expression analysis of EndMT marker genes using snap frozen atrial appendage tissue harvested from 9 individuals—3 with preserved renal function, 3 with CKD, and 3 with ESRD—undergoing cardiac surgery. Despite the small sample size, the results were suggestive of an increase in SLUG, TWIST and SNAIL expression consistent with an increase in myocardial EndMT with worsening renal function (Fig. 2E–G).

### 3.2. Effects of uremic serum on human coronary endothelial cells

We aimed to test whether uremic serum could mediate such EndMT. Among 162 individuals enrolled in our serologic cohort, 30 had preserved renal function, 58 stage 2, 60 stage 3–4, and 14 stage 5 CKD, the majority of whom were on dialysis (Table 3). Compared

to the individuals with preserved function (57.2 ± 8.3 years old), age was higher in subjects with stage 2 (61.1 ± 11.4 years) and with stage 3–4 CKD (67.0 ± 11.8 years) but was decreased among the individuals with stage 5 CKD (48.9 ± 20.0 years,  $P < 0.001$ ). Diabetes ( $P = 0.003$ ) and hypertension ( $P = 0.07$ ) were more frequent with more advanced CKD (Table 3).

We first assessed if serum from patients with CKD affected human coronary endothelial cells differently than serum from healthy individuals. Upon treatment with CKD serum, cell number decreased and HCAECs changed towards more spindle-shaped cell morphology as compared to treatment with serum from healthy individuals (Fig. 3A). Accordingly, quantification of apoptosis showed an increase ( $P_{\text{trend}} = 0.02$ ) while proliferation of HCAEC decreased ( $P_{\text{trend}} = 0.03$ ) after incubation in serum from individuals with more severe CKD (Table 4, Fig. 3C–D). In addition, exposure to serum from individuals with more severe CKD also increased expression of the EndMT-related transcripts TWIST ( $P_{\text{trend}} = 0.03$ ) and SNAIL in HCAEC ( $P_{\text{trend}} = 0.012$ , Fig. 3F–G).

### 3.3. Serologic factors affecting human coronary endothelial cells in CKD

In CKD the overall production of NO is decreased [5]. Several serologic factors have been found to be associated with both lower NO and increased cardiovascular disease in animal models, such as the NO-synthase inhibitor ADMA and the angiogenesis inhibitors ANG, TSP and END [6–8,15–23]. In order to identify specific serologic



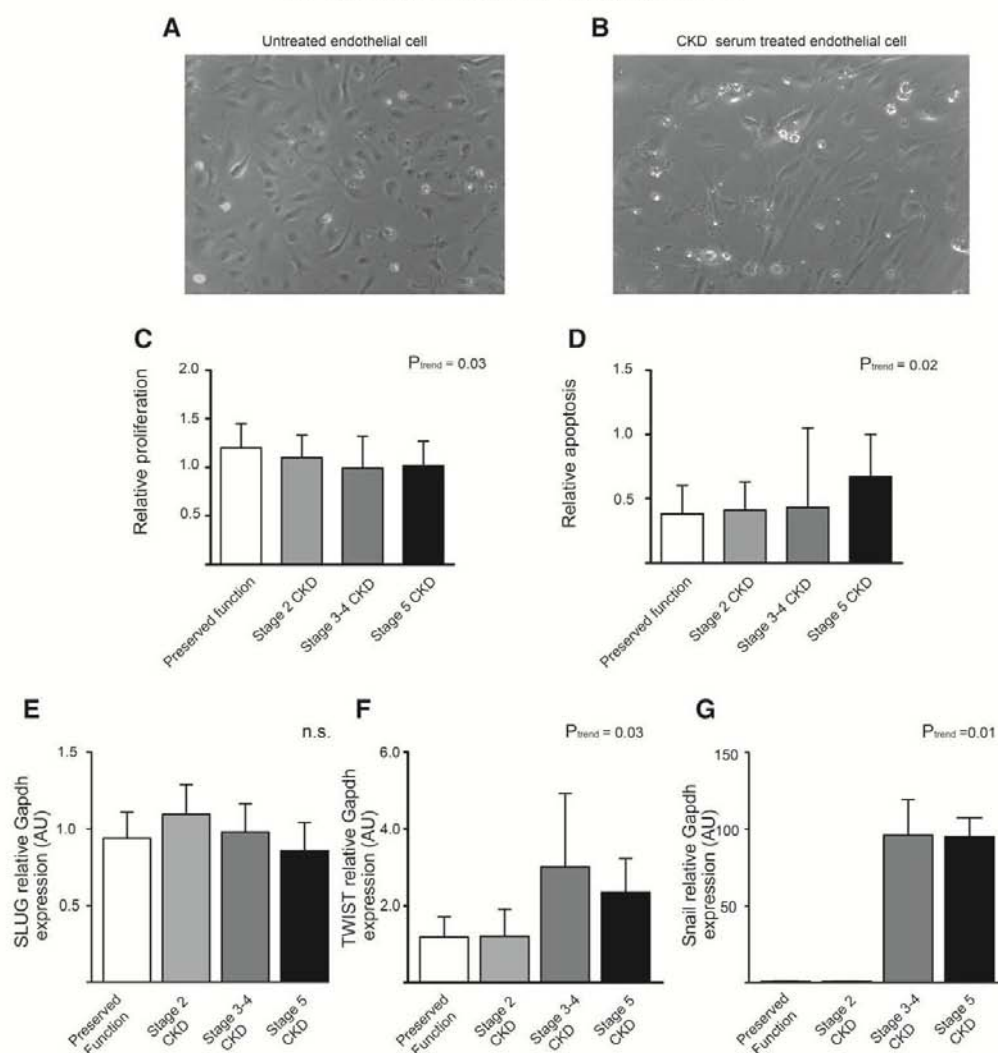


**Fig. 3.** Effect of CKD serum on human coronary artery endothelial cells (HCAECs): proliferation, apoptosis, and EndMT. (A, B) Representative light microscopy images of HCAEC after 6 days of incubation with serum from subjects with preserved renal function (A) and with CKD (B). Medium with serum was changed every other day. Number of cells decreased upon CKD serum incubation and cell morphology of surviving cells changed towards more spindle shaped as compared to incubation with serum from an individual with preserved renal function. (C, D) HCAECs were incubated with serum from individuals with preserved renal function ( $n = 30$ ), or from CKD patients stage 2 ( $n = 58$ ), stage 3–4 ( $n = 60$ ), or stage 5 ( $n = 14$ ), and relative apoptosis (as assessed by the Caspase-Glo 3/7 assay) and proliferation (as assessed by the WST-1 assay) were measured. (C) Relative proliferation of HCAECs decreased with more severe CKD. (D) Relative apoptosis of HCAEC increased with increasing CKD severity. (E–G) Bar graphs show quantitative real time PCR for EndMT marker genes *SLUG* (E), *SNAIL* (F), and *TWIST* (G) (all relative to *GAPDH*) in HCAEC upon incubation with healthy ( $n = 3$ ) versus CKD ( $n = 9$ , 3 per stage) serum. Both *TWIST* and *SNAIL* are increased upon incubation with serum from CKD stages 3 through 5.

**Table 4**  
Factor concentrations, HCAEC apoptosis, and proliferation.

Factor, median (IQR)	Preserved function (N = 30)	Stage 2 CKD (N = 58)	Stage 3–4 CKD (N = 60)	Stage 5 CKD (N = 14)	P value <sup>a</sup>
Log endostatin, (ng/mL)	4.5 ± 0.3	4.7 ± 0.5	5.4 ± 0.4 <sup>b</sup>	6.7 ± 0.4 <sup>b</sup>	<0.001
Log thrombospondin-2, (pg/mL)	9.9 ± 0.6	9.9 ± 0.5	10.3 ± 0.6 <sup>b</sup>	10.1 ± 0.8	0.01
Log angiotensin-2, (ng/mL)	0.7 ± 0.6	0.7 ± 0.5	1.3 ± 0.6 <sup>b</sup>	1.9 ± 0.7 <sup>b</sup>	<0.001
Log ADMA (μmol/L)	-0.8 ± 0.2	-0.8 ± 0.2	-0.7 ± 0.2	-0.5 ± 0.3 <sup>b</sup>	<0.001
Log apoptosis (relative units)	-1.2 ± 0.7	-1.0 ± 0.6	-1.1 ± 0.6	-0.6 ± 0.7 <sup>b</sup>	0.02
Proliferation (relative units), mean ± SD	1.2 ± 0.25	1.1 ± 0.23	0.99 ± 0.33 <sup>b</sup>	1.02 ± 0.25	0.03

SD = standard deviation. IQR = interquartile range.

<sup>a</sup> ANOVA and non-parametric trend test for normally and non-normally distributed continuous variables, respectively.

<sup>b</sup>  $P < 0.05$  for comparison with preserved function by Tukey–Kramer post-hoc test.

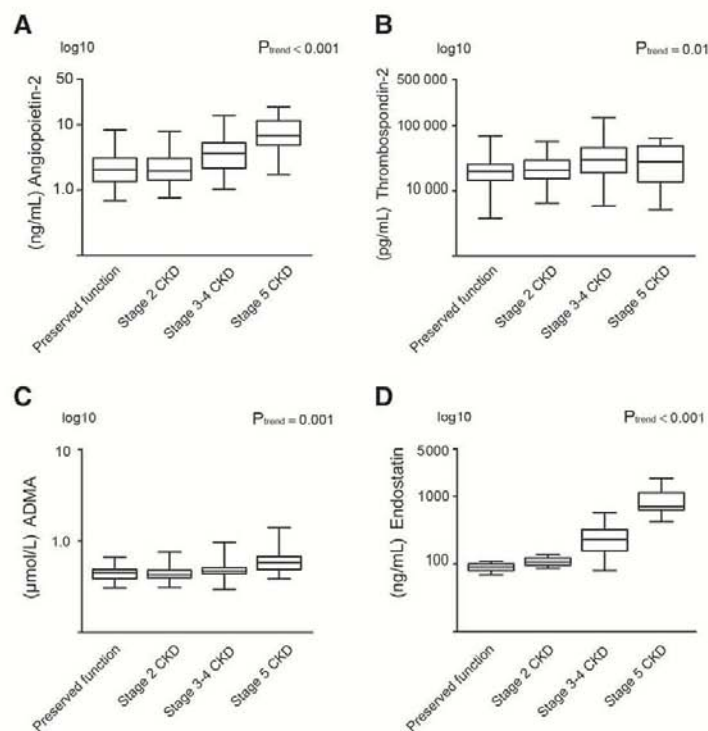


**Fig. 4.** Serum concentrations of anti-angiogenic factors in CKD patients. Box plots show serum levels of (A) the NO-synthase inhibitor ADMA and (B–D) the angiogenesis inhibitors (B) endostatin, (C) thrombospondin-2 and (D) angiotensin-2. Boxes span the minimum and maximum values (log transformed). Horizontal lines represent the median. Vertical lines above and below each box encompass maximal and minimal values. Serum of individuals with preserved renal function ( $n = 30$ ), or from CKD patients stage 2 ( $n = 58$ ), stage 3–4 ( $n = 60$ ), or stage 5 ( $n = 14$ ) was used for all of these measurements.

factors which could mediate the observed effect of uremic serum on coronary endothelial cells, we measured serum ADMA, ANG, TSP and END in our cohort ( $n = 162$ ). All were increased in serum of patients with CKD: END concentration was nearly 10-fold higher in stage 5 CKD (879.6 ng/mL, IQR 631.4–1129.3) than with preserved renal function (91.1 ng/mL, IQR 69.4–109.6) and concentrations of END, TSP, ANG and ADMA increased significantly across categories of CKD and were independently associated with renal function (Table 4, Fig. 4, Supplementary Table A.3). END, ANG and ADMA concentrations were significantly higher in stage 5 CKD than with preserved function. Similarly, END, TSP and ANG concentrations were higher with stage 5 CKD compared with preserved kidney function. ADMA concentration was correlated with END ( $r = 0.34$ ,  $P < 0.001$ ) and ANG ( $r = 0.38$ ,  $P < 0.001$ ).

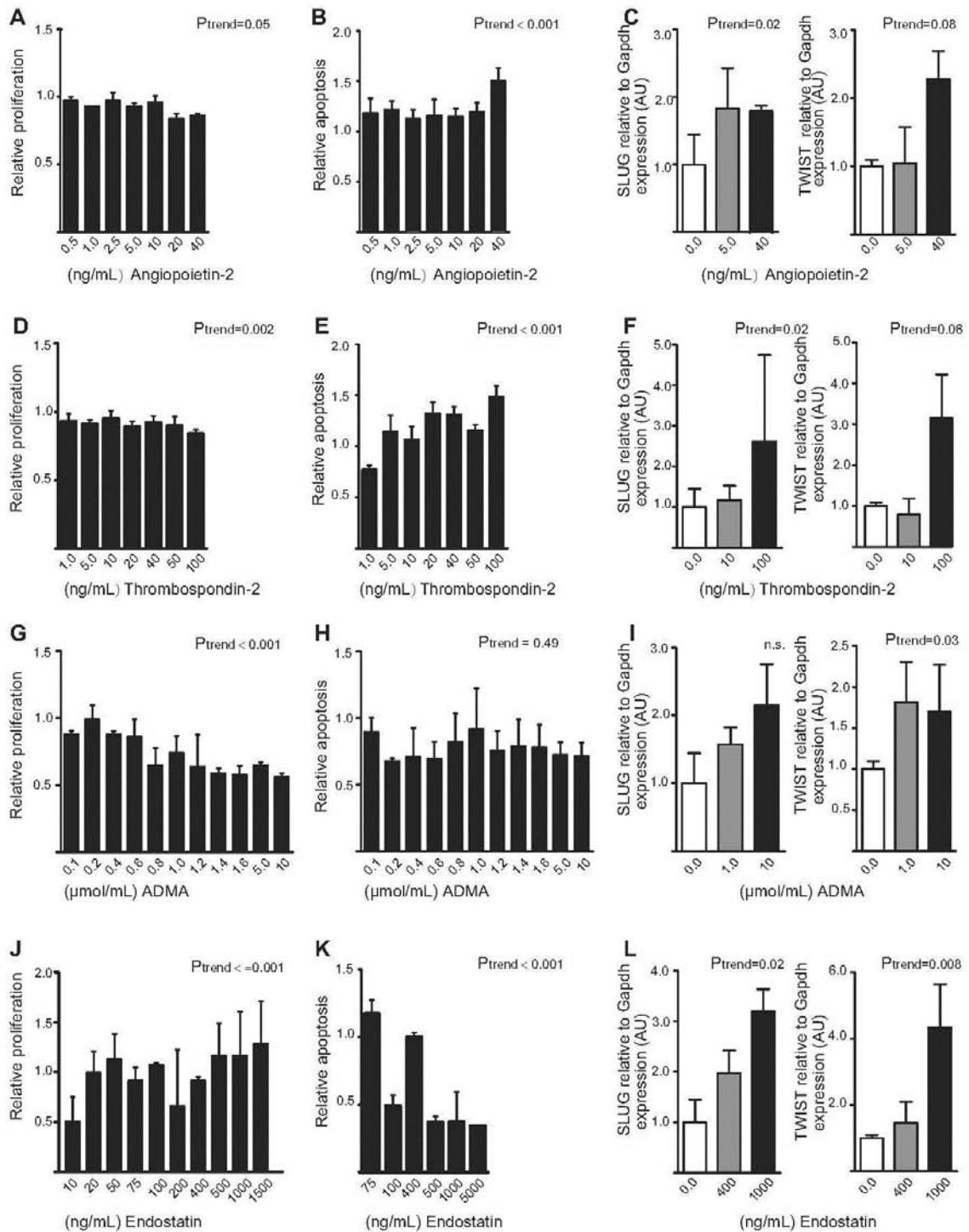
HCAEC apoptosis and END, TSP, ANG, and ADMA concentrations were independently associated with CKD class in multivariable models adjusted for age, race, sex, diabetes, hypertension, smoking, history of myocardial infarction, recruitment site, and presence of acute coronary syndrome. However, the association with HCAEC proliferation was attenuated after multivariable adjustment (Supplementary Table A.3). Results were similar with further adjustment for anemia or use of angiotensin blockers and angiotensin converting enzyme inhibitors, but the association of CKD class with TSP concentration was slightly attenuated.

To assess whether these factors could mediate the effects of uremic serum on apoptosis, proliferation, and EndMT of HCAEC, we tested the effects of a wide range of concentrations (which included the previously documented range among healthy and CKD patients) of purified, recombinant ADMA, END, TSP and ANG on HCAEC. Recombinant ANG increased apoptosis of HCAEC at all concentrations tested (Fig. 5B) and both ANG ( $P_{\text{trend}} < 0.001$ ) and TSP ( $P_{\text{trend}} < 0.001$ ) increased apoptosis at increasing concentrations within the physiologic range (Fig. 5B, E). Similarly, HCAEC proliferation was inversely proportional to the concentrations of ADMA ( $P_{\text{trend}} < 0.001$ ), ANG ( $P_{\text{trend}} = 0.05$ ) and TSP ( $P_{\text{trend}} = 0.002$ ) added to the medium (Fig. 5A, D, G). Each of these proteins also induced EndMT of HCAEC, as reflected by increased expression of TWIST and SLUG RNA (Fig. 5C, F, I, L). In contrast, physiologic concentrations of END decreased apoptosis and increased HCAEC proliferation ( $P < 0.001$ , Fig. 5J, K).

#### 4. Discussion

We found that myocardial fibrosis and EndMT increased while microvascular supply decreased significantly with CKD severity. In addition, the concentration of circulating angiogenesis and NO inhibitors increased with CKD severity while serum from patients with more severe CKD inhibited proliferation and increased apoptosis of cultured coronary endothelial cells. Finally, ADMA, ANG, TSP and

**Fig. 5** Effect of recombinant angiotensin-2, thrombospondin-2, ADMA and endostatin on proliferation, apoptosis and EndMT of HCAECs. HCAECs were treated with different concentrations of recombinant angiotensin-2 (A–C), thrombospondin-2 (D–F), ADMA (G–I), or endostatin (J–L). Bar graphs show the effect of these factors on HCAEC proliferation (A, D, G, J), HCAEC apoptosis (B, E, H, K), and EndMT marker expression *SLUG* and *TWIST* (C, F, I, L).





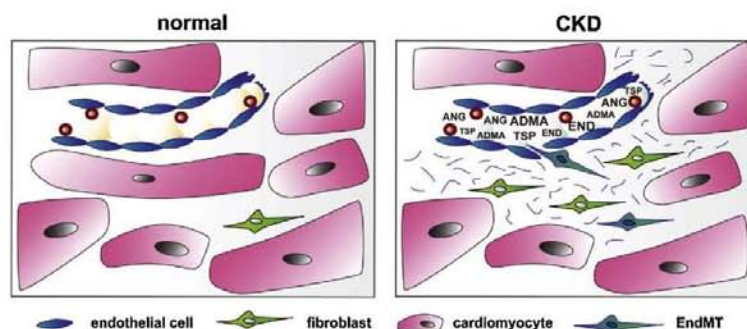


Fig. 6. Schematic for mechanisms of fibrosis and capillary rarefaction in CKD. High circulating concentrations of the angiogenesis inhibitors asymmetric dimethylarginine (ADMA), endostatin (END), angiotensin-2 (ANG), and thrombospondin-2 (TSP) in CKD lead to EndMT causing microvascular rarefaction, fibroblast accumulation, and cardiac fibrosis.

END had qualitatively similar effects on cultured endothelial cells as uremic serum.

CKD is strongly associated with CVD, especially heart failure and sudden death [1]. Experimental studies suggest that renal impairment inhibits ischemia-driven angiogenesis [4] and induces myocardial capillary rarefaction and fibrosis [3], but evidence of these processes in humans is limited. In one study comparing 9 dialysis patients with 9 hypertensive and 10 non-hypertensive controls—all free from coronary disease and with non-CV causes of death—LV capillary density decreased by 49% and 21% and interstitial tissue increased by 65% and 44% compared with normal and hypertensive controls, respectively [24]. Conversely, in endomyocardial biopsies of 90 patients with dilated cardiomyopathy, myocyte diameter was significantly increased in the dialysis group. However, in this cohort with advanced cardiomyopathy, LV fibrosis did not differ between dialysis patients and controls [25].

Our findings add to these studies by demonstrating significant increases in myocardial fibrosis and capillary rarefaction in a less highly-selected population of dialysis patients, and by showing that changes in capillary supply and myocardial fibrosis begin relatively early in CKD before accelerating in ESRD. Whether differences in technique (measurement of myocyte area vs. diameter), patient population, or statistical power explain the divergent findings on myocyte size requires further study. Finally, our findings of an increase in cells dual positive for endothelial and fibroblastic markers (as well as trends consistent with an increase in *SNAIL* and *SLUG* mRNA expression) provide the first evidence that EndMT [26] with transformation of endothelial cells into fibroblasts has a role in the capillary rarefaction and myocardial fibrosis characterizing the uremic myocardium.

NO homeostasis is abnormally regulated in experimental uremia [5], and in experimental models NO deficiency induces myocardial fibrosis and capillary rarefaction [27] while lowering NO concentrations induces END, ANG, and TSP synthesis and the exocytosis of ANG from endothelial cells [6–8,15]. Our observation that ADMA—a potent inhibitor of NO synthase—increases with CKD severity and is accompanied by analogous changes in END, ANG, and TSP, suggests a model of CVD in CKD in which NO deficiency—partly driven by increased ADMA—leads to myocardial fibrosis and microvascular dropout through direct effects on endothelial cells and fibroblasts and by indirectly stimulating production of additional, potent angiogenesis inhibitors (Fig. 6). These novel pathways are likely to synergize with other traditional risk factors common in CKD such as volume overload, anemia, as well as abnormalities in insulin signaling, parathyroid hormone, calcium and phosphorous.

These results are consistent with prior studies demonstrating that ADMA and ANG-2 concentrations are increased in CKD and associated with higher risks of CV and all-cause death [16–19]. They also confirm studies demonstrating that END concentration rises in both pre-

dialysis and dialysis-dependent CKD [20,21]. Our study extends these observations by demonstrating the independence of these associations from other standard risk factors and by showing analogous changes in an additional potent angiogenesis inhibitor, TSP, which is known to promote renal capillary rarefaction and to promote fibrosis and inhibit vascularization of experimental cardiac allografts [22,23], but whose association with kidney function has not been previously assessed [20–23].

We also demonstrated potent effects of uremic serum on endothelial cells as well as specific effects of ADMA, ANG, END, and TSP on endothelial apoptosis, proliferation, and EndMT at their circulating concentrations. The *in vitro* and *in vivo* evidence of EndMT that we observed suggests that induction of EndMT with a resultant loss of endothelial cells and increase in myocardial fibroblasts (together with endothelial apoptosis and inhibited proliferation) play key roles in the characteristic myocardial pathology of uremia and are consistent with experimental studies suggesting a mechanistic role for EndMT in cardiac fibrosis [26].

In contrast to prior studies [28,29], END did not impair proliferation or promote apoptosis at the studied concentrations. This could reflect a difference in cell lines (HCAEC vs. cow pulmonary artery and human umbilical vein cells), but our preliminary observations showed inhibition of HCAEC proliferation for concentrations of END above 1  $\mu\text{g}/\text{mL}$  (data not shown) suggesting that the lower concentrations tested (ng/mL vs.  $\mu\text{g}/\text{mL}$ ) underlie the divergence. Our data thus suggests a complex biology in which increasing END levels initially increase proliferation and inhibit apoptosis, but which is reversed at higher concentrations. Although the moderate rise in circulating END in CKD is thus unlikely to be a major factor underlying endothelial apoptosis or proliferation, these levels may induce EndMT. Furthermore, local myocardial concentrations of END may also be crucial. Tissue levels of endostatin are inversely correlated with myocardial capillary density in experimental models [30] while inhibition of NO synthesis increases both *in vitro* production of END by endothelial cells and *in vivo* tissue END levels [6]. Thus, high circulating levels of ADMA in CKD likely increase both serum and tissue END concentration. Myocardial END concentrations derived from local endothelial synthesis may thus be sufficient to promote apoptosis and inhibit endothelial proliferation regardless of circulating concentrations. Further studies to fully elucidate END's role and to measure myocardial tissue levels in CKD are warranted.

#### 4.1. Strengths and limitations

This study has several strengths. In particular we used a multifaceted approach with consistent data from histopathological (autopsy), serological, and *in vitro* studies, encompassing cell biology and cardiac structure and function. There were several limitations: The number of ESRD patients was small, and additional studies including more dialysis



patients are needed. The number of post-mortem samples was particularly small. Our ability to simultaneously adjust for relevant covariates in the analysis of these samples was limited, and although our findings appeared robust, we cannot rule out the possibility that residual confounding may partly explain the observed associations with CKD. Our findings should thus be confirmed using detailed, multi-variable adjustment and larger multi-center cohorts before they can be broadly generalized. Finally, our studies were associative in nature. Although interventional studies are needed for causality, our studies provide novel insights into the potential mechanisms underlying uremic CVD.

#### 4.2. Conclusions

In conclusion, we found significant associations between the severity of CKD, myocardial fibrosis and capillary rarefaction as well as significant increases in the circulating concentrations of ADMA, END, TSP and ANG in individuals with CKD. Our human data support experimental animal studies suggesting that capillary rarefaction and fibrosis underlie the high risk of CV death in CKD, particularly in ESRD, while suggesting an important role for ADMA-related inhibition of NO homeostasis and related increases in END, TSP, ANG and EndMT in those pathologic changes (Fig. 6). Further studies are needed to determine whether restoring NO homeostasis or inhibiting ADMA, END, TSP, or ANG can improve CV histology or outcomes in CKD.

#### Funding

This work was supported by funds of the University Medical Center of Göttingen (EMZ and MZ); the Paul Teschan Research Fund; the Carl Gottschalk Award of the American Society of Nephrology; the American Heart Association Scientist Development Grant [0735638N] (DMC), NIH RO1 HL070938 (JH), grants ZE523/3-1 and ZE523/2-1 by the Deutsche Forschungsgemeinschaft (MZ), the Cancer Prevention and Research Institute of Texas, the Metastasis Research Center at MD Anderson Cancer Center, and NIH grants DK055001, DK081576, CA125550, CA155370, CA151925 and CA163191 (RK). Elisabeth Zeisberg is further supported by the SFB1002/C01 DFG grant.

#### Conflict of interest

None declared. Author contributions—DMC and EMZ—study design, conduct of experiments, analysis of data, and drafting of manuscript. RP, RK, AMH—study design, conduct of experiments, and analysis of study. MZ and JH—analysis of data and drafting of manuscripts. AC, XX, XL—conduct of experiments and analysis of data. All authors approved the final draft.

#### Appendix A. Supplementary data

Supplementary data to this article can be found online at <http://dx.doi.org/10.1016/j.ijcard.2014.06.062>.

#### References

- [1] Go AS, Chertow GM, Fan D, McCulloch CE, Hsu CY. Chronic kidney disease and the risks of death, cardiovascular events, and hospitalization. *N Engl J Med* 2004;351:1296–305.
- [2] Herzog CA, Asinger RW, Berger AK, et al. Cardiovascular disease in chronic kidney disease. A clinical update from kidney disease: improving global outcomes (KDIGO). *Kidney Int* 2011;80:572–86.
- [3] Amann K, Neimeier KA, Schwarz U, et al. Rats with moderate renal failure show capillary deficit in heart but not skeletal muscle. *Am J Kidney Dis* 1997;30:382–8.
- [4] Jacobi J, Porst M, Cordasic N, et al. Subtotal nephrectomy impairs ischemia-induced angiogenesis and hindlimb re-perfusion in rats. *Kidney Int* 2006;69:2013–21.
- [5] Baylis C. Nitric oxide deficiency in chronic kidney disease. *Am J Physiol Ren Physiol* 2008;294:F1–9.
- [6] O'Riordan E, Mendeleev N, Patschan S, et al. Chronic NOS inhibition actuates endothelial–mesenchymal transformation. *Am J Physiol Heart Circ Physiol* 2007;292:H285–94.
- [7] Bhandari V, Choo-Wing R, Hanjith A, et al. Increased hyperoxia-induced lung injury in nitric oxide synthase 2 null mice is mediated via angiotensin II. *Am J Respir Cell Mol Biol* 2012;46:668–76.
- [8] MacLaughlan S, Yu J, Parrish M, et al. Endothelial nitric oxide synthase controls the expression of the angiogenesis inhibitor thrombospondin 2. *Proc Natl Acad Sci U S A* 2011;108:E1137–45.
- [9] Levey AS, Coresh J, Greene T, et al. Using standardized serum creatinine values in the modification of diet in renal disease study equation for estimating glomerular filtration rate. *Ann Intern Med* 2006;145:247–54.
- [10] Ekroyan G, Hostetter T, Bakris GL, et al. Proteinuria and other markers of chronic kidney disease: a position statement of the national kidney foundation (NKF) and the national institute of diabetes and digestive and kidney diseases (NIDDK). *Am J Kidney Dis* 2003;42:617–22.
- [11] Teerlink T. HPLC analysis of ADMA and other methylated L-arginine analogs in biological fluids. *J Chromatogr B Anal Technol Biomed Life Sci* 2007;851:21–9.
- [12] Medici D, Kalluri R. Endothelial–mesenchymal transition and its contribution to the emergence of stem cell phenotype. *Semin Cancer Biol* 2012;22:379–84.
- [13] Pun PH, Smarz TR, Honeycutt EF, Shaw LK, Al-Khatib SM, Middleton JP. Chronic kidney disease is associated with increased risk of sudden cardiac death among patients with coronary artery disease. *Kidney Int* 2009;76:652–8.
- [14] Gulati A, Jabbar A, Ismail TF, et al. Association of fibrosis with mortality and sudden cardiac death in patients with nonischemic dilated cardiomyopathy. *JAMA* 2013;309:896–908.
- [15] Matsushita K, Morrell CN, Cambien B, et al. Nitric oxide regulates exocytosis by S-nitrosylation of N-ethylmaleimide-sensitive factor. *Cell* 2003;115:139–50.
- [16] Fleck C, Janz A, Schweitzer F, Karge E, Schwertfeger M, Stein G. Serum concentrations of asymmetric (ADMA) and symmetric (SDMA) dimethylarginine in renal failure patients. *Kidney Int Suppl* 2001;78:S14–8.
- [17] Zoccali C, Bode-Boger S, Mallamaci F, et al. Plasma concentration of asymmetrical dimethylarginine and mortality in patients with end-stage renal disease: a prospective study. *Lancet* 2001;358:2113–7.
- [18] David S, Kumpers P, Lukasz A, et al. Circulating angiotensin-2 levels increase with progress of chronic kidney disease. *Nephrol Dial Transplant* 2010;25:2571–6.
- [19] David S, John SG, Jefferies HJ, et al. Angiotensin-2 levels predict mortality in CKD patients. *Nephrol Dial Transplant* 2012;27:1867–72.
- [20] Chen J, Hamm LL, Kleinpeter MA, et al. Elevated plasma levels of endostatin are associated with chronic kidney disease. *Am J Nephrol* 2012;35:335–40.
- [21] Watorek E, Paprocka M, Dus D, Kopec W, Klinger M. Endostatin and vascular endothelial growth factor: potential regulators of endothelial progenitor cell number in chronic kidney disease. *Pol Arch Med Wewn* 2011;121:296–301.
- [22] Daniel C, Amann K, Hohenstein B, Bornstein P, Hugo C. Thrombospondin 2 functions as an endogenous regulator of angiogenesis and inflammation in experimental glomerulonephritis in mice. *J Am Soc Nephrol* 2007;18:788–98.
- [23] Reinecke H, Robey TE, Mignone JL, Muskheili V, Bornstein P, Murray CE. Lack of thrombospondin-2 reduces fibrosis and increases vascularity around cardiac cell grafts. *Cardiovasc Pathol* 2013;22:91–5.
- [24] Amann K, Breitbach M, Ritz E, Mall G. Myocyte/capillary mismatch in the heart of uremic patients. *J Am Soc Nephrol* 1998;9:1018–22.
- [25] Aoki J, Ikari Y, Nakajima H, et al. Clinical and pathologic characteristics of dilated cardiomyopathy in hemodialysis patients. *Kidney Int* 2005;67:333–40.
- [26] Zeisberg EM, Tarnavski O, Zeisberg M, et al. Endothelial-to-mesenchymal transition contributes to cardiac fibrosis. *Nat Med* 2007;13:952–61.
- [27] Kazakov A, Muller P, Jagoda P, Semenov A, Bohm M, Laufs U. Endothelial nitric oxide synthase of the bone marrow regulates myocardial hypertrophy, fibrosis, and angiogenesis. *Cardiovasc Res* 2012;93:397–405.
- [28] Dhanabal M, Volk R, Ramchandran R, Simons M, Sukhatme VP. Cloning, expression, and in vitro activity of human endostatin. *Biochem Biophys Res Commun* 1999;258:345–52.
- [29] Dhanabal M, Ramchandran R, Waterman MJ, et al. Endostatin induces endothelial cell apoptosis. *J Biol Chem* 1999;274:11721–6.
- [30] Gu JW, Shparago M, Tan W, Bailey AP. Tissue endostatin correlates inversely with capillary network in rat heart and skeletal muscles. *Angiogenesis* 2006;9:93–9.

## Appendix

Supplementary Table A.1—Correlations of Pathologic Findings with Glomerular Filtration Rate

<i>Characteristic Mean ± SD</i>	<b>Correlation Coefficient</b>	<b>P Value</b>
<b>Histology (N=45)</b>		
<i>Percent fibrosis</i>	-0.33	0.03
<i>Number of vessels per cross-section</i>	0.30	0.05
<i>Number of cardiomyocytes per cross-section</i>	0.40	0.01
<i>Myocyte size (uM<sup>2</sup>)</i>	-0.08	0.62
<i>Myocyte density (n/uM<sup>2</sup>)</i>	0.40	0.01
<i>Vessels per myocyte</i>	-0.02	0.91
<b>Immunofluorescence (N=23)</b>		
<i>FSP+ cells/field</i>	-0.40	0.06
<i>Double FSP/CD-31 positive cells/field</i>	-0.53	0.01
<i>Ratio of double positive to all FSP-positive cells/field</i>	-0.58	0.003

S.D.=Standard deviation, I.Q.R.=Interquartile Range, eGFR=estimated glomerular filtration rate.

Charytan *et al.* : *Circulating Inhibitors and myocardial pathology in CKD*

2

## Appendix

Supplementary Table A.2 Multivariable associations of fibrosis and microvascular supply with renal function

Factor	CKD Class (per 1 class change)	
	$\beta$ (95% CI)	P
<b>Fibrosis</b>		
Model 1	3.08 (0.36, 5.81)	0.03
Model 2	3.22 (0.26, 6.18)	0.03
Model 3	2.93 (0.13-5.73)	0.04
<b>Number of Vessels/Field</b>		
Model 1	-54.6 (-107.03, -2.12)	0.04
Model 2	-62.2 (-117.69, -6.75)	0.03
Model 3	-58.6 (-109.99 -7.28)	0.03

Adjusted associations of CKD class with fibrosis and microvascular supply in post-mortem samples. Model 1 includes age, sex, hypertension, and diabetes. Model 2 includes age, sex, diabetes, and anemia. Model 3 includes age, sex, diabetes, and use of angiotensin converting enzyme inhibitors or ACE inhibitors. CI-confidence interval. GFR-glomerular filtration rate. CKD-chronic kidney disease.

Charytan *et al.*, : *Circulating Inhibitors and myocardial pathology in CKD*

3

**Supplementary Table A.3. Multivariable associations of circulating factors, endothelial cell proliferation and endothelial cell apoptosis with renal function**

Factor	CKD Class (per 1 class change)		GFR (per 10 mL/min/1.73m <sup>2</sup> )	
	$\beta$ (95% CI)	P	$\beta$ (95% CI)	P
<b>Model 1</b>				
Log Endostatin, ng/mL	0.39 (0.32, 0.45)	<0.001	-0.19 (-0.22, -0.17)	<0.001
Log Thrombospondin-2, pg/mL	0.09 (0.01, 0.16)	0.03	-0.03 (-0.07, 0.00)	0.08
Log Angiopoietin-2, ng/mL	0.19 (0.10, 0.27)	<0.001	-0.09 (-0.13, -0.06)	<0.001
Log ADMA, $\mu$ mol/L	0.06 (0.03, 0.08)	<0.001	-0.03 (-0.04, -0.02)	<0.001
Log Apoptosis, relative units	0.13 (0.05, 0.20)	0.001	-0.06 (-0.09, -0.02)	0.001
Proliferation, relative units	-0.003 (-0.04, 0.03)	0.87	0.01 (-0.01, 0.02)	0.49
<b>Model 2</b>				
Log Endostatin, ng/mL	0.36 (0.30, 0.43)	<0.001	-0.18 (-0.21, -0.15)	<0.001
Log Thrombospondin-2, pg/mL	0.08 (-0.00, 0.16)	0.06	-0.03 (-0.07, 0.01)	0.15
Log Angiopoietin-2, ng/mL	0.18 (0.10, 0.27)	<0.001	-0.09 (-0.13, -0.05)	<0.001
Log ADMA, $\mu$ mol/L	0.06 (0.03, 0.08)	<0.001	-0.03 (-0.05, -0.02)	<0.001
Log Apoptosis, relative units	0.14 (0.06, 0.22)	0.001	-0.06 (-0.10, -0.03)	0.001
Proliferation, relative units	0.002 (-0.03, 0.04)	0.91	0.003 (-0.01, 0.02)	0.71
<b>Model 3</b>				
Log Endostatin, ng/mL	0.36 (0.30, 0.43)	<0.001	-0.18 (-0.21, -0.16)	<0.001
Log Thrombospondin-2, pg/mL	0.08 (-0.00, 0.16)	0.06	-0.03 (-0.07, 0.01)	0.15
Log Angiopoietin-2, ng/mL	0.18 (0.10, 0.27)	<0.001	-0.09 (-0.13, -0.05)	<0.001
Log ADMA, $\mu$ mol/L	0.06 (0.03, 0.08)	<0.001	-0.03 (-0.05, -0.02)	<0.001
Log Apoptosis, relative units	0.14 (0.06, 0.22)	0.001	-0.06 (-0.10, -0.03)	0.001
Proliferation, relative units	0.002 (-0.03, 0.04)	0.89	0.003 (-0.01, 0.02)	0.71

Adjusted associations of CKD class or GFR with circulating factor concentration, and HCAEC apoptosis, or proliferation after exposure to subject serum. Model 1- adjusted for age, race, sex, diabetes, hypertension, smoking, history of myocardial infarction, recruitment site, and presence of acute coronary syndrome. Model 2 includes all factors in model 1 with the addition of anemia. Model 3 includes all factors in Model 2 with addition of use of angiotensin receptor blockers or ACE inhibitors. CI-confidence interval. GFR-glomerular filtration rate. CKD-chronic kidney disease.



### 3. Unpublished data

*In this section, these unpublished data are about the establishment of HLHS-hiPSC disease model, which was used for exploring the potential pathological mechanism of HLHS.*

#### 3.1 Patient-specific iPSC models for HLHS

##### 3.1.1 Abstract

*HLHS is a rare but lethal congenital heart disease. EFE is a hallmark of HLHS. Aberrant EndMT is believed to be a common denominator of EFE generation. This provides evidence for assumption that dysfunctional endothelial cells may contribute to pathological process in HLHS. Surgical intervention can largely increase the survival rate of HLHS patient, but the lack of the etiological understanding impedes the development of new therapies. Another limitation of HLHS research is that such a complex syndrome could not be fully represented by animal models. With the development of stem cell technology, hiPSC disease model provides a powerful tool to study the underlying etiology of HLHS. In this study, endothelial cells derived from hiPSCs are used to test if the aberrant EndMT could contribute to EFE generation in HLHS. Firstly, we generated hiPSC lines from two unrelated HLHS patients. These HLHS-hiPSC lines were characterized to be pluripotent, which together with WT-hiPSC lines were differentiated into functional endothelial cells by using our reported protocol. EndMT assay showed that there seemed no significant difference of the susceptibility to TGF $\beta$  and hypoxia of HLHS-hiPSC-ECs compared to WT-hiPSC-ECs with respect to EndMT. This finding suggests that hiPSC-EC system should be optimized for modeling HLHS in the future.*

### 3.1.2 Introduction

*HLHS is a rare birth defect, which is represented by the undeveloped and small left heart, especially the left ventricle (Tchervenkov et al., 2006). The hypoplasia of the left heart included left ventricle, aortic valve, aorta and mitral valve. Interestingly, EFE is found in a large number of HLHS cases and could be considered as one of the hallmarks (Feinstein et al., 2012; Xu et al., 2015a). Results of both mouse experiments and patient data strongly suggested that endothelial cell dysfunction, like EndMT, might contribute to the EFE generation (Xu et al., 2015a).*

*hiPSCs is a powerful tool for drug screening and provides an alternative model for the study of pathological mechanism of diseases (Takahashi and Yamanaka, 2006; Yu et al., 2007). In this study, hiPSC lines were generated from two HLHS patients. By using our reported endothelial cell differentiation method, patient-specific endothelial cells were successfully generated. The susceptibility of hiPSC-ECs to pro-fibrotic factors (TGF $\beta$  and hypoxia) was tested by EndMT assay.*

### 3.1.3 Materials and Methods

#### 3.1.3.1 HLHS-hiPSC generation

*Dermal fibroblasts were isolated from skin biopsies of HLHS1 patient (kindly supplied by Dr. Maria Iascone, Bergamo). Fibroblasts of HLHS2 patient were purchased from the Coriell Institute for Medical Research (GM12601). Both patients were clinically diagnosed with HLHS. All the dermal fibroblasts were cultured in DMEM (Dulbecco's Modified Eagle Medium) supplemented with 10% FBS. The disease-specific hiPSCs were generated from these HLHS1 and HLHS2 fibroblast by Sendai virus (Life Technologies) or STMCCA virus (all related plasmids were provided by Prof. Kotton, Boston University School of Medicine) carrying reprogramming factors OCT4, SOX2, KLF4 and C-MYC, respectively.*

*hiPSCs generation from HLHS patient was supported by the technicians in the stem cell unit (UMG, Gottingen).  $2 \times 10^4$  fibroblasts were seeded into in a well of a 12 well plate and transduced with STEMCCA virus plus polybrene or Sendai virus for 24 hours. hiPSC colonies were picked and cultured in Essential 8 medium supplemented with Essential 8 Supplement (Life Technologies) on the dish coated with Geltrex (Life Technologies).*

### **3.1.3.2 Alkaline phosphatase (ALP) staining**

*Alkaline phosphatase is a widely accepted marker for stem cells, which has been used to label different types of pluripotent stem cells. The experiment was performed according to the manufacturer instructions (Sigma Aldrich). Briefly, hiPSCs were fixed by citrate-acetone-formaldehyde at room temperature. Thereafter fixed cells were washed with PBS for 3 times, alkaline-dye mixed solutions were sequentially added and kept for 15 min in dark. After washing 3 times in PBS, the cells were dried in the air. The stained samples were analyzed under microscope (Carl Zeiss).*

### **3.1.3.3 *In vitro* ECs differentiation**

*As we reported before, hiPSCs were seeded onto Geltrex coated 6-well plates with Essential 8 Medium supplemented with 6  $\mu$ M ROCK inhibitor (Millipore). 24 hours later, DMEM/F12 supplemented with 4  $\mu$ M CHIR (Millipore) was used for medium change. At day 2, medium was exchanged with endothelial cell basal medium (Promocell) supplemented with growth factors 5 ng/ml bFGF (Peprotech) and 10 ng/ml VEGFA (R&D). At day 4, medium was changed with EMV2 medium (Promocell) supplemented with 10 ng/ml VEGFA. After 10 days of differentiation, the primary hiPSCs derived endothelial cells were ready for sorting.*

### **3.1.3.4 Flow cytometry and fluorescence-activated cell sorting**

*Cells were dissociated into single cells with trypsin-EDTA. All the cell pellets were collected and re-suspended in 2% bovine serum albumin (BSA). Directly-labeled*

antibodies against CD31 (BD) and VE-cadherin (BD) were added to the samples and incubated for 1 hour. Samples were resuspended in ice-cold dilution buffer (2% BSA in PBS) to adjust the final concentrations of  $1 \times 10^6$  cells/ml. Cells were then filtrated through cell strainers and used for flow cytometry or fluorescence-activated cell sorting (FACS) analysis.

### **3.1.3.5 Immunofluorescence staining**

All the cells were seeded on Geltrex (Life technologies) or gelatin (Sigma Aldrich) coated coverslips. When cells reached 80% confluence, fixation was performed by 4% paraformaldehyde. Then cells were permeabilized in 0.1% TritonX-100 for 10 minutes and then blocked in 5% BSA for 30 minutes. Primary antibodies were incubated with the cells and kept at 4 °C overnight. After washing with PBS, proper secondary antibodies were added. After 1 hour incubation, the stained cells on the coverslips were analyzed by fluorescence microscopy (Carl Zeiss).

Primary antibodies used: AFP (Dako), CD31 (Dako), LIN28 (R&D), NANOG (Thermo Fisher Scientific), OCT4 (R&D), SMA (Sigma Aldrich), VE-cadherin (Cell Signal Tech), von Willebrand factor (VWF) (Abcam), SSEA4 (Thermo Fisher Scientific), TRA-1-60 (Abcam), and  $\beta$ -III-TUBULIN (Covance). Secondary antibodies used: goat anti-rabbit Alexa Fluor 546 (Life Technologies), goat anti-mouse Alexa Fluor 546 (Life Technologies) and goat anti-mouse Alexa Fluor 488 (Life Technologies).

### **3.1.3.6 RNA isolation and real-time PCR**

RNA was extracted using Trizol™ (Invitrogen) and reverse transcribed using SuperScript™ reverse transcriptase (RT) kit (Promega) according to manufacturers' recommendations. Real-time polymerase chain reaction (qPCR) was performed using SYBR Master Mix kit (Applied Biosystems) on an ABI StepOne PCR instrument (Applied Biosystems). Real-time PCR primers are listed in Table 2.

**Table 2. PCR primers list:**

Real-time PCR primers list:			
Gene name	F/R	Sequence	Reference
<i>CD31(PECAM1)</i>	Forward	5'-ATTGCAGTGGTTATCATCGGAGTG-3'	Self-designed
	Reverse	5'-CTCGTTGTTGGAGTTCAGAAAGTGG-3'	Self-designed
<i>VE-cadherin(CDH5)</i>	Forward	5'-AGACACCCCAACATGCTAC-3'	Self-designed
	Reverse	5'-GCAAACCTCTCCTTGGAGCAC-3'	Self-designed
<i>VWF</i>	Forward	5'-GGGGTCATCTCTGGATTCAAG-3'	Primerdesign
	Reverse	5'-TCTGTCTCCTCTTAGCTGAA-3'	Primerdesign
<i>SNAIL(SNAIL1)</i>	Forward	5'-GGCAATTTAAACAATGTCTGAAAAGG-3'	Primerdesign
	Reverse	5'-GAATAGTTCTGGGAGACACATCG-3'	Primerdesign
<i>SLUG(SNAIL2)</i>	Forward	5'-ACTCCGAAGCCAAATGACAA-3'	Primerdesign
	Reverse	5'-CTCTCTCTGTGGGTGTGTGT-3'	Primerdesign
RT-PCR primers list:			
<i>GAPDH</i>	Forward	5'-AGAGGCAGGGATGATGTTCT-3'	Self-designed
	Reverse	5'-TCTGCTGATGCCCCCATGTT-3'	Self-designed
<i>OCT4</i>	Forward	5'-GACAACAATGAAAATCTTCAGGAGA-3'	Self-designed
	Reverse	5'-TTCTGGCGCCGGTTACAGAACCA-3'	Self-designed
<i>NANOG</i>	Forward	5'-AGTCCCAAAGGCAAACAACCCACTTC-3'	Self-designed
	Reverse	5'-ATCTGCTGGAGGCTGAGGTATTTCTGTCTC-3'	Self-designed
<i>LIN28</i>	Forward	5'-AGTAAGCTGCACATGGAAGG-3'	Self-designed
	Reverse	5'-ATTGTGGCTCAATTCTGTGC-3'	Self-designed
<i>FOXD3</i>	Forward	5'-GTGAAGCCGCCTTACTCGTAC-3'	Self-designed
	Reverse	5'-CCGAAGCTCTGCATCATGAG-3'	Self-designed

**Table 2.** *Primerdesign* is the supplier who supplied all these primers marked as 'Primerdesign'. *GAPDH* primers for real-time PCR are also supplied by *Primerdesign*.

### 3.1.3.7 Reverse transcription PCR (RT-PCR)

*RT-PCR* was used to check the expression of pluripotency-related genes. The sequences of forward and reverse primers of *RT-PCR* are shown in Table 2. By using the *PCR* kit (*Sigma Aldrich*), DNA fragments of pluripotency-related genes were amplified. The *RT-PCR* products were analyzed by gel electrophoresis on 1.5% agarose gel.

### 3.1.3.8 Statistical Analysis

All results were presented as means  $\pm$  SD (standard deviation). Statistical differences between different samples were evaluated by Student's *t* test,



*Differences were considered statistically significant when p values  $\leq 0.05$ .*

### **3.1.4 Results**

#### **3.1.4.1 Generation of HLHS-hiPSCs**

*At first, HLHS patients' fibroblasts were isolated and prepared for hiPSCs generation. There were no morphological differences between HLHS fibroblasts and healthy controls. During the reprogramming process, the efficiency of hiPSCs generation was not influenced severely by the patient's pathological background in this study. The WT-hiPSCs were obtained from Prof. Dr. Kaomei Guan (Now Dresden), and had been utilized in previous published projects (WT1-hiPSCs, WT2-hiPSCs) (Dudek et al., 2013; Streckfuss-Bomeke et al., 2013).*

*After HLHS-hiPSCs were established, pluripotency characterizations were performed according to the former studies (Dudek et al., 2013; Streckfuss-Bomeke et al., 2013). All HLHS-hiPSC lines showed typical stem cell-like morphology and were positive for alkaline phosphatase staining (figure3 A). At RNA level, the expression of pluripotency-related genes including OCT4, NANOG, LIN28 and FOXD3, were compared to hESCs (figure3 B). At protein level, all the HLHS-hiPSC lines expressed pluripotency-related proteins: OCT4, SOX2, NANOG, LIN28, SSEA4 and TRA-1-60 (figure3 C). Furthermore, the HLHS-hiPSCs were able to differentiate into different cell types of the three embryonic germ layers in vitro. The differentiated cells were identified as positive for the markers AFP (endoderm), SMA (mesoderm), and  $\beta$ -III-TUBULIN (ectoderm), respectively (figure3 D). In summary, the HLHS-hiPSCs cell lines were pluripotent and were ready for endothelial cell differentiation.*

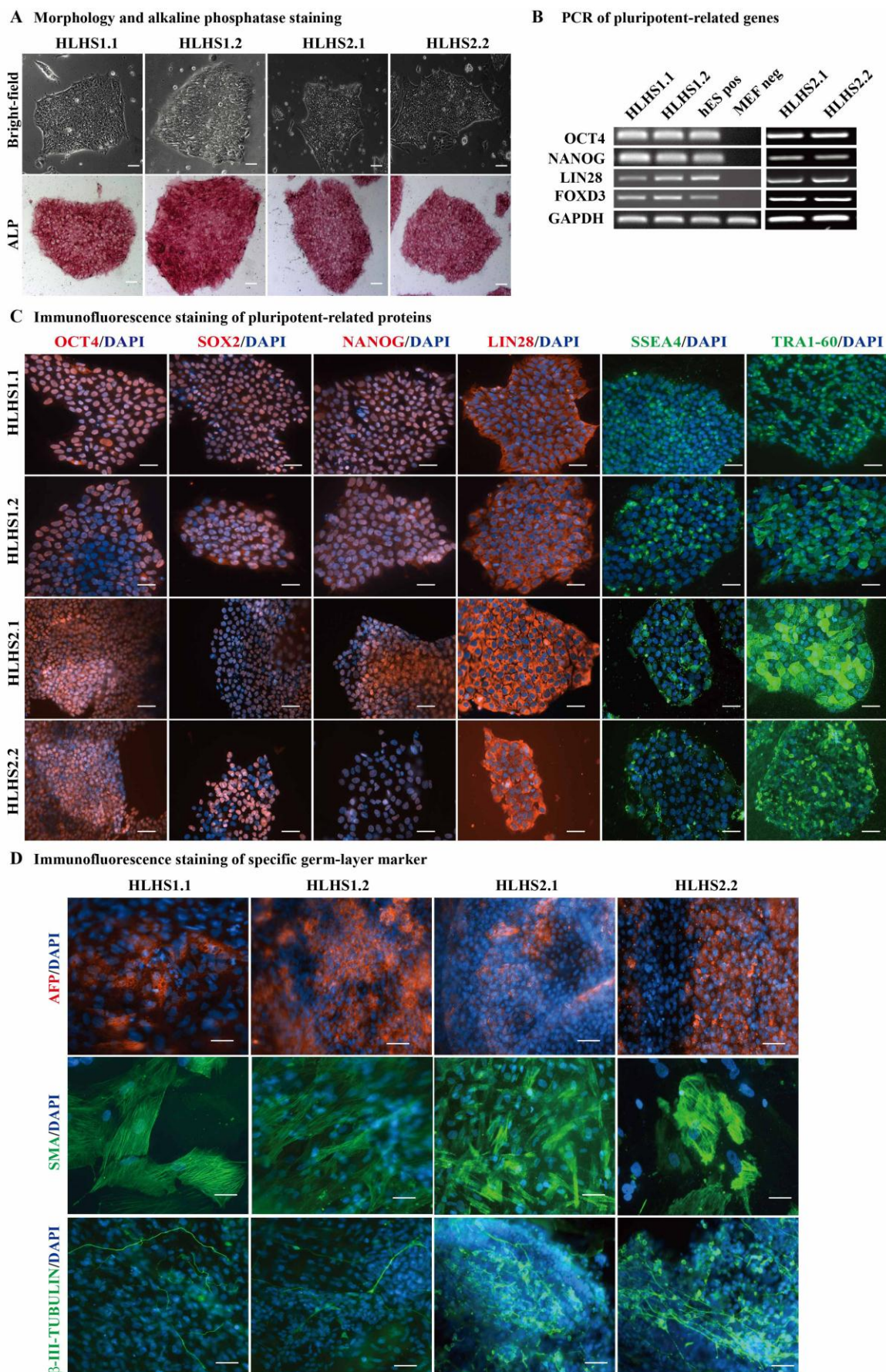


**Figure 3. Pluripotency characterization of HLHS-hiPSCs.**

*HLHS-hiPSC lines were successfully generated from HLHS patient 1 and HLHS patient*

2, named as HLHS1.1, HLHS1.2, HLHS2.1 and HLHS2.2. (A) All of the established HLHS-hiPSC lines at passage 8 showed typical stem cell colony shape and were positive for alkaline phosphatase. (B) The pluripotency-related genes OCT4, NANOG, LIN28 and FOXD3 were expressed in all HLHS-hiPSC lines. (C) HLHS-hiPSCs showed typical pluripotency-related proteins OCT4, SOX2, NANOG, LIN28 and SSEA4. Cell nucleus was stained with DAPI. (D) Immunofluorescence staining results showed the representative markers of endoderm (AFP), mesoderm (SMA) and ectoderm ( $\beta$ -III-TUBULIN) in all HLHS-hiPSC lines. Scale bar: 50  $\mu$ m.

#### **3.1.4.2 Generation and characterization of HLHS-hiPSC-ECs and WT-hiPSC-ECs**

hiPSC-ECs were generated with the endothelial cell differentiation method as previously reported (Liu et al., 2016). HLHS-hiPSCs showed similar capabilities of endothelial cell differentiation with WT-hiPSCs. Briefly, the efficiency and duration of endothelial differentiation were not altered in HLHS-hiPSCs compared to WT-hiPSCs. For morphological features, HLHS-hiPSC-EC colonies presented a similar “cobblestone” arrangement as WT-hiPSC-ECs (figure4 A). Furthermore, immunofluorescence staining showed that both HLHS-hiPSC-ECs and WT-hiPSC-ECs highly expressed the specific markers of endothelial cells, e.g. CD31, VE-cadherin and VWF (figure4 A). At RNA level, HLHS-hiPSC-ECs and WT-hiPSC-ECs expressed typical RNA expression patterns of endothelial cells (figure4 B). Altogether, our results demonstrated that HLHS-hiPSC-ECs expressed specific markers of endothelial cells at RNA and protein level similar to WT-hiPSC-ECs (figure4 A and B).



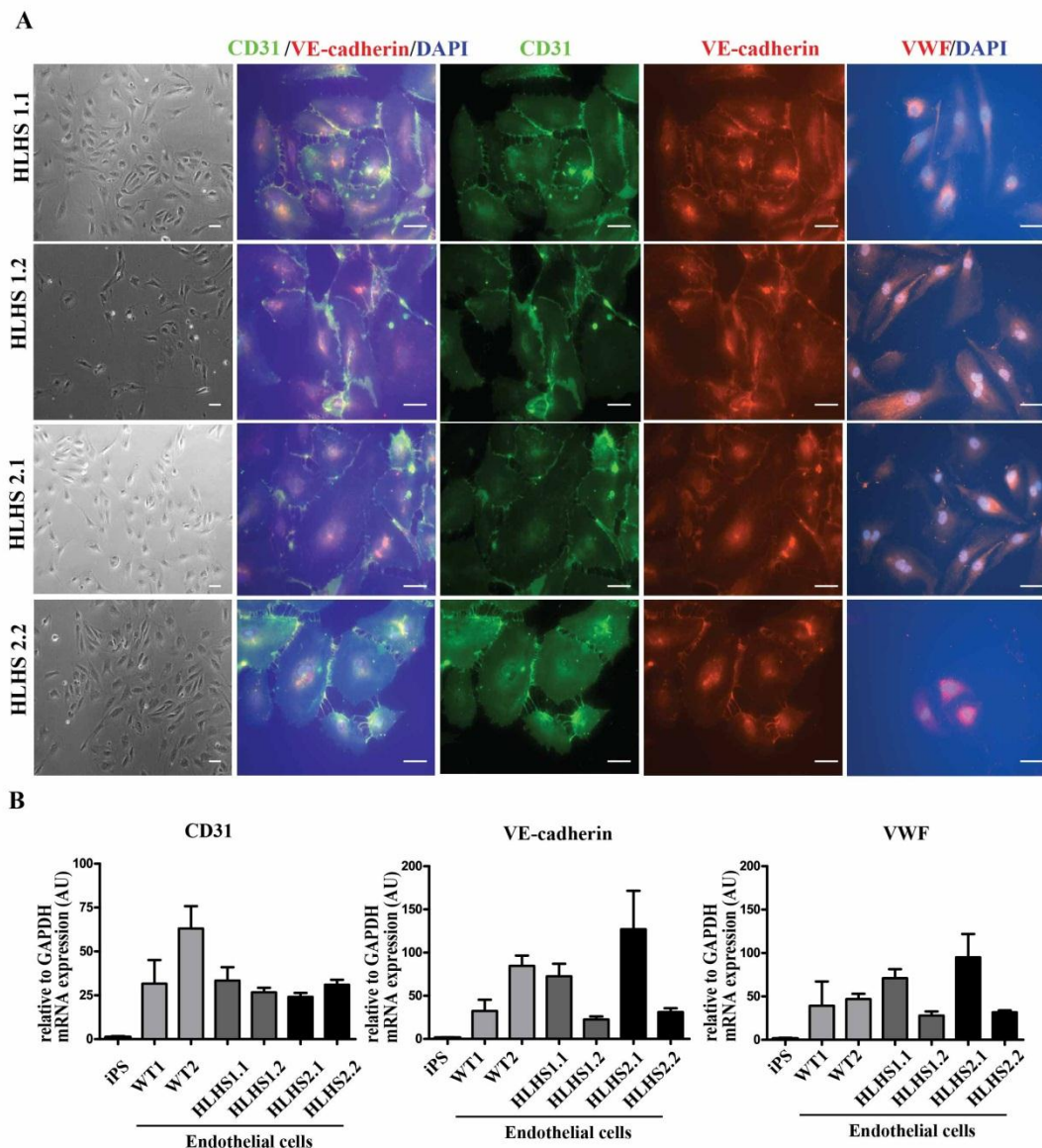


**Figure 4. Characterization of HLHS-hiPSC-ECs.**

(A) Immunofluorescence staining results showed that the representative markers of endothelial cells including CD31, VE-cadherin and VWF were expressed in the HLHS-hiPSC-ECs. Cell nucleus was stained with DAPI. Scale bar: 50  $\mu$ m. (B) Expression of CD31, VE-cadherin and VWF at RNA level were checked with real-time PCR.

### 3.1.4.3 Susceptibility of hiPSC-ECs to EndMT

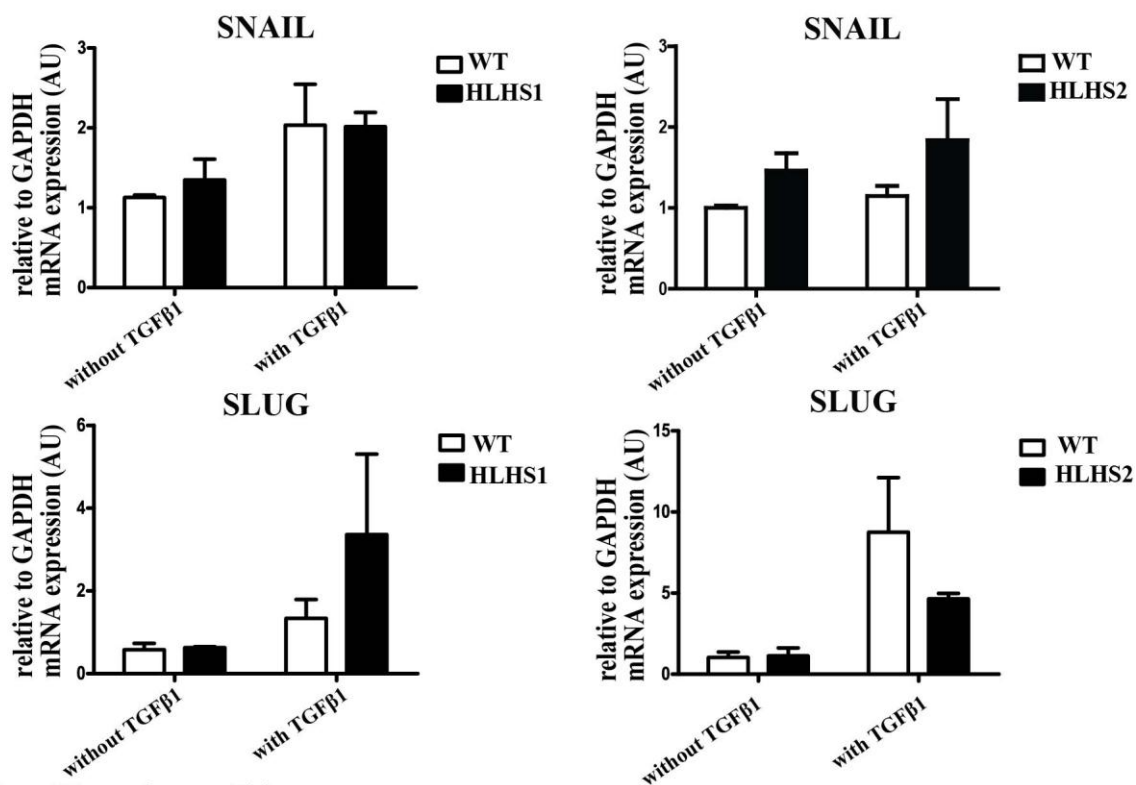
Disruption of endothelial cell development or pathological EndMT could contribute to the EFE tissue generation (Xu et al., 2015a). According to our hypothesis, if the HLHS-hiPSC-ECs are susceptible to TGF $\beta$  treatment, the expression of EndMT master regulator genes should be upregulated in TGF $\beta$ 1 mediated EndMT assay comparing to WT-hiPSC-ECs. Here, TGF $\beta$ 1 exposure for 6 days was used to

*induce EndMT in both HLHS-hiPSC-ECs and WT-hiPSC-ECs (Xu et al., 2015b). Analysis of the gene expression of EndMT key regulators SNAIL and SLUG illustrated that there seems no obvious differences between HLHS-hiPSC-ECs and WT-hiPSC-ECs in response to TGF $\beta$ 1, suggesting that HLHS-hiPSC-ECs are not more susceptible to TGF $\beta$ 1 treatment with respect to EndMT (figure5 A).*

*Hypoxic damage has been proven to be another pro-fibrotic factor which also induces EndMT. Hypoxic damage furthermore increases DNA damages, DNA replication arrest, and even genomic instability. Interestingly, genomic instability was demonstrated previously to be associated with HLHS in several case reports (Fakhro et al., 2011; Gaber et al., 2013). There is also evidence that the genomic instability could increase the susceptibility of the oxidative stress or other injuries (Gaber et al., 2013). In HLHS, HIF-1 $\alpha$  has been found to translocate into the nucleus in left ventricle samples (Gaber et al., 2013). HIF-1 $\alpha$  signaling pathway is also a crucial factor for the fetal heart development (Patterson and Zhang, 2010). To investigate the susceptibility to hypoxia-induced EndMT of HLHS-hiPSC-ECs, a hypoxia-mimetic agent was used to induce EndMT as has been previously described (Xu et al., 2015c). Briefly, 4 days of the chemical CoCl<sub>2</sub> treatment was sufficient to mimic HIF-1 activation effectively by stabilizing HIF-1. The CoCl<sub>2</sub> mimetic hypoxia condition is similar to the hypoxic microenvironment in vivo (Dai et al., 2012; Zhou et al., 2004). The CoCl<sub>2</sub> treatment of HLHS-hiPSC-ECs and WT-hiPSC-ECs showed a significant upregulation of EndMT key regulators when compared to normal condition (figure5 B). In addition, there seemed no observable differences of the gene expression of EndMT key regulators SNAIL and SLUG between HLHS-hiPSC-ECs and WT-hiPSC-ECs (figure5 B).*



**A TGFβ<sub>1</sub> treatment**



**B Hypoxia condition**

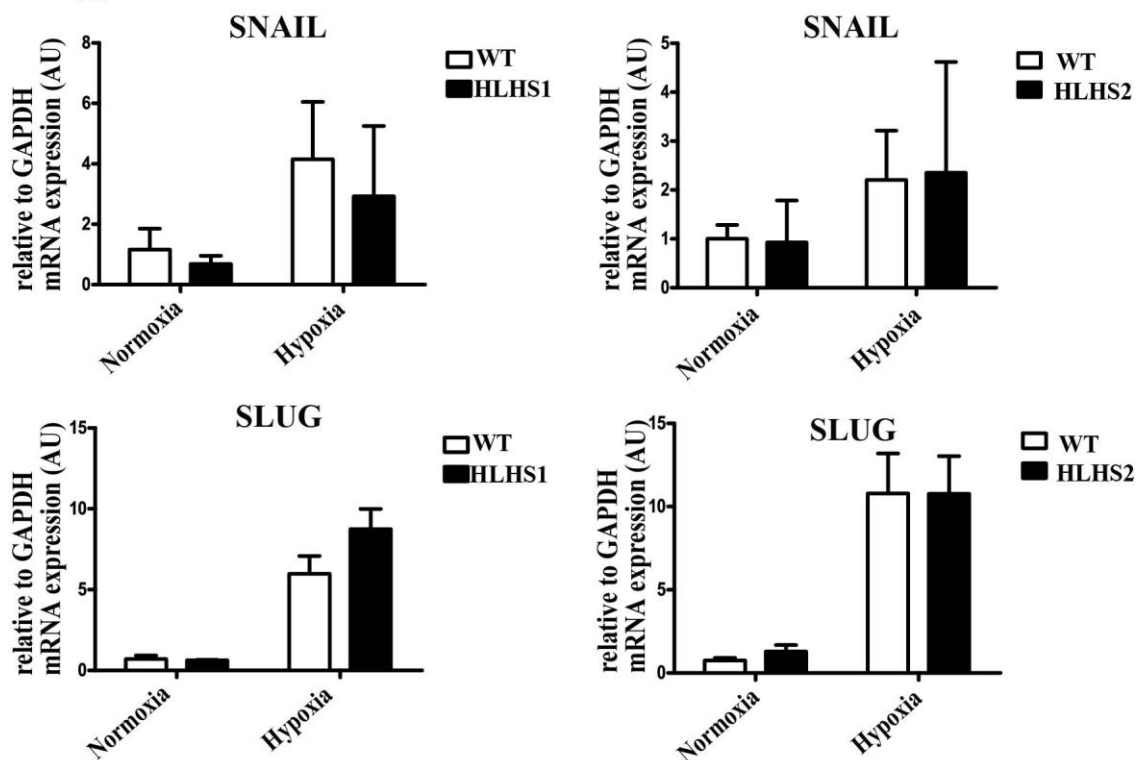


**Figure 5. Susceptibility of HLHS-hiPSC-ECs to TGFβ<sub>1</sub> treatment and hypoxia condition.** (A) With the pro-fibrotic factor TGFβ<sub>1</sub> treatment (final concentration 10 ng/ml), the expression of EndMT key regulators SNAIL and SLUG were similar between HLHS-hiPSC-ECs and WT-hiPSC-ECs. (B) CoCl<sub>2</sub> (final concentration 400 μM) was used for mimicking the hypoxia condition, it seemed no difference of the expression of EndMT

*key regulators SNAIL and SLUG comparing HLHS-hiPSC-ECs to WT-hiPSC-ECs.*

### **3.1.5 Discussion**

*Here, HLHS-hiPSCs were generated from fibroblasts of two individual HLHS patients, and further characterization showed that all HLHS-hiPSC lines were pluripotent and had the capability to differentiate into endothelial cells. Endothelial cells derived from WT-hiPSCs and HLHS-hiPSCs were used for further functional comparisons and mechanism studies.*

*Development of fibrosis, like scarring process, is a repair mechanism for acute or chronic injuries (Krenning et al., 2010; Moncrieff et al., 2004; Weber, 2000). Previous studies confirmed that EndMT contribute to the progression of fibrosis in different organs, suggesting that EndMT could be the responsible source of fibroblast during EFE tissue formation (Krenning et al., 2010; Piera-Velazquez et al., 2011; Xu et al., 2015a). Many factors such as TGF $\beta$  and hypoxia also contribute to EndMT.*

*To test the susceptibility of HLHS-hiPSC-ECs to TGF $\beta$ 1 and hypoxia condition, EndMT assay was performed in this study. The results showed that HLHS-hiPSC-ECs were not significantly susceptible to TGF $\beta$ 1 or hypoxia condition compared to WT-hiPSC-ECs. However, the aforementioned observation cannot be used to rule out the susceptibility of endothelial cells to pro-fibrotic factors in HLHS. The previous study revealed that higher expression levels of TGF $\beta$ 1 was observed in myocardial samples of HLHS compared to the healthy control. It was also confirmed that TGF $\beta$ 1 co-localized with fibroblast specific protein 1 (FSP1) in the hearts of HLHS patient (Gaber et al., 2013), which suggests that TGF $\beta$ 1 still play an important role in EFE generation. In addition, it has been proved that the perturbed TGF $\beta$ 1 might be caused by the aberrant secretion from damaged or abnormal cells (Hung et al., 2013). Particularly, malfunctioned cardiomyocytes may contribute to the accumulation of pro-fibrotic*

factors, like TGF $\beta$  or chronic hypoxia condition (Bujak and Frangogiannis, 2007; Song and Wang, 2015).

*The HLHS-hiPSC disease model is only able to explain one aspect of phenotypes and molecular mechanisms. Generally, different endothelial cell lineages share the same molecular markers, e.g. CD31, VE-cadherin, and VWF. Therefore, the endothelial cells derived from hiPSCs show heterogeneity in this protocol (Liu et al., 2016). Furthermore, different endothelial cell lineages express their distinct gene expression patterns and possess unique biological characteristics. These limitations of hiPSC-ECs could have an impact on the EndMT assay, which might hide the susceptibility to TGF $\beta$ 1 or hypoxia in HLHS samples.*

## 4. Discussion

*Despite the cause of HLHS is still unknown, strong evidence propose that HLHS is a genetic disease (Grossfeld, 1999; Hinton et al., 2007; lascone et al., 2012). Abnormal EndMT has been shown to contribute to the generation of EFE, which supposes that endothelial cell malfunctions may play an important role in the pathological development of heart in HLHS (Xu et al., 2015a). The purpose of this study is to analyze HLHS pathological disorder by using a patient-specific hiPSC system, and differentiate the patient-specific hiPSCs into endothelial cells for pathological analysis in vitro. At first, a highly efficient and simple protocol for the differentiation of endothelial cells was established. Furthermore, HLHS-hiPSC-ECs were generated and applied for further investigation of HLHS etiology.*

### 4.1 Establishment of a novel endothelial cell differentiation method

*Direct monolayer differentiation approach was established for endothelial cell differentiation in this study. Three steps, including mesoderm induction, endothelial cell differentiation and endothelial cell expansion, are involved in the differentiation of endothelial cells. During the first phase of endothelial cell differentiation, mesodermal cells were induced by the treatment of GSK3 $\beta$  inhibitor CHIR. The combinations of cytokines facilitate generation of endothelial cells by the activation of sequential endothelial cell differentiation cascades. After the generation of endothelial progenitor cells, complete endothelial cell growth medium was used for the acclimating progenitor cells into matured functional endothelial cells. In vitro functional characterizations of hiPSC-ECs further demonstrated that hiPSCs could be successfully differentiated into endothelial cells.*

*Since hESCs were isolated for the first time, efforts for developing different somatic cell differentiation protocols have never ceased (Thomson et al., 1998). In*

*the beginning, a method with three-dimensional aggregates called embryoid body was used for the differentiation of various cell types, which undergo differentiation of three-germ lineages in vitro. Several reports have illustrated that generation of endothelial cells from iPSCs through embryoid bodies (EBs) formation is reliable (Choi et al., 2009; James et al., 2010; Li et al., 2009; Rufaihah et al., 2013; Yang et al., 2008). However, this three-dimensional method could give rise to some undesired cell types and low differentiation efficiency. In contrast, direct monolayer differentiation creates a controllable microenvironment and overcomes the disadvantages associated with the spontaneous differentiation approach using embryoid body. Monolayer differentiation of endothelial cells was then developed later to improve this approach (Li et al., 2011a; Li et al., 2009; Lian et al., 2014; Orlova et al., 2014) and showed many advantages compared to EB methods, such as time-saving and cost efficiency. Besides, in some of endothelial cell differentiation methods, endothelial cell progenitors were enriched by cell sorting and then differentiated into endothelial cells (Tatsumi et al., 2011; Yang et al., 2008). The process of enrichment is time-consuming and was soon replaced by direct differentiation method (Lian et al., 2014; Patsch et al., 2015; Sahara et al., 2014). Due to the optimization of different cytokines and chemicals, the efficiency and duration of direct endothelial cell differentiation increased significantly in the protocols published recently (Bao et al., 2015; Sahara et al., 2014; Wu et al., 2015). Although there are several ready-to-use medium available now, it would be a large expenditure using of these commercial differentiation medium, which might be a limitation for their applications (Orlova et al., 2014; Patsch et al., 2015). Considering about all these pros and cons, medium and reagents used in this protocol was simplified and optimized. Therefore, a fast, high-efficiency and cost-effective endothelial cell differentiation protocol was established.*

*In our protocol, to shrink the time expansion of differentiation, endothelial cells were enriched with only one-step of cell sorting within 10 days. Here, the*



*differentiation efficiency of endothelial cells was improved to be more than 80% by the indication of double positive of CD31 and VE-cadherin. Moreover, this protocol could provide a more efficient approach for the generation of endothelial cells subtypes. We speculate that after further refinement of the protocol with proper characterization and modulation of different cytokines, a novel method for enrichment of particular subtypes of endothelial cells, namely arterial, venous or lymphatic endothelial cells could also be developed.*

#### **4.2 Modeling of HLHS by hiPSCs**

*In HLHS, patients have different levels of the heart defects. In particular, undeveloped left ventricle phenotype is associated with other heart disease, like mitral valve atresia and heterotaxy defects (Lin et al., 2008). EFE is reported in some HLHS cases, and further evidence showed that EFE originates from aberrant EndMT (Xu et al., 2015a). Additionally, fetal left ventricle in HLHS patient shows a decrease of the cardiomyocyte population and an increase of the fibroblast population (Gaber et al., 2013; Jiang et al., 2014).*

*For modeling the human cardiovascular diseases in vitro, hiPSCs provide a new method to recapitulate the complex pathophysiology of HLHS. Using the advantages of hiPSCs, HLHS-hiPSCs was used for modeling the cardiomyopathy in HLHS in several studies (Jiang et al., 2014; Kobayashi et al., 2014). It was reported that the properties and the gene expression profiles of HLHS-hiPSCs derived cardiomyocyte was perturbed by comparing with the cardiomyocyte from WT-hiPSCs, but the potential endothelial cell disorder was not addressed yet.*

*In this study, fibroblasts were isolated from diagnosed HLHS patients, which could be used for hiPSCs generation. After the patient-specific fibroblasts were successfully reprogrammed to hiPSCs, which were sequentially differentiated into endothelial cells. hiPSC-ECs were characterized with the expression of specific markers. Thereafter, EndMT assays were carried on to test the susceptibility of*

*HLHS-hiPSC-ECs to TGF $\beta$ 1 and hypoxia condition, the results revealed no differences between HLHS-hiPSC-ECs and WT-hiPSC-ECs.*

*The hypothesis of susceptibility of HLHS-hiPSC-ECs to TGF $\beta$ 1 and hypoxia condition could not be fully proved in this hiPSCs model. There could be some limitations of the hiPSCs derived endothelial cells. On one hand, hiPSC-ECs derived from this differentiation method contain a mixture of different subtypes of endothelial cells. It assumed that TGF $\beta$ 1 or hypoxic condition could trigger the susceptibility in a specific endothelial subtype, e.g. endocardial endothelial cells. On the other hand, it is speculated that endothelial cell progenitors are not synchronously differentiated into endothelial cells at the same stage. In detail, the gene expression profile varies in the enriched endothelial cell populations. Furthermore, the hiPSC-ECs may be not mature enough compared to the endothelial cells in normal physiological conditions. Therefore, hiPSCs derived endothelial cells may not re-implement the susceptibility to TGF $\beta$  or hypoxia as we expected.*

*For the further application, we provide a possibility of manipulating growth factors and chemicals for particular endothelial cell lineage generation. Treatment with the BMP4 and low level of VEGF, the generation of venous EC could be promoted. Stimulation with VEGF-C or Ang1 at the early stage could lead to lymphatic differentiation; beside, combination of BMP4, high level of VEGF concentration and cAMP were proven to enhance specific arterial EC differentiation (Atkins et al., 2011a; Kume, 2010; Le Bras et al., 2010; Li et al., 2009; Rufaihah et al., 2013; Yamashita, 2007). Based on all of these findings, it might be possible to enrich one particular EC lineages in a controllable microenvironment, particularly the endocardial endothelial cells.*

*Previous studies also reported gene mutations and CNVs in HLHS cases, which are associated with the gene regulatory pathways of EndMT or cardiac*

development (Gioli-Pereira et al., 2010; Hitz et al., 2012; Silversides et al., 2012; Stallmeyer et al., 2010; Zhao et al., 2015). In this study, the patient HLHS1 was identified with mutations in two genes including GSE1 and LRP6, while gene mutations were not found in another patient HLHS2 in former studies. Although several reported genetic mutations in HLHS, it is still unclear if these genetic mutations are responsible for disease progression or as non-disease-causing single nucleotide polymorphisms (SNPs). The interactions between these gene mutations and TGF $\beta$ 1 or TGF $\beta$ 1 induced EndMT require further investigations. According to the existential viewpoint, one of the reasonable explanations of HLHS malformation could result from the changes in the gene background combined with the toxic environmental factors (Benson et al., 2016; Grossfeld, 2007a; Grossfeld et al., 2009; Grossfeld, 2007b; Hinton et al., 2007).

## 5. Conclusion and future perspectives

*A simple and highly efficient differentiation method of functional endothelial cell from hiPSCs was established. HLHS-hiPSC lines were demonstrated to be pluripotent and differentiated into functional endothelial cells. There was no differences in susceptibility to TGF $\beta$ 1 or hypoxia condition comparing HLHS-hiPSC-ECs with WT-hiPSC-ECs.*

*In future studies, new differentiation protocols of specific subtypes of endothelial cell including the arterial, venous and lymphatic endothelial cells may be established based on current protocols. The pathological mechanisms of HLHS require individual assessment on a case-by-case basis. The development of precise medicine is becoming an option for the understanding of HLHS. Understanding of the genetic basis of HLHS would be achieved with the development of better analytical tools and more functional disease models.*

## 6 Reference

- Adams, W.J., Zhang, Y., Cloutier, J., Kuchimanchi, P., Newton, G., Sehrawat, S., Aird, W.C., Mayadas, T.N., Lusinskas, F.W., and Garcia-Cardena, G. (2013). Functional vascular endothelium derived from human induced pluripotent stem cells. *Stem cell reports* 1, 105-113.
- Al Turki, S., Manickaraj, A.K., Mercer, C.L., Gerety, S.S., Hitz, M.P., Lindsay, S., D'Alessandro, L.C.A., Swaminathan, G.J., Bentham, J., Arndt, A.K., *et al.* (2014). Rare Variants in NR2F2 Cause Congenital Heart Defects in Humans. *Am J Hum Genet* 94, 574-585.
- Andersen, N.D., Ramachandran, K.V., Bao, M.M., Kirby, M.L., Pitt, G.S., and Hutson, M.R. (2015). Calcium signaling regulates ventricular hypertrophy during development independent of contraction or blood flow. *Journal of molecular and cellular cardiology* 80, 1-9.
- Asuthkar, S., Guda, M.R., Martin, S.E., Antony, R., Fernandez, K., Lin, J.L., Tsung, A.J., and Velpula, K.K. (2016). Hand1 overexpression inhibits medulloblastoma metastasis. *Biochem Bioph Res Co* 477, 215-221.
- Atkins, G.B., Jain, M.K., and Hamik, A. (2011a). Endothelial Differentiation Molecular Mechanisms of Specification and Heterogeneity. *Arterioscl Throm Vas* 31, 1476-1484.
- Atkins, G.B., Jain, M.K., and Hamik, A. (2011b). Endothelial differentiation: molecular mechanisms of specification and heterogeneity. *Arterioscler Thromb Vasc Biol* 31, 1476-1484.
- Baekvad-Hansen, M., Tumer, Z., Delicado, A., Erdogan, F., Tommerup, N., and Larsen, L.A. (2006). Delineation of a 2.2 Mb microdeletion at 5q35 associated with microcephaly and congenital heart disease. *American Journal of Medical Genetics Part A* 140A, 427-433.
- Bao, X., Lian, X., Dunn, K.K., Shi, M., Han, T., Qian, T., Bhute, V.J., Canfield, S.G., and Palecek, S.P. (2015). Chemically-defined albumin-free differentiation of human pluripotent stem cells to endothelial progenitor cells. *Stem Cell Res* 15, 122-129.
- Beggah, A.T., Escoubet, B., Puttini, S., Cailmail, S., Delage, V., Ouvrard-Pascaud, A., Bocchi, B., Peuchmaur, M., Delcayre, C., Farman, N., and Jaisser, F. (2002). Reversible cardiac fibrosis and heart failure induced by conditional expression of an antisense mRNA of the mineralocorticoid receptor in cardiomyocytes. *P Natl Acad Sci USA* 99, 7160-7165.
- Belaousoff, M., Farrington, S.M., and Baron, M.H. (1998). Hematopoietic induction and respecification of A-P identity by visceral endoderm signaling in the mouse



embryo. *Development* 125, 5009-5018.

Benson, D.W., Martin, L.J., and Lo, C.W. (2016). Genetics of Hypoplastic Left Heart Syndrome. *J Pediatr-Us* 173, 25-31.

Bertram, H., Hitz, M.P., Ono, M., Sasse, M., Wessel, A., Breymann, T., and Yelbuz, T.M. (2008). Hypoplastic left heart syndrome with left ventricular myocardial sinusoids: Echocardiographic and angiographic findings in the first neonate surviving the Norwood I and II procedure. *Circulation* 117, E319-E321.

Bokesch, P.M., Appachi, E., Cavaglia, M., Mossad, E., and Mee, R.B.B. (2002). A glial-derived protein, S100B, in neonates and infants with congenital heart disease: Evidence for preexisting neurologic injury. *Anesth Analg* 95, 889-892.

Borchin, B., Chen, J., and Barberi, T. (2013). Derivation and FACS-mediated purification of PAX3+/PAX7+ skeletal muscle precursors from human pluripotent stem cells. *Stem cell reports* 1, 620-631.

Breckpot, J., Thienpont, B., Arens, Y., Tranchevent, L.C., Vermeesch, J.R., Moreau, Y., Gewillig, M., and Devriendt, K. (2011). Challenges of Interpreting Copy Number Variation in Syndromic and Non-Syndromic Congenital Heart Defects. *Cytogenet Genome Res* 135, 251-259.

Brito-Zeron, P., Izmirly, P.M., Ramos-Casals, M., Buyon, J.P., and Khamashta, M.A. (2015). The clinical spectrum of autoimmune congenital heart block. *Nat Rev Rheumatol* 11, 301-312.

Bruneau, B.G. (2013). Signaling and transcriptional networks in heart development and regeneration. *Cold Spring Harbor perspectives in biology* 5, a008292.

Bujak, M., and Frangogiannis, N.G. (2007). The role of TGF-beta signaling in myocardial infarction and cardiac remodeling. *Cardiovasc Res* 74, 184-195.

Burlew, B.S., and Weber, K.T. (2002). Cardiac fibrosis as a cause of diastolic dysfunction. *Herz* 27, 92-98.

Cao, N., Liang, H., Huang, J.J., Wang, J., Chen, Y.X., Chen, Z.Y., and Yang, H.T. (2013). Highly efficient induction and long-term maintenance of multipotent cardiovascular progenitors from human pluripotent stem cells under defined conditions. *Cell Res* 23, 1119-1132.

Capone, C., Buyon, J.P., Friedman, D.M., and Frishman, W.H. (2012). Cardiac Manifestations of Neonatal Lupus: A Review of Autoantibody-associated Congenital Heart Block and its Impact in an Adult Population. *Cardiol Rev* 20, 72-76.

Chakraborty, S., Zawieja, D.C., Davis, M.J., and Muthuchamy, M. (2015). MicroRNA signature of inflamed lymphatic endothelium and role of miR-9 in lymphangiogenesis and inflammation. *American journal of physiology. Cell*

physiology 309, C680-692.

Chiang, P.M., and Wong, P.C. (2011). Differentiation of an embryonic stem cell to hemogenic endothelium by defined factors: essential role of bone morphogenetic protein 4. *Development* 138, 2833-2843.

Choi, K.D., Yu, J., Smuga-Otto, K., Salvagiotto, G., Rehrauer, W., Vodyanik, M., Thomson, J., and Slukvin, I. (2009). Hematopoietic and endothelial differentiation of human induced pluripotent stem cells. *Stem Cells* 27, 559-567.

Choi, S.H., Hong, Z.Y., Nam, J.K., Lee, H.J., Jang, J., Yoo, R.J., Lee, Y.J., Lee, C.Y., Kim, K.H., Park, S., *et al.* (2015a). A Hypoxia-Induced Vascular Endothelial-to-Mesenchymal Transition in Development of Radiation-Induced Pulmonary Fibrosis. *Clinical cancer research : an official journal of the American Association for Cancer Research* 21, 3716-3726.

Choi, S.H., Hong, Z.Y., Nam, J.K., Lee, H.J., Jang, J., Yoo, R.J., Lee, Y.J., Lee, C.Y., Kim, K.H., Park, S., *et al.* (2015b). A Hypoxia-Induced Vascular Endothelial-to-Mesenchymal Transition in Development of Radiation-Induced Pulmonary Fibrosis. *Clinical cancer research : an official journal of the American Association for Cancer Research* 21, 3716-3726.

Chu, Y., Lund, D.D., Doshi, H., Keen, H.L., Knudtson, K.L., Funk, N.D., Shao, J.Q., Cheng, J., Hajj, G.P., Zimmerman, K.A., *et al.* (2016). Fibrotic Aortic Valve Stenosis in Hypercholesterolemic/Hypertensive Mice. *Arterioscler Thromb Vasc Biol* 36, 466-474.

Cooley, B.C., Nevado, J., Mellad, J., Yang, D., St Hilaire, C., Negro, A., Fang, F., Chen, G.B., San, H., Walts, A.D., *et al.* (2014). TGF-beta Signaling Mediates Endothelial-to-Mesenchymal Transition (EndMT) During Vein Graft Remodeling. *Science translational medicine* 6.

Dai, Z.J., Gao, J., Ma, X.B., Yan, K., Liu, X.X., Kang, H.F., Ji, Z.Z., Guan, H.T., and Wang, X.J. (2012). Up-regulation of hypoxia inducible factor-1alpha by cobalt chloride correlates with proliferation and apoptosis in PC-2 cells. *Journal of experimental & clinical cancer research : CR* 31, 28.

Dasgupta, C., Martinez, A.M., Zuppan, C.W., Shah, M.M., Bailey, L.L., and Fletcher, W.H. (2001). Identification of connexin43 (alpha1) gap junction gene mutations in patients with hypoplastic left heart syndrome by denaturing gradient gel electrophoresis (DGGE). *Mutat Res* 479, 173-186.

Denham, M., Bye, C., Leung, J., Conley, B.J., Thompson, L.H., and Dottori, M. (2012). Glycogen Synthase Kinase 3 beta and Activin/Nodal Inhibition in Human Embryonic Stem Cells Induces a Pre-Neuroepithelial State That Is Required for Specification to a Floor Plate Cell Lineage. *Stem Cells* 30, 2400-2411.

- Drawnel, F.M., Boccardo, S., Prummer, M., Delobel, F., Graff, A., Weber, M., Gerard, R., Badi, L., Kam-Thong, T., Bu, L., *et al.* (2014). Disease Modeling and Phenotypic Drug Screening for Diabetic Cardiomyopathy using Human Induced Pluripotent Stem Cells. *Cell Rep* 9, 810-820.
- Dudek, J., Cheng, I.F., Balleininger, M., Vaz, F.M., Streckfuss-Bomeke, K., Hubscher, D., Vukotic, M., Wanders, R.J.A., Rehling, P., and Guan, K.M. (2013). Cardiolipin deficiency affects respiratory chain function and organization in an induced pluripotent stem cell model of Barth syndrome. *Stem Cell Res* 11, 806-819.
- Ebert, A.D., Liang, P., and Wu, J.C. (2012). Induced Pluripotent Stem Cells as a Disease Modeling and Drug Screening Platform. *J Cardiovasc Pharm* 60, 408-416.
- Ebnet, K., Aurrand-Lions, M., Kuhn, A., Kiefer, F., Butz, S., Zander, K., Meyer zu Brickwedde, M.K., Suzuki, A., Imhof, B.A., and Vestweber, D. (2003). The junctional adhesion molecule (JAM) family members JAM-2 and JAM-3 associate with the cell polarity protein PAR-3: a possible role for JAMs in endothelial cell polarity. *J Cell Sci* 116, 3879-3891.
- Eisenberg, L.M., and Markwald, R.R. (1995). Molecular regulation of atrioventricular valvuloseptal morphogenesis. *Circulation research* 77, 1-6.
- Elliott, D.A., Kirk, E.P., Yeoh, T., Chandar, S., McKenzie, F., Taylor, P., Grossfeld, P., Fatkin, D., Jones, O., Hayes, P., *et al.* (2003). Cardiac homeobox gene NKX2-5 mutations and congenital heart disease: associations with atrial septal defect and hypoplastic left heart syndrome. *J Am Coll Cardiol* 41, 2072-2076.
- Emani, S.M., McElhinney, D.B., Tworetzky, W., Myers, P.O., Schroeder, B., Zurakowski, D., Pigula, F.A., Marx, G.R., Lock, J.E., and del Nido, P.J. (2012). Staged left ventricular recruitment after single-ventricle palliation in patients with borderline left heart hypoplasia. *J Am Coll Cardiol* 60, 1966-1974.
- Ezon, D., Maskatia, S., Jeewa, A., and Denfield, S. (2012). Morphologic Heterogeneity in Left Ventricular Noncompaction Resulting in Accessory Left Ventricular Chambers. *Circ-Heart Fail* 5, E94-E95.
- Fakhro, K.A., Choi, M., Ware, S.M., Belmont, J.W., Towbin, J.A., Lifton, R.P., Khokha, M.K., and Brueckner, M. (2011). Rare copy number variations in congenital heart disease patients identify unique genes in left-right patterning. *Proc Natl Acad Sci U S A* 108, 2915-2920.
- Feinstein, J.A., Benson, D.W., Dubin, A.M., Cohen, M.S., Maxey, D.M., Mahle, W.T., Pahl, E., Villafane, J., Bhatt, A.B., Peng, L.F., *et al.* (2012). Hypoplastic Left Heart Syndrome Current Considerations and Expectations. *J Am Coll Cardiol* 59, S1-S42.
- Friehs, I., Illigens, B., Melnychenko, I., Zhong-Hu, T., Zeisberg, E., and Del Nido, P.J. (2012). An animal model of endocardial fibroelastosis. *The Journal of surgical*

research.

Fruitman, D.S. (2000). Hypoplastic left heart syndrome: Prognosis and management options. *Paediatrics & child health* 5, 219-225.

Fusaki, N., Ban, H., Nishiyama, A., Saeki, K., and Hasegawa, M. (2009). Efficient induction of transgene-free human pluripotent stem cells using a vector based on Sendai virus, an RNA virus that does not integrate into the host genome. *P Jpn Acad B-Phys* 85, 348-362.

Gaber, N., Gagliardi, M., Patel, P., Kinnear, C., Zhang, C., Chitayat, D., Shannon, P., Jaeggi, E., Tabori, U., Keller, G., and Mital, S. (2013). Fetal Reprogramming and Senescence in Hypoplastic Left Heart Syndrome and in Human Pluripotent Stem Cells during Cardiac Differentiation. *Am J Pathol* 183, 720-734.

Garg, V., Muth, A.N., Ransom, J.F., Schluterman, M.K., Barnes, R., King, I.N., Grossfeld, P.D., and Srivastava, D. (2005). Mutations in NOTCH1 cause aortic valve disease. *Nature* 437, 270-274.

Gioli-Pereira, L., Pereira, A.C., Mesquita, S.M., Xavier-Neto, J., Lopes, A.A., and Krieger, J.E. (2010). NKX2.5 mutations in patients with non-syndromic congenital heart disease. *Int J Cardiol* 138, 261-265.

Glaser, D.E., Gower, R.M., Lauer, N.E., Tam, K., Blancas, A.A., Shih, A.J., Simon, S.I., and McCloskey, K.E. (2011). Functional Characterization of Embryonic Stem Cell-Derived Endothelial Cells. *Journal of vascular research* 48, 415-428.

Glessner, J.T., Bick, A.G., Ito, K., Homsy, J.G., Rodriguez-Murillo, L., Fromer, M., Mazaika, E., Vardarajan, B., Italia, M., Leipzig, J., *et al.* (2014). Increased frequency of de novo copy number variants in congenital heart disease by integrative analysis of single nucleotide polymorphism array and exome sequence data. *Circulation research* 115, 884-896.

Glidewell, S.C., Miyamoto, S.D., Grossfeld, P.D., Clouthier, D.E., Coldren, C.D., Stearman, R.S., and Geraci, M.W. (2015). Transcriptional Impact of Rare and Private Copy Number Variants in Hypoplastic Left Heart Syndrome. *Clinical and translational science* 8, 682-689.

Gotzsche, C.O., Krag-Olsen, B., Nielsen, J., Sorensen, K.E., and Kristensen, B.O. (1994). Prevalence of cardiovascular malformations and association with karyotypes in Turner's syndrome. *Archives of disease in childhood* 71, 433-436.

Grant, C.A., and Robertson, B. (1972). Microangiography of the pulmonary arterial system in "hypoplastic left heart syndrome". *Circulation* 45, 382-388.

Gridley, T. (2007). Notch signaling in vascular development and physiology. *Development* 134, 2709-2718.

- Gros, J., and Tabin, C.J. (2014). Vertebrate Limb Bud Formation Is Initiated by Localized Epithelial-to-Mesenchymal Transition. *Science* 343, 1253-1256.
- Grossfeld, P. (2007a). Hypoplastic left heart syndrome: new insights. *Circulation research* 100, 1246-1248.
- Grossfeld, P., Ye, M., and Harvey, R. (2009). Hypoplastic left heart syndrome: new genetic insights. *J Am Coll Cardiol* 53, 1072-1074.
- Grossfeld, P.D. (1999). The genetics of hypoplastic left heart syndrome. *Cardiology in the young* 9, 627-632.
- Grossfeld, P.D. (2007b). Hypoplastic left heart syndrome: it is all in the genes. *J Am Coll Cardiol* 50, 1596-1597.
- Grossfeld, P.D., Mattina, T., Lai, Z., Favier, R., Jones, K.L., Cotter, F., and Jones, C. (2004a). The 11q terminal deletion disorder: a prospective study of 110 cases. *American journal of medical genetics. Part A* 129A, 51-61.
- Grossfeld, P.D., Mattina, T., Lai, Z., Favier, R., Jones, K.L., Cotter, F., Jones, C., and Consortium, q. (2004b). The 11q terminal deletion disorder: A prospective study of 110 cases. *American Journal of Medical Genetics Part A* 129A, 51-61.
- Guan, J., and Couldwell, W.T. (2013). Evaluating the Role of CCM1 Loss-of-Function-Induced Endothelial-to-Mesenchymal Transition in Cavernous Malformation Development. *World Neurosurgery* 80, 444-446.
- Hashimoto, N., Phan, S.H., Imaizumi, K., Matsuo, M., Nakashima, H., Kawabe, T., Shimokata, K., and Hasegawa, Y. (2010). Endothelial-mesenchymal transition in bleomycin-induced pulmonary fibrosis. *Am J Respir Cell Mol Biol* 43, 161-172.
- Hickey, E.J., Caldarone, C.A., and McCrindle, B.W. (2012). Left ventricular hypoplasia: a spectrum of disease involving the left ventricular outflow tract, aortic valve, and aorta. *J Am Coll Cardiol* 59, S43-54.
- Higgins, D.F., Kimura, K., Iwano, M., and Haase, V.H. (2008). Hypoxia-inducible factor signaling in the development of tissue fibrosis. *Cell Cycle* 7, 1128-1132.
- Hinton, R.B., Martin, L.J., Tabangin, M.E., Mazwi, M.L., Cripe, L.H., and Benson, D.W. (2007). Hypoplastic left heart syndrome is heritable. *J Am Coll Cardiol* 50, 1590-1595.
- Hirashima, M. (2009). Regulation of endothelial cell differentiation and arterial specification by VEGF and Notch signaling. *Anat Sci Int* 84, 95-101.
- Hitz, M.P., Lemieux-Perreault, L.P., Marshall, C., Feroz-Zada, Y., Davies, R., Yang, S.W., Lionel, A.C., D'Amours, G., Lemyre, E., Cullum, R., *et al.* (2012). Rare copy number variants contribute to congenital left-sided heart disease. *PLoS genetics* 8,



e1002903.

Hou, P.P., Li, Y.Q., Zhang, X., Liu, C., Guan, J.Y., Li, H.G., Zhao, T., Ye, J.Q., Yang, W.F., Liu, K., *et al.* (2013). Pluripotent Stem Cells Induced from Mouse Somatic Cells by Small-Molecule Compounds. *Science* *341*, 651-654.

Hung, S.P., Yang, M.H., Tseng, K.F., and Lee, O.K. (2013). Hypoxia-induced secretion of TGF-beta1 in mesenchymal stem cell promotes breast cancer cell progression. *Cell Transplant* *22*, 1869-1882.

Iascone, M., Ciccone, R., Galletti, L., Marchetti, D., Seddio, F., Lincesso, A.R., Pezzoli, L., Vetro, A., Barachetti, D., Boni, L., *et al.* (2012). Identification of de novo mutations and rare variants in hypoplastic left heart syndrome. *Clin Genet* *81*, 542-554.

James, D., Nam, H.S., Seandel, M., Nolan, D., Janovitz, T., Tomishima, M., Studer, L., Lee, G., Lyden, D., Benezra, R., *et al.* (2010). Expansion and maintenance of human embryonic stem cell-derived endothelial cells by TGF beta inhibition is Id1 dependent. *Nature biotechnology* *28*, 161-U115.

Jiang, Y., Habibollah, S., Tilgner, K., Collin, J., Barta, T., Al-Aama, J.Y., Tesarov, L., Hussain, R., Trafford, A.W., Kirkwood, G., *et al.* (2014). An Induced Pluripotent Stem Cell Model of Hypoplastic Left Heart Syndrome (HLHS) Reveals Multiple Expression and Functional Differences in HLHS-Derived Cardiac Myocytes. *Stem Cell Transl Med* *3*, 416-423.

Kalluri, R., and Weinberg, R.A. (2009). The basics of epithelial-mesenchymal transition. *Journal of Clinical Investigation* *119*, 1420-1428.

Kanady, J.D., Dellinger, M.T., Munger, S.J., Witte, M.H., and Simon, A.M. (2011). Connexin37 and Connexin43 deficiencies in mice disrupt lymphatic valve development and result in lymphatic disorders including lymphedema and chylothorax. *Dev Biol* *354*, 253-266.

Katsura, A., Suzuki, H.I., Ueno, T., Mihira, H., Yamazaki, T., Yasuda, T., Watabe, T., Mano, H., Yamada, Y., and Miyazono, K. (2016). MicroRNA-31 is a positive modulator of endothelial-mesenchymal transition and associated secretory phenotype induced by TGF-beta. *Genes to cells : devoted to molecular & cellular mechanisms* *21*, 99-116.

Kim, D., Kim, C.H., Moon, J.I., Chung, Y.G., Chang, M.Y., Han, B.S., Ko, S., Yang, E., Cha, K.Y., Lanza, R., and Kim, K.S. (2009). Generation of human induced pluripotent stem cells by direct delivery of reprogramming proteins. *Cell stem cell* *4*, 472-476.

Kisanuki, Y.Y., Hammer, R.E., Miyazaki, J., Williams, S.C., Richardson, J.A., and Yanagisawa, M. (2001). Tie2-Cre transgenic mice: A new model for endothelial cell-lineage analysis in vivo. *Developmental Biology* *230*, 230-242.

Kobayashi, J., Yoshida, M., Tarui, S., Hirata, M., Nagai, Y., Kasahara, S., Naruse, K., Ito, H., Sano, S., and Oh, H. (2014). Directed Differentiation of Patient-Specific Induced

Pluripotent Stem Cells Identifies the Transcriptional Repression and Epigenetic Modification of NKX2-5, HAND1, and NOTCH1 in Hypoplastic Left Heart Syndrome. *Plos One* 9.

Kondratyeva, L.G., Sveshnikova, A.A., Grankina, E.V., Chernov, I.P., Kopantseva, M.R., Kopantzev, E.P., and Sverdlov, E.D. (2016). Downregulation of expression of mater genes SOX9, FOXA2, and GATA4 in pancreatic cancer cells stimulated with TGFbeta1 epithelial-mesenchymal transition. *Doklady. Biochemistry and biophysics* 469, 257-259.

Kovacic, J.C., Mercader, N., Torres, M., Boehm, M., and Fuster, V. (2012). Epithelial-to-Mesenchymal and Endothelial-to-Mesenchymal Transition From Cardiovascular Development to Disease. *Circulation* 125, 1795-1808.

Krenning, G., Zeisberg, E.M., and Kalluri, R. (2010). The Origin of Fibroblasts and Mechanism of Cardiac Fibrosis. *J Cell Physiol* 225, 631-637.

Kumarswamy, R., Volkmann, I., Jazbutyte, V., Dangwal, S., Park, D.H., and Thum, T. (2012). Transforming growth factor-beta-induced endothelial-to-mesenchymal transition is partly mediated by microRNA-21. *Arterioscler Thromb Vasc Biol* 32, 361-369.

Kume, T. (2010). Specification of arterial, venous, and lymphatic endothelial cells during embryonic development. *Histology and histopathology* 25, 637-646.

Kume, T. (2012). The Role of FoxC2 Transcription Factor in Tumor Angiogenesis. *J Oncol* 2012, 204593.

Lahm, H., Schon, P., Doppler, S., Dressen, M., Cleuziou, J., Deutsch, M.A., Ewert, P., Lange, R., and Krane, M. (2015). Tetralogy of Fallot and Hypoplastic Left Heart Syndrome - Complex Clinical Phenotypes Meet Complex Genetic Networks. *Current genomics* 16, 141-158.

Le Bras, A., Vijayaraj, P., and Oettgen, P. (2010). Molecular mechanisms of endothelial differentiation. *Vasc Med* 15, 321-331.

Li, C., Dong, F., Jia, Y.N., Du, H.Y., Dong, N., Xu, Y.J., Wang, S., Wu, H.P., Liu, Z.G., and Li, W. (2013). Notch Signal Regulates Corneal Endothelial-to-Mesenchymal Transition. *Am J Pathol* 183, 786-795.

Li, Z., Hu, S., Ghosh, Z., Han, Z., and Wu, J.C. (2011a). Functional characterization and expression profiling of human induced pluripotent stem cell- and embryonic stem cell-derived endothelial cells. *Stem cells and development* 20, 1701-1710.

Li, Z.J., Hu, S.J., Ghosh, Z., Han, Z.C., and Wu, J.C. (2011b). Functional Characterization and Expression Profiling of Human Induced Pluripotent Stem Cell- and Embryonic Stem Cell-Derived Endothelial Cells. *Stem cells and development* 20, 1701-1710.

- Li, Z.J., Wilson, K.D., Smith, B., Kraft, D.L., Jia, F.J., Huang, M., Xie, X.Y., Robbins, R.C., Gambhir, S.S., Weissman, I.L., and Wu, J.C. (2009). Functional and Transcriptional Characterization of Human Embryonic Stem Cell-Derived Endothelial Cells for Treatment of Myocardial Infarction. *Plos One* 4.
- Lian, X., Bao, X., Al-Ahmad, A., Liu, J., Wu, Y., Dong, W., Dunn, K.K., Shusta, E.V., and Palecek, S.P. (2014). Efficient differentiation of human pluripotent stem cells to endothelial progenitors via small-molecule activation of WNT signaling. *Stem cell reports* 3, 804-816.
- Lian, X.J., Hsiao, C., Wilson, G., Zhu, K.X., Hazeltine, L.B., Azarin, S.M., Raval, K.K., Zhang, J.H., Kamp, T.J., and Palecek, S.P. (2012). Robust cardiomyocyte differentiation from human pluripotent stem cells via temporal modulation of canonical Wnt signaling. *P Natl Acad Sci USA* 109, E1848-E1857.
- Lian, X.J., Zhang, J.H., Zhu, K.X., Kamp, T.J., and Palecek, S.P. (2013). Insulin Inhibits Cardiac Mesoderm, Not Mesendoderm, Formation During Cardiac Differentiation of Human Pluripotent Stem Cells and Modulation of Canonical Wnt Signaling Can Rescue This Inhibition. *Stem Cells* 31, 447-457.
- Lin, A.E., Basson, C.T., Goldmuntz, E., Magoulas, P.L., McDermott, D.A., McDonald-McGinn, D.M., McPherson, E., Morris, C.A., Noonan, J., Nowak, C., *et al.* (2008). Adults with genetic syndromes and cardiovascular abnormalities: clinical history and management. *Genet Med* 10, 469-494.
- Lin, F., Wang, N., and Zhang, T.C. (2012a). The role of endothelial-mesenchymal transition in development and pathological process. *IUBMB Life* 64, 717-723.
- Lin, F.J., You, L.R., Yu, C.T., Hsu, W.H., Tsai, M.J., and Tsai, S.Y. (2012b). Endocardial Cushion Morphogenesis and Coronary Vessel Development Require Chicken Ovalbumin Upstream Promoter-Transcription Factor II. *Arterioscl Throm Vas* 32, E135-+.
- Liu, X., Qi, J., Xu, X., Zeisberg, M., Guan, K., and Zeisberg, E.M. (2016). Differentiation of functional endothelial cells from human induced pluripotent stem cells: A novel, highly efficient and cost effective method. *Differentiation; research in biological diversity*.
- Liu, X., Sun, H., Qi, J., Wang, L., He, S., Liu, J., Feng, C., Chen, C., Li, W., Guo, Y., *et al.* (2013). Sequential introduction of reprogramming factors reveals a time-sensitive requirement for individual factors and a sequential EMT-MET mechanism for optimal reprogramming. *Nature cell biology* 15, 829-838.
- Lopez, B., Gonzalez, A., Hermida, N., Laviades, C., and Diez, J. (2008). Myocardial fibrosis in chronic kidney disease: potential benefits of torasemide. *Kidney international* 74, S19-S23.

Marcelo, K.L., Goldie, L.C., and Hirschi, K.K. (2013). Regulation of endothelial cell differentiation and specification. *Circulation research* 112, 1272-1287.

Markwald, R.R., Fitzharris, T.P., and Manasek, F.J. (1977). Structural Development of Endocardial Cushions. *Am J Anat* 148, 85-119.

Marom, K., Levy, V., Pillemer, G., and Fainsod, A. (2005). Temporal analysis of the early BMP functions identifies distinct anti-organizer and mesoderm patterning phases. *Developmental Biology* 282, 442-454.

McBride, K.L., Zender, G.A., Fitzgerald-Butt, S.M., Koehler, D., Menesses-Diaz, A., Fernbach, S., Lee, K., Towbin, J.A., Leal, S., and Belmont, J.W. (2009). Linkage analysis of left ventricular outflow tract malformations (aortic valve stenosis, coarctation of the aorta, and hypoplastic left heart syndrome). *Eur J Hum Genet* 17, 811-819.

McElhinney, D.B., Geiger, E., Blinder, J., Benson, D.W., and Goldmuntz, E. (2003a). NKX2.5 mutations in patients with congenital heart disease. *J Am Coll Cardiol* 42, 1650-1655.

McElhinney, D.B., Geiger, E., Blinder, J., Benson, D.W., and Goldmuntz, E. (2003b). NKX2.5 mutations in patients with congenital heart disease. *J Am Coll Cardiol* 42, 1650-1655.

McElhinney, D.B., Vogel, M., Benson, C.B., Marshall, A.C., Wilkins-Haug, L.E., Silva, V., and Tworetzky, W. (2010). Assessment of left ventricular endocardial fibroelastosis in fetuses with aortic stenosis and evolving hypoplastic left heart syndrome. *The American journal of cardiology* 106, 1792-1797.

McLean, A.B., D'Amour, K.A., Jones, K.L., Krishnamoorthy, M., Kulik, M.J., Reynolds, D.M., Sheppard, A.M., Liu, H.Q., Xu, Y., Baetge, E.E., and Dalton, S. (2007). Activin efficiently specifies definitive endoderm from human embryonic stem cells only when phosphatidylinositol 3-kinase signaling is suppressed. *Stem Cells* 25, 29-38.

Medici, D., and Kalluri, R. (2012). Endothelial-mesenchymal transition and its contribution to the emergence of stem cell phenotype. *Seminars in cancer biology* 22, 379-384.

Medici, D., Potenta, S., and Kalluri, R. (2011). Transforming growth factor-beta2 promotes Snail-mediated endothelial-mesenchymal transition through convergence of Smad-dependent and Smad-independent signalling. *The Biochemical journal* 437, 515-520.

Mohamed, S.A., Aherrahrou, Z., Liptau, H., Erasmi, A.W., Hagemann, C., Wrobel, S., Borzym, K., Schunkert, H., Sievers, H.H., and Erdmann, J. (2006). Novel missense mutations (p.T596M and p.P1797H) in NOTCH1 in patients with bicuspid aortic valve. *Biochem Biophys Res Commun* 345, 1460-1465.

Moncrieff, J., Lindsay, M.M., and Dunn, F.G. (2004). Hypertensive heart disease and

fibrosis. *Curr Opin Cardiol* 19, 326-331.

Moskowitz, I.P., Wang, J., Peterson, M.A., Pu, W.T., Mackinnon, A.C., Oxburgh, L., Chu, G.C., Sarkar, M., Berul, C., Smoot, L., *et al.* (2011). Transcription factor genes Smad4 and Gata4 cooperatively regulate cardiac valve development. [corrected]. *Proc Natl Acad Sci U S A* 108, 4006-4011.

Nakano, Y., Oyamada, M., Dai, P., Nakagami, T., Kinoshita, S., and Takamatsu, T. (2008). Connexin43 knockdown accelerates wound healing but inhibits mesenchymal transition after corneal endothelial injury in vivo. *Invest Ophthalmol Vis Sci* 49, 93-104.

Orlova, V.V., van den Hil, F.E., Petrus-Reurer, S., Drabsch, Y., ten Dijke, P., and Mummery, C.L. (2014). Generation, expansion and functional analysis of endothelial cells and pericytes derived from human pluripotent stem cells. *Nat Protoc* 9, 1514-1531.

Ozgur, S., Senocak, F., Orun, U.A., Ocal, B., Karademir, S., Dogan, V., and Yilmaz, O. (2011). Ventricular non-compaction in children: clinical characteristics and course. *Interact Cardiovasc Thromb* 12, 370-373.

Patsch, C., Challet-Meylan, L., Thoma, E.C., Urich, E., Heckel, T., O'Sullivan, J.F., Grainger, S.J., Kapp, F.G., Sun, L., Christensen, K., *et al.* (2015). Generation of vascular endothelial and smooth muscle cells from human pluripotent stem cells. *Nature cell biology*.

Patterson, A.J., and Zhang, L. (2010). Hypoxia and fetal heart development. *Current molecular medicine* 10, 653-666.

Pearson, S., Sroczynska, P., Lacaud, G., and Kouskoff, V. (2008). The stepwise specification of embryonic stem cells to hematopoietic fate is driven by sequential exposure to Bmp4, activin A, bFGF and VEGF. *Development* 135, 1525-1535.

Peinado, H., Olmeda, D., and Cano, A. (2007). Snail, ZEB and bHLH factors in tumour progression: an alliance against the epithelial phenotype? *Nat Rev Cancer* 7, 415-428.

Peinado, H., Portillo, F., and Cano, A. (2004). Transcriptional regulation of cadherins during development and carcinogenesis. *Int J Dev Biol* 48, 365-375.

Phillips, H.M., Renforth, G.L., Spalluto, C., Hearn, T., Curtis, A.R.J., Craven, L., Havarani, B., Clement-Jones, M., English, C., Stumper, O., *et al.* (2002). Narrowing the critical region within 11q24-qter for hypoplastic left heart and identification of a candidate gene, JAM3, expressed during cardiogenesis. *Genomics* 79, 475-478.

Piera-Velazquez, S., Li, Z., and Jimenez, S.A. (2011). Role of endothelial-mesenchymal transition (EndoMT) in the pathogenesis of fibrotic disorders. *Am J Pathol* 179, 1074-1080.

- Reamon-Buettner, S.M., Ciribilli, Y., Inga, A., and Borlak, J. (2008). A loss-of-function mutation in the binding domain of HAND1 predicts hypoplasia of the human hearts. *Hum Mol Genet* 17, 1397-1405.
- Rieder, F., Kessler, S.P., West, G.A., Bhilocha, S., de la Motte, C., Sadler, T.M., Gopalan, B., Stylianou, E., and Fiocchi, C. (2011). Inflammation-Induced Endothelial-to-Mesenchymal Transition A Novel Mechanism of Intestinal Fibrosis. *Am J Pathol* 179, 2660-2673.
- Rufaihah, A.J., Huang, N.F., Kim, J., Herold, J., Volz, K.S., Park, T.S., Lee, J.C., Zambidis, E.T., Reijo-Pera, R., and Cooke, J.P. (2013). Human induced pluripotent stem cell-derived endothelial cells exhibit functional heterogeneity. *Am J Transl Res* 5, 21-U122.
- Rychik, J., Rome, J.J., Collins, M.H., DeCampi, W.M., and Spray, T.L. (1999). The hypoplastic left heart syndrome with intact atrial septum: Atrial morphology, pulmonary vascular histopathology and outcome. *J Am Coll Cardiol* 34, 554-560.
- Sahara, M., Hansson, E.M., Wernet, O., Lui, K.O., Spater, D., and Chien, K.R. (2014). Manipulation of a VEGF-Notch signaling circuit drives formation of functional vascular endothelial progenitors from human pluripotent stem cells. *Cell Res* 24, 820-841.
- Saito, A. (2013). EMT and EndMT: regulated in similar ways? *Journal of Biochemistry* 153, 493-495.
- Saxton, T.M., and Pawson, T. (1999). Morphogenetic movements at gastrulation require the SH2 tyrosine phosphatase Shp2. *P Natl Acad Sci USA* 96, 3790-3795.
- Seki, A., Patel, S., Ashraf, S., Perens, G., and Fishbein, M.C. (2013). Primary endocardial fibroelastosis: an underappreciated cause of cardiomyopathy in children. *Cardiovascular Pathology* 22, 345-350.
- Shay, A., Kirwin, S., and Funanage, V. (2011). Hypoplastic Left Heart Syndrome: Molecular Consequences of Transcription Factor Mutations. *Faseb J* 25.
- Shimada, S., Robles, C., Illigens, B.M.W., Berazaluze, A.M.C., del Nido, P.J., and Friehs, I. (2015). Distention of the Immature Left Ventricle Triggers Development of Endocardial Fibroelastosis: An Animal Model of Endocardial Fibroelastosis Introducing Morphopathological Features of Evolving Fetal Hypoplastic Left Heart Syndrome. *Biomed Res Int*.
- Sifrim, A., Hitz, M.P., Wilsdon, A., Breckpot, J., Al Turki, S.H., Thienpont, B., Mcrae, J., Fitzgerald, T.W., Singh, T., Swaminathan, G.J., *et al.* (2016). Distinct genetic architectures for syndromic and nonsyndromic congenital heart defects identified by exome sequencing. *Nat Genet* 48, 1060-+.
- Silversides, C.K., Lionel, A.C., Costain, G., Merico, D., Migita, O., Liu, B., Yuen, T.,



- Rickaby, J., Thiruvahindrapuram, B., Marshall, C.R., *et al.* (2012). Rare copy number variations in adults with tetralogy of Fallot implicate novel risk gene pathways. *PLoS genetics* 8, e1002843.
- Sjoberg, G., Chow, C.W., Cooper, S., and Weintraub, R.G. (2007). X-linked cardiomyopathy presenting as contracted endocardial fibroelastosis. *J Heart Lung Transpl* 26, 293-295.
- Song, W., and Wang, X. (2015). The role of TGFbeta1 and LRG1 in cardiac remodelling and heart failure. *Biophysical reviews* 7, 91-104.
- Stallmeyer, B., Fenge, H., Nowak-Gottl, U., and Schulze-Bahr, E. (2010). Mutational spectrum in the cardiac transcription factor gene NKX2.5 (CSX) associated with congenital heart disease. *Clinical Genetics* 78, 533-540.
- Streckfuss-Bomeke, K., Wolf, F., Azizian, A., Stauske, M., Tiburcy, M., Wagner, S., Hubscher, D., Dressel, R., Chen, S., Jende, J., *et al.* (2013). Comparative study of human-induced pluripotent stem cells derived from bone marrow cells, hair keratinocytes, and skin fibroblasts. *European heart journal* 34, 2618-2629.
- Takahashi, K., Tanabe, K., Ohnuki, M., Narita, M., Ichisaka, T., Tomoda, K., and Yamanaka, S. (2007). Induction of pluripotent stem cells from adult human fibroblasts by defined factors. *Cell* 131, 861-872.
- Takahashi, K., and Yamanaka, S. (2006). Induction of pluripotent stem cells from mouse embryonic and adult fibroblast cultures by defined factors. *Cell* 126, 663-676.
- Tan, J.Y., Sriram, G., Rufaihah, A.J., Neoh, K.G., and Cao, T. (2013). Efficient Derivation of Lateral Plate and Paraxial Mesoderm Subtypes from Human Embryonic Stem Cells Through GSKi-Mediated Differentiation. *Stem cells and development* 22, 1893-1906.
- Tatsumi, R., Suzuki, Y., Sumi, T., Sone, M., Suemori, H., and Nakatsuji, N. (2011). Simple and Highly Efficient Method for Production of Endothelial Cells From Human Embryonic Stem Cells. *Cell Transplant* 20, 1423-1430.
- Tchervenkov, C.I., Jacobs, J.P., Weinberg, P.M., Aiello, V.D., Beland, M.J., Colan, S.D., Elliott, M.J., Franklin, R.C.G., Gaynor, J.W., Krogmann, O.N., *et al.* (2006). The nomenclature, definition and classification of hypoplastic left heart syndrome. *Cardiology in the young* 16, 339-368.
- Thiery, J.P., Acloque, H., Huang, R.Y.J., and Nieto, M.A. (2009). Epithelial-Mesenchymal Transitions in Development and Disease. *Cell* 139, 871-890.
- Thomson, J.A., Itskovitz-Eldor, J., Shapiro, S.S., Waknitz, M.A., Swiergiel, J.J., Marshall, V.S., and Jones, J.M. (1998). Embryonic stem cell lines derived from human blastocysts. *Science* 282, 1145-1147.
- Tripathi, R.R., Sridhar, A., and Chidambaram, S. (2012). Unusual combination of

hypoplastic left ventricle, atrioventricular septal defect with restrictive ventricular septal defect, and common arterial trunk. *World journal for pediatric & congenital heart surgery* 3, 396-398.

van Meeteren, L.A., and ten Dijke, P. (2012). Regulation of endothelial cell plasticity by TGF-beta. *Cell Tissue Res* 347, 177-186.

Vokes, S.A., and Krieg, P.A. (2002). Endoderm is required for vascular endothelial tube formation, but not for angioblast specification. *Development* 129, 775-785.

Voyta, J.C., Via, D.P., Butterfield, C.E., and Zetter, B.R. (1984). Identification and Isolation of Endothelial-Cells Based on Their Increased Uptake of Acetylated-Low Density Lipoprotein. *J Cell Biol* 99, 2034-2040.

Warren, L., Manos, P.D., Ahfeldt, T., Loh, Y.H., Li, H., Lau, F., Ebina, W., Mandal, P.K., Smith, Z.D., Meissner, A., *et al.* (2010). Highly Efficient Reprogramming to Pluripotency and Directed Differentiation of Human Cells with Synthetic Modified mRNA. *Cell stem cell* 7, 618-630.

Weber, K.T. (2000). Fibrosis and hypertensive heart disease. *Curr Opin Cardiol* 15, 264-272.

Wu, Y.T., Yu, I.S., Tsai, K.J., Shih, C.Y., Hwang, S.M., Su, I.J., and Chiang, P.M. (2015). Defining minimum essential factors to derive highly pure human endothelial cells from iPS/ES cells in an animal substance-free system. *Scientific reports* 5, 9718.

Wu, Y.Y., Ai, Z.Y., Yao, K.Z., Cao, L.X., Du, J., Shi, X.Y., Guo, Z.K., and Zhang, Y. (2013). CHIR99021 promotes self-renewal of mouse embryonic stem cells by modulation of protein-encoding gene and long intergenic non-coding RNA expression. *Exp Cell Res* 319, 2684-2699.

Wu, Z.Q., Rowe, R.G., Lim, K.C., Lin, Y., Willis, A., Tang, Y., Li, X.Y., Nor, J.E., Maillard, I., and Weiss, S.J. (2014). A Snail1/Notch1 signalling axis controls embryonic vascular development. *Nat Commun* 5, 3998.

Xiong, Y., Zhou, B., and Chang, C.P. (2012). Analysis of the endocardial-to-mesenchymal transformation of heart valve development by collagen gel culture assay. *Methods Mol Biol* 843, 101-109.

Xu, X.B., Friehs, I., Hu, T.Z., Melnychenko, I., Tampe, B., Alnour, F., Iascone, M., Kalluri, R., Zeisberg, M., del Nido, P.J., and Zeisberg, E.M. (2015a). Endocardial Fibroelastosis Is Caused by Aberrant Endothelial to Mesenchymal Transition. *Circulation research* 116, 857-866.

Xu, X.B., Tan, X.Y., Tampe, B., Nyamsuren, G., Liu, X.P., Maier, L.S., Sossalla, S., Kalluri, R., Zeisberg, M., Hasenfuss, G., and Zeisberg, E.M. (2015b). Epigenetic balance of aberrant Rasal1 promoter methylation and hydroxymethylation regulates cardiac fibrosis. *Cardiovasc Res* 105, 279-291.

- Xu, X.B., Tan, X.Y., Tampe, B., Sanchez, E., Zeisberg, M., and Zeisberg, E.M. (2015c). Snail Is a Direct Target of Hypoxia-inducible Factor 1 alpha (HIF1 alpha) in Hypoxia-induced Endothelial to Mesenchymal Transition of Human Coronary Endothelial Cells. *J Biol Chem* 290, 16653-16664.
- Xu, X.F., Su, B., Xie, C.G., Wei, S.M., Zhou, Y.Q., Liu, H., Dai, W.Q., Cheng, P., Wang, F., Xu, X.R., and Guo, C.Y. (2014). Sonic Hedgehog-Gli1 Signaling Pathway Regulates the Epithelial Mesenchymal Transition (EMT) by Mediating a New Target Gene, S100A4, in Pancreatic Cancer Cells. *Plos One* 9.
- Yamaguchi, T.P., Harpal, K., Henkemeyer, M., and Rossant, J. (1994). Fgfr-1 Is Required for Embryonic Growth and Mesodermal Patterning during Mouse Gastrulation. *Gene Dev* 8, 3032-3044.
- Yamashita, J.K. (2007). Differentiation of arterial, venous, and lymphatic endothelial cells from vascular progenitors. *Trends Cardiovasc Med* 17, 59-63.
- Yan, W., Bentley, B., and Shao, R. (2008). Distinct angiogenic mediators are required for basic fibroblast growth factor- and vascular endothelial growth factor-induced angiogenesis: the role of cytoplasmic tyrosine kinase c-Abl in tumor angiogenesis. *Molecular biology of the cell* 19, 2278-2288.
- Yang, L., Soonpaa, M.H., Adler, E.D., Roepke, T.K., Kattman, S.J., Kennedy, M., Henckaerts, E., Bonham, K., Abbott, G.W., Linden, R.M., *et al.* (2008). Human cardiovascular progenitor cells develop from a KDR+ embryonic-stem-cell-derived population. *Nature* 453, 524-528.
- Yu, J.Y., Vodyanik, M.A., Smuga-Otto, K., Antosiewicz-Bourget, J., Frane, J.L., Tian, S., Nie, J., Jonsdottir, G.A., Ruotti, V., Stewart, R., *et al.* (2007). Induced pluripotent stem cell lines derived from human somatic cells. *Science* 318, 1917-1920.
- Yu, W.J., Liu, Z., An, S., Zhao, J.Y., Xiao, L., Gou, Y.C., Lin, Y.F., and Wang, J. (2014). The Endothelial-Mesenchymal Transition (EndMT) and Tissue Regeneration. *Curr Stem Cell Res T* 9, 196-204.
- Zeisberg, E., Melnychenko, I., Hu, T.Z., Fries, I., Kalluri, R., and del Nido, P. (2009). Endocardial Fibroelastosis in Hypoplastic Left Heart Syndrome is Caused by Aberrant Endothelial to Mesenchymal Transition. *Circulation* 120, S603-S603.
- Zeisberg, E.M., Potenta, S., Xie, L., Zeisberg, M., and Kalluri, R. (2007a). Discovery of endothelial to mesenchymal transition as a source for carcinoma-associated fibroblasts. *Cancer Res* 67, 10123-10128.
- Zeisberg, E.M., Potenta, S.E., Sugimoto, H., Zeisberg, M., and Kalluri, R. (2008). Fibroblasts in kidney fibrosis emerge via endothelial-to-mesenchymal transition. *Journal of the American Society of Nephrology : JASN* 19, 2282-2287.
- Zeisberg, E.M., Tarnavski, O., Zeisberg, M., Dorfman, A.L., McMullen, J.R., Gustafsson,

E., Chandraker, A., Yuan, X.L., Pu, W.T., Roberts, A.B., *et al.* (2007b). Endothelial-to-mesenchymal transition contributes to cardiac fibrosis. *Nat Med* 13, 952-961.

Zhang, C., Han, Y., Huang, H., Qu, L., and Shou, C. (2014). High NR2F2 transcript level is associated with increased survival and its expression inhibits TGF-beta-dependent epithelial-mesenchymal transition in breast cancer. *Breast cancer research and treatment* 147, 265-281.

Zhao, L., Li, B., Dian, K., Ying, B.W., Lu, X.J., Hu, X.J., An, Q., Chen, C.X., Huang, C.Y., Tan, B., and Qin, L. (2015). Association between the European GWAS-Identified Susceptibility Locus at Chromosome 4p16 and the Risk of Atrial Septal Defect: A Case-Control Study in Southwest China and a Meta-Analysis. *Plos One* 10.

Zhou, H.Y., Wu, S.L., Joo, J.Y., Zhu, S.Y., Han, D.W., Lin, T.X., Trauger, S., Bien, G., Yao, S., Zhu, Y., *et al.* (2009). Generation of Induced Pluripotent Stem Cells Using Recombinant Proteins. *Cell stem cell* 4, 381-384.

Zhou, J., Schmid, T., Frank, R., and Brune, B. (2004). PI3K/Akt is required for heat shock proteins to protect hypoxia-inducible factor 1alpha from pVHL-independent degradation. *J Biol Chem* 279, 13506-13513.

Zhou, T., Benda, C., Dunzinger, S., Huang, Y.H., Ho, J.C., Yang, J.Y., Wang, Y., Zhang, Y., Zhuang, Q., Li, Y.H., *et al.* (2012). Generation of human induced pluripotent stem cells from urine samples. *Nat Protoc* 7, 2080-2089.

## 7 Acknowledgement

*Thanks for the kind support and help from all the people around me.*

*At first, I would like to thank my supervisor Prof. Dr. Elisabeth Zeisberg for her help, advice and support. Advice given by my supervisor has been a great help in my research and thesis preparations. Thank you for setting up a series of clear goals for me in my academic road.*

*Thanks for all my colleges in Zeisberg's lab who provided support in many different ways. It is a great team just like a big family to work together.*

*Besides, I have to thank for all the technology support from Prof. Dr. Kaomei Guan and the stem cell lab. Thanks for my thesis committee members Prof. Dr. Frauke Alves for her advice and kind support.*

*Thanks a lot for Dr. Poh Loong Soong and Dr. Xingbo Xu, who helps me about the thesis writing and scientific writing. Thanks for the proofreading from Andreas Maus and Sarah Henze. Thanks for the technology support from Stem cell unit, FACS and TAL faculty Universitätsmedizin Göttingen.*

*I would like to express my deep thanks to my family. They help me to find the right way when I am lost. Thanks for Jing Qi, for her patience and support. She always trusts me and encourages me to be a good scientist and good husband.*

*I really appreciate the peaceful and memorable time in Göttingen.*

## Curriculum Vitae

### Personal details:

---

Name: Xiaopeng Liu  
Date of birth: 05.11.1987  
Place of birth: Chifeng, Inner Mongolia, China  
Nationality: Chinese

### Education and Work Experiences

---

Sep,2004-Jun,2008 Anhui University  
Sep,2008-Jun,2011 University of Science and Technology of China  
Jul,2013- present Georg-August-Universität Göttingen

### Work Experiences

---

Jul,2011- Mar,2013 Guangzhou Institute of Biomedicine and Health,  
Chinese Academy of Sciences

### Publications and academic performance

---

- **Xiaopeng Liu**, J. Qi, X. Xu, M. Zeisberg, K. Guan and E. M. Zeisberg (2016). Differentiation of functional endothelial cells from human induced pluripotent stem cells: A novel, highly efficient and cost effective method. *Differentiation*, doi: 10.1016/j.diff.2016.05.004.
- **Xiaopeng Liu**, H. Sun, J. Qi, L. Wang, S. He, J. Liu, C. Feng, et al. Sequential introduction of reprogramming factors reveals a time-sensitive requirement for individual factors and a sequential EMT-MET mechanism for optimal reprogramming. *Nature Cell Biology*. 15 (2013), pp. 829 – 838.
- H. Zheng, H. Zou, **Xiaopeng Liu**, et al. Cholesterol level influences opioid signaling in cell models and analgesia in mice and humans. *Journal of Lipid Research*. 2012;53(6):1153–1162.
- Miguel Angel Esteban, Tao Wang, Baoming Qin, Jiayin Yang, Dajiang Qin, Jinglei Cai, Wen Li, Zihui Weng, Jiekai Chen, Su Ni, Keshi Chen, Yuan Li, **Xiaopeng Liu**,.... Duanqing Pei. Vitamin C enhances the generation of mouse and human induced pluripotent stem cells. *Cell Stem Cell*. 6(1):71-9. 2010.
- David M. Charytan, Robert Padera, Alexander M. Helfand, Michael Zeisberg, Xingbo Xu, **Xiaopeng Liu**,.... Elisabeth M. Zeisberg. Increased concentration of circulating angiogenesis and nitric oxide inhibitors induces endothelial to mesenchymal transition and myocardial fibrosis in patients with chronic kidney disease. *International Journal of Cardiology*. 176(1). 2014.
- Xingbo Xu, Xiaoying Tan, Bjorn Tampe, Gunsmaa Nyamsuren, **Xiaopeng Liu**,.... Elisabeth M. Zeisberg .Epigenetic balance of aberrant Rasal1 promoter methylation and hydroxymethylation regulates cardiac fibrosis. *Cardiovascular Research*. 105(3). 2015.